2018

Effect of glycerine and water emulsion of diesel-biodiesel blends on engine performance and emissions with EGR

Sidhu, Manpreet Singh

Effect of Glycerine and Water Emulsion of Diesel-Biodiesel Blends on Engine Performance and Emissions with EGR

By: Manpreet Singh Sidhu

Supervised By

Dr. Murari Mohon Roy, Associate Professor, Department of Mechanical Engineering

Dr. Wilson Wang, Professor, Department of Mechanical Engineering

April 2018

A Thesis Submitted in the Partial Fulfilment of the Requirement for the Degree of Masters in Science

In Mechanical Engineering

Faculty of Engineering

Lakehead University, Thunder Bay, Ontario, Canada P7B 5E1

Abstract

The globally rising temperatures and its impact on our ecosystem and earth's natural processes have raised an environmental concern worldwide. The pollution caused due to the burning of fossil fuels has resulted in climate change, thus, compelling the researchers to look for eco-friendly fuels. Biodiesel derived from biomass have emerged recently as a possible fuel due to their role in decreasing CO emissions. However, the excessive production of biodiesel has raised a disposal concern for its by-product glycerine and higher NOx emissions produced through its use has initiated the need to look for other alternative fuels. In the present study, a systematic comparison was performed with multiple blends of diesel-biodiesel and their glycerine emulsions to compare it with water emulsion and investigate the performance and emissions of the related fuels along with the EGR system. All fuel blends and their emulsions were tested on a light-duty and heavy-duty engine. Hydrophilic-lipophilic balance (HLB) was formulated using suitable surfactants to attain the desired stability for various emulsion fuels. Emulsion stability, mean particle droplet size, fuel properties, engine performance, and emissions were observed. It was concluded that brake-specific fuel consumption (BSFC) and brake-thermal efficiency (BTE) increased with the increase in biodiesel and water-glycerine concentration. For emissions, the rise in CO and HC were noted but reductions in exhaust gas temperature, smoke and NO_x were observed with emulsion fuels without EGR. Also, there was a significant decrease in smoke (approximately 80%) with increased concentration of glycerine at 3000 rpm, at high load. With the use of EGR, an increase in BSFC and decrease in BTE was observed. Additionally, EGR was seen to increase smoke, CO and HC emissions but lowers NOx and exhaust gas temperatures. The reduction of NOx in B100 was 20.41% and 16.39% when compared to water emulsion and glycerine emulsion at 10% concentration without EGR, and this reduction continued to 44.07% and 43.25% at maximum EGR % at 3000 rpm and high load respectively.

Acknowledgment

I would like to thank my professor Dr. Roy for helping me in this study. His guidance served as the backbone for the completion of my thesis. I am sincerely grateful to have worked under his supervision. He gave me the theoretical as well as practical knowledge for this work.

I would also like to extend my gratitude to Dr. Wang whose constant support helped me in fulfilling the requirements of my studies. I am thankful for his supervision, advice and support. I felt great working under his direction.

I would also like to acknowledge my appreciation for the committee members Dr. Pakzad and Dr. Tarokh, for their helping commentaries without which I would not have completed my thesis.

I want to thank Joe Ripku (Mechanical Department Technician), Greg Kepka (Instrumentation Lab Technician) and Debbie Puumala (Chemistry Lab Technician) for their assistance.

Lastly, I would like to thank my family and colleagues for being my moral support whenever I needed them.

Table of Contents

Caption for Figures

Caption for Tables

NOMENCLATURE

ASTM	American Society of Testing and Materials
BSFC	Brake-specific fuel consumption
BTDC	Before top dead center
BTE	Brake thermal
cc	Cubic centimeter
CN	Cetane number
CO	Carbon monoxide
CO_2	Carbon dioxide
cP	Centipoise
cSt	Centistokes
°C	Degree Celsius
EGR	Exhaust gas recirculation
EGT	Exhaust gas temperature
FAME	Fatty acid methyl esters
g/kWh	Gram per kilowatt-hour
HC	Hydrocarbon
HLB	Hydrophilic-lipophilic balance
kg/m^3	Kilogram per cubic meter
kJ/kg	Kilojoule per kilogram
kW	Kilowatt
mg/m^3	Milligram per cubic meter
ml/min	Milliliter per minute
mm	Millimeter
MPa	Mega pascal
NO	Nitric oxide
NO_2	Nitrogen dioxide
NO_x	Oxides of nitrogen
O_2	Oxygen
pH	Potential of hydrogen
PM	Particulate matter
ppm	Parts per million
RL	Rhamnolipid biosurfactant
rpm	Revolutions per minute
Span 80	Sorbitan monooleate
Tween 80	Polyoxyethylene sorbitan monooleate
w.r.t.	with respect to
µm	Micrometer

CHAPTER 1: INTRODUCTION

1.1 OVERVIEW

The world population tends to grow every year at an amazing rate, and this leads to an increased demand for energy resources to sustain the growing human population. Among all the resources used to produce energy, fossil fuels continue to play a dominant role in global energy production. Fossil fuels are the primary source of energy consumption which is growing by almost 2% with every passing year [1]. Fossil fuels are formed because of natural processes such as decomposition of dead organisms. The sources of fossil fuels include oil, coal and natural gas which are a non-renewable source of energy and will not last forever. Besides its being an exhaustible energy source it usage and extraction can result in serious health problems and has adverse effects on the environment because these stand as a dominant source in the production of carbon dioxide.

Most of the carbon emissions that affect the climate of the earth are released into the atmosphere through the burning of fossil fuels for energy and transportation. Primary source of carbon emission across the world remains to be transportation, which contributed to almost 26 percent in of all carbon emission in the year 2000 and out of these can attribute to road transport that was responsible for about 65% of those emissions [2]. These figures, however, are not final figures and are estimated to increase in future due to the overreliance of people on transportation. According to the International Energy Agency (IEA), the carbon emissions emitted by the transport sector will rise by 92% till 2020, and it is projected that from 2020 to 2035, 8.6 billion metric tons carbon emissions will be released into the earth's atmosphere [3]. The primary production of carbon emissions can be attributed to the usage of diesel engines used in both private and public transportation sectors owing to its efficiency and improved durability. Also, the extensive use of diesel engines makes it a major contributor to the inhalation of the air-suspended particulate matters [4]. Thus, scientists and researchers are looking for more eco-friendly options in the transportation sector.

Therefore, owing to the effects that fossil fuels have on climate and growing debates on its continued usage has led to an increased demand to look for alternative ways of energy production which can reduce our reliance on fossil fuels and can help people make possible a transition towards a low-carbon producing society. After examining the various fuels, researchers found biodiesel which is an organic fuel to be the most promising alternative which can take the place of the conventional diesel fuel without having to make many alternations in the existing diesel engine [5].

Biodiesel is a biodegradable fuel and can be defined as a mono alkyl ester that is obtained through transesterification with methanol from either vegetable or animal fat [6]–[10]. Fatty acid methyl esters (FAME) which are the primary molecule present in biodiesel has been proven to be useful in the reduction of fossil fuels usage, in improving energy efficiency in various sectors and its usage can be seen as a step towards sustainable energy [10]–[12]. Biodiesel has been seen to be effective in the reduction of harmful exhaust emissions, which include, particulate matter (PM), carbon monoxide (CO), and unburnt hydrocarbons (HC), however, it results in a slight of nitrogen oxides (NOx) due to presence of oxygen that facilitates proper fuel combustion [9], [13], [14].

The organic and eco-friendly quality of biodiesel has resulted in an increased demand among researchers to explore its use as an alternative fuel. The demand to test biodiesel as an alternative fuel has resulted in the overproduction of biodiesel which in turn has led to the oversupply of glycerine in the market, which in turn has decreased the prices of glycerine and the problem of its disposal has raised another environmental concern [15]–[19]. Thus, the large surplus of glycerine has stressed the need to examine different strategies that can be employed to counter this oversupply.

Glycerine (glycerine or 1,2,3- Propanetriol), which is a by-product of biodiesel, through transesterification has most recently being tested as a possible alternative fuel in the production of energy [19], [20]. Although, glycerine, in the past, has been successfully used in cosmetics, soaps, food and beverage industries after purification [21]. If used as a fuel to produced electricity and heat in boilers or furnaces, glycerine can aid in reducing the harmful emissions and improve the sustainability of biodiesel [22]. However, there is a need to explore different ways in which glycerine can be utilized as possible fuel in the transport sector and assist in countering the problem faced due to its excessive supply.

1.2 PROPERTIES OF BIODIESEL

1.2.1 Flash Point

Flashpoint of a liquid may be referred to as the lowest temperature at which it starts to produce vapors that can be ignited through contact with an ignition source. The flash point temperature of biodiesel is higher when compared to that of diesel which makes it less volatile and safer to store and use in transportation [23], [24]. However, several factors influence the flash point of biodiesel are identified as the residual alcohol content and the number of carbon atoms and double bonds present in the biodiesel [25].

1.2.2 Viscosity

Viscosity measures the resistance of a fluid to flow caused by the internal friction of the moving fluid over another at a specified temperature. When compared to diesel, biodiesel is said to have a higher viscosity which may because of the raw material that is used in its production [23], [26]. The high viscosity of biodiesel leads to reduced fuel atomization, incomplete combustion and results in carbon accumulation on the injectors, however, if the viscosity is low, it may not provide sufficient lubrication to the engine [23]. The kinematic viscosity of biodiesel at 40 °C is limited 1.9–6.0 mm^2/s in ASTM D6751 [26].

1.2.3 Density

Engine performance is significantly affected by the density of the fuel. Density has an essential part to play in determining the correlation of the fuel injection property with the air-fuel ratio and energy content present within the combustion chamber [26]–[28]. Biodiesel has a slightly higher density than petrol or diesel, however; its density is affected by the chain length and degree of unsaturation, where higher chain length signifies lower fuel density, whereas, higher unsaturation signifies an increase in density [26].

1.2.4 Cetane Number

Cetane number (CN) refers to the property of fuel that measures the ignition properties of fuel regarding ignition and combustion. The cetane number of biodiesel depending on the feedstock and process of its production, can either be lower which hinders engine start in cold weather and results in pollution due to poor combustion and higher which causes instant ignition that reduces fuel efficiency [28], [29]. The cetane number of biodiesel is higher than diesel fuel owing to its long-chain hydrocarbon groups which result in higher combustion efficiency and better ignition property [25], [27], [30].

1.2.5 Lubricity

Lubricity refers to the measure of reduction in friction between moving solid surfaces. Due to the high oxygen content present in biodiesel, its lubricity value is better than diesel fuel which may help to reduce friction loss, hence, improving the brake power efficiency [31]–[33]. The high lubricity of biodiesel can be attributed to the impurities present in the biodiesel, and its purification results in the removal of its impurities which in turn, reduces the lubricity [27].

1.2.6 Calorific Value (Heating value)

Calorific value refers to total amount of heat produced by the complete combustion of a fuel. The calorific value of the fuel is mainly used to measure the energy released when a substance is burned and is an essential factor that effects engine power. Therefore, the higher calorific value is an essential factor in combustion. However, biodiesel has a calorific value than diesel fuel [34]. Thus, the increase of biodiesel content decreases the engine power [32].

1.3 THESIS SCOPE

Biodiesel has many advantages over diesel engine due to its organic and renewable quality, but it also has a downside that it increases the NOx emissions which are proven to be toxic for human beings and the atmosphere. Through this research, an attempt will be made to looks for alternative techniques with different fuel types to reduce the NOx and smoke capacity emitted from a diesel engine and to improve the performance the engine.

CHAPTER 2: LITERATURE REVIEW

2.1 INTERNAL COMBUSTION ENGINE (IC)

Internal combustion engines (IC) is a heat engine which facilitates the fuel combustion usually in the presence of an oxidizer in a confined space called combustion chamber. IC engines are the most widely used engines in buses, trucks or other automobiles. IC engines are mainly of two types: spark engines (petrol and gasoline), and compression engines (diesel engine) [35]. Both gasoline and diesel engines are the pillar of the transportation sector. However, diesel engines have been proven to be superior in terms of regulating losses, thermal efficiency and fuel consumption than gasoline engines with the exception of formation of nitrogen oxide (NOx) [36].

2.2 BIODIESEL

Technological advancement in fuel technology, increasing demand for energy and strict emission laws that are enforced to lower harmful emissions that have resulted in climate change had led to an increased demand to search for alternative fuels that can be used in CI engines and help in reducing fossil fuel consumption [37]. This problem has compelled researchers to look for such alternative fuels and has brought their attention to biodiesel.

Biodiesel, if used as a fuel, is nominally toxic due to its biodegradable nature and can easily be used without any modification in the present CI engines [36]. Biodiesel has many advantages, such as renewability, non-toxic and safe for the environment when compared with petroleum diesel [38], [39]. Due to the high oxygen content present in biodiesel, it facilitates complete combustion, therefore, reducing particulate matter (PM), carbon monoxide (CO), and, hydrocarbon (HC) emissions, however, it causes a slight increase in NOx emissions [14], [40]–[44].

2.3 REGULATED EMISSIONS

The world is now confronted with the problem of increased pollution produced because of emissions and the severe effects it has on our climate. This has led to an increased demand to regulate emissions that are released into the atmosphere and to create look for innovative ways to produce clean energy. This problem has initiated a need to regulate the number of emissions released into the atmosphere. Based on engine power, exhaust emission standards are divided into various class in Canada that establish maximum levels of particulate matter (PM), carbon monoxide (CO), hydrocarbons (HC) and nitrogen oxides (NOx) [45].

2.3.1 Particulate Matter (PM) Emissions

Particulate matter is a combination of solid particles and a liquid droplet that can include organic and inorganic particles that remain suspended in air. PM is also known as total particulate matter (TPM), or diesel particulate matter (DPM) which is blend of carbon soot and other solid and liquid materials [46]. Particulate matters are formed because of incomplete combustion of hydrocarbons [47], [48]. PM emission of a diesel engine when compared with gasoline engines

are six to ten times higher, and more than 50 percent of these emissions are soot (black smoke) that adversely impact the environment and human health [47].

2.3.2 Carbon Monoxide (CO) Emissions

Carbon monoxide is a poisonous, colorless and odorless gas that is formed due to the lack of oxygen which leads to the incomplete combustion of hydrocarbons [49]. CO is most commonly formed in rich mixtures where there is an insufficient quantity of oxygen all carbon molecules cannot be converted into carbon dioxide thus resulting in the formation of CO[47], [50].

2.3.3 Hydrocarbon (HC) Emissions

Hydrocarbon emissions are produced by the internal combustion engine due to incomplete combustion of hydrocarbon fuels. Higher oxygen quantity and cetane number help to reduce HC emissions. Therefore, in case of biodiesel, hydrocarbons are reduced because of the high oxygen content that facilitated complete combustion, and high cetane number helps to reduce ignition delay [51].

2.3.4 Nitrogen Oxides (NOx) Emissions

NOx emissions are the most toxic pollutants that negatively effect human health and, contributes to climate change as it results atmospheric ozone formation [52]. NOx is formed in the combustion chamber due to the high combustion temperature which results in oxidization of nitrogen present in the intake air [53]. NOx formation is affected by the combustion temperature, oxygen content and residence time [54]. To decrease NOx, Exhaust Gas Recirculation (EGR) has been proven to be the most efficient method as it reduces the oxygen by re-circulating the exhaust gas back to inlet air [36], [55], [56].

The formation of NO in the combustion chamber has been studied extensively using the extended Zeldovich mechanism [57], [58]. It has been found that NO is formed during the combustion process due to the oxidation of nitrogen present in the atmospheric air.

$$N_2 + O \longrightarrow NO + N$$

$$N + O_2 \longrightarrow NO + O$$

$$N + OH \longrightarrow NO + H \quad \ldots\ldots\ldots\ldots \quad (1)$$

NO is converted to NO_2 by its oxidation using the following reactions:

$$NO + HO_2 \longrightarrow NO_2 + OH$$

$$NO_2 + O \longrightarrow NO + O_2 \quad \ldots\ldots\ldots\ldots \quad (2)$$

From the total amount of NO present in the exhaust gases around 10-30% is comprised of NO_2 which is five times more toxic than NO. The idle temperature for the formation of NOx is estimated to be above 2000 K [59].

2.4 PERFORMANCE AND EMISSIONS OF BIODIESEL/BIODIESEL BLENDS FUEL

The increasing levels of pollution that have resulted in a change of earth's climate and depletion of fossil fuels have initiated a demand to seek cleaner and renewable methods of energy production and use in transportation. In the search for the invention of alternative fuels that can take the place of the depleting fossil fuels, biodiesel has attracted considerable attention [60]. Biodiesel fuels have the potential to reduce the emissions such as CO, SO_2, HC and particulate matters that cause global warming although it increases NOx concentration in comparison to diesel fuel [61].

Zhang et al. [6] experimented with a marine diesel engine to investigate the emissions and characteristics of the various biodiesel fuel blends and found that the oxygen content present in biodiesel decreased HC and CO emission and increased NOx emissions when compared with pure diesel. Soto et al. [8] explored from two different techniques (Thermal analysis and engine experiments) using diesel and biodiesel to determine which fuel or fuel blend aids in better combustion and observed that B20 blend increased power, torque and thermal efficiency by 1.2%, 1.0%, and 1.2% respectively and reduced soot emissions up to 8.9%, when compared to diesel fuel. Ali et al. [62] investigated the feasibility of blended biodiesel-diesel fuel and noted that engine brake power reduced by 2.6 % and the brake specific fuel consumption increased by 3% with the increase in biodiesel ratios.

Nabi et al. [44] examined the influence of biodiesel blends at 20%, 40%, and 60% (by volume) on engine performance and emissions in comparison to diesel fuel and observed that biodiesel blends reduced CO, HC, PM and increased the NOx emissions. Roy et al. [63] conducted experiments on DI diesel engine using biodiesel–diesel, biodiesel–diesel-additive and kerosene–biodiesel to test the performance and emissions of the blends and observed that BSFC and NOx increased with the increase in biodiesel, whereas, CO and HC decreased with the use of biodiesel blends. Qi et al. [64] tested the effect of biodiesel regarding combustion, performance, and emissions on a diesel engine and found out that the low heating value of biodiesel increased brake specific fuel consumption and showed a reduction in CO, HC, NOx and smoke at full engine load.

Hasan and Rahman [65] explored engine performance and emission characteristics of biodiesel-diesel blends on CI engines and observed that biodiesel-diesel blend provided shorter ignition as compared to diesel, and also noted that biodiesel-diesel reduced HC, CO, and PM emissions but increased NOx emissions. Emiroğlu et al. [66] experimented with turkey rendering fat biodiesel (TRFB) to investigate its effects on combustion, performance and exhaust emissions at different loads on CI engine and found that due to lower heating value of biodiesel than diesel fuel, the BSFC values of TRFB blends were higher in comparison to diesel fuel and also, TRFB10, TRFB20, and TRFB50 blends decreased smoke opacity by 20%, 25% and 40% respectively, however, caused NOx emissions to increase slightly. Pinzi et al. [66] investigated the effect of biodiesel chemical structure on combustion and emissions properties in a diesel engine and observed that HC, CO, soot, and NOx emissions are higher when FAME chain length is increased. Roy et al. [9] conducted experiments on DI diesel engine using biodiesel–diesel, biodiesel–diesel-additive and kerosene–biodiesel to test the performance and emissions of the blends and observed

that BSFC and NOx increased with the increase in biodiesel, whereas, CO and HC decreased with the use of biodiesel blends.

2.5 BIODIESEL FUEL BLENDING

Fuel blending is an important factor for the improvement of cold flow property. Diesel and kerosene have the high CFPs than biodiesel which is -40°C for diesel and -2.6°C for canola oil biodiesel [67]. So, blending can be helpful in CFPs. Roy et al. [68] experimented on DI engine using biodiesel-diesel and canola oil-diesel blends to study the performance and emissions of the engine at idling speed and observed considerably low CO and HC emissions for biodiesel-diesel blends where B20 and UCB20 exhibited 13% reduction in CO and 22% in HC as compared to neat diesel fuel. It was further noted that CO emissions were substantially low with the addition of 5% pure canola oil in diesel fuel. Roy et al. [67] did experiment with two different additives ethanol and diethyl ether in biodiesel-diesel blends (B20, B50 and B100) as these help in improving the cold flow properties of diesel-biodiesel blends and noted that cloud point for B20 was below -20°C whereas for ethanol blends it was below -25°C and furthermore it was observed that biodiesel blends and biodiesel blend with ethanol 5% (except B100) reduced CO more than neat diesel.

2.6 METHODS TO REDUCE OXIDES OF NITROGEN

2.6.1 Emulsion

Emulsion is defined as a mixture of two or more immiscible liquids (polar and non-polar) [69]–[71] which is kinetically stable system and has recognized to be a promising fuel upgrading process [19], [72], [73]. Polar liquids have an unequal charge due to the presence of a significant negative charge on its oxygen molecules, whereas non-polar liquids have an equal charge due to the even distribution of positive and negative on each of its molecule [71], [74]. Surfactant plays a vital role in the process of formation of a kinetically stable emulsion fuel by reducing the oil and water surface tension [75], [76]. The formation of a stable emulsion depends on the hydrophilic-lipophilic balance (HLB) of a surfactant which is used to measure the hydrophilic or lipophilic degree [77]. HLB value ranges from 1 to 20, where low HLB value (1-9) tends to be attracted towards non-polar liquids (oil-loving/lipophilic), making a stable water-in-oil emulsion and high HLB value (11-20) tends to be attracted to polar liquids (water-loving/hydrophilic), making a stable oil-in-water emulsion [75], [78]–[80]. Emulsion can be categorized into two types, firstly, depending on the droplet size of the particles, that is, microemulsions, macroemulsions and nanoemulsions respectively [81]. Secondly, based on phase which are: two-phase (water-in-oil and oil-in-water) and three-phase (oil-in-water-in-oil and water-in-oil-in-water) as seen in Figure 1 [71], [82]. Two-phase emulsion is preferred more than three-phase emulsion to be used in the production of combustion fuels, due to the smaller mean droplet size and higher heating value whereas three-phase emulsion is mostly used in food, medicine, and cosmetics industries [82], [83]. Emulsion can be prepared using electronic, mechanical, ultrasonic and magnetic forces [78], [84], [85].

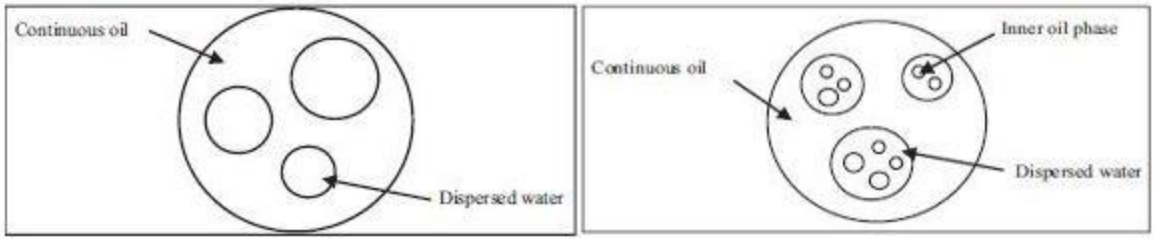

(a) Two-Phase Emulsion (b) Three-Phase Emulsion

Figure 1: Different Phases of Emulsion [71]

Neat biodiesel as a fuel is estimated to produce 10% more NOx than diesel engines, however, by using emulsification technique NOx emissions can be reduced [86]. Various studies have investigated the role of emulsion in the reduction of NOx emissions. Debnath et al. [71] examined the role of emulsified fuel technology to reduce diesel engine emissions and critically analysed the studies performed using emulsified fuel and observed that the application of water-diesel emulsion increases engine brake power (BP), BSFC and CO whereas due to the presence of water aids in reducing NOx and smoke and HC emissions. Attia and Kulchitskiy [87] investigated the performance of water-in-diesel fuel emulsion on a diesel engine and found out that emulsion with the larger size of water droplets result in the reducing of NOx emissions, whereas emulsion with finer droplets reduced smoke and HC and increased engine efficiency. Alahmer et al. [88] studied the performance of an engine powered by pure diesel and emulsified fuel and noted that with the increase in water content BSFC increased at high engine speeds, whereas, due to the high amount of water, BTE, exhaust gas temperature, and NOx decreased. Emulsion fuel combustion can be seen in Figure 2 and the atomization of emulsion fuel molecule in Figure 3.

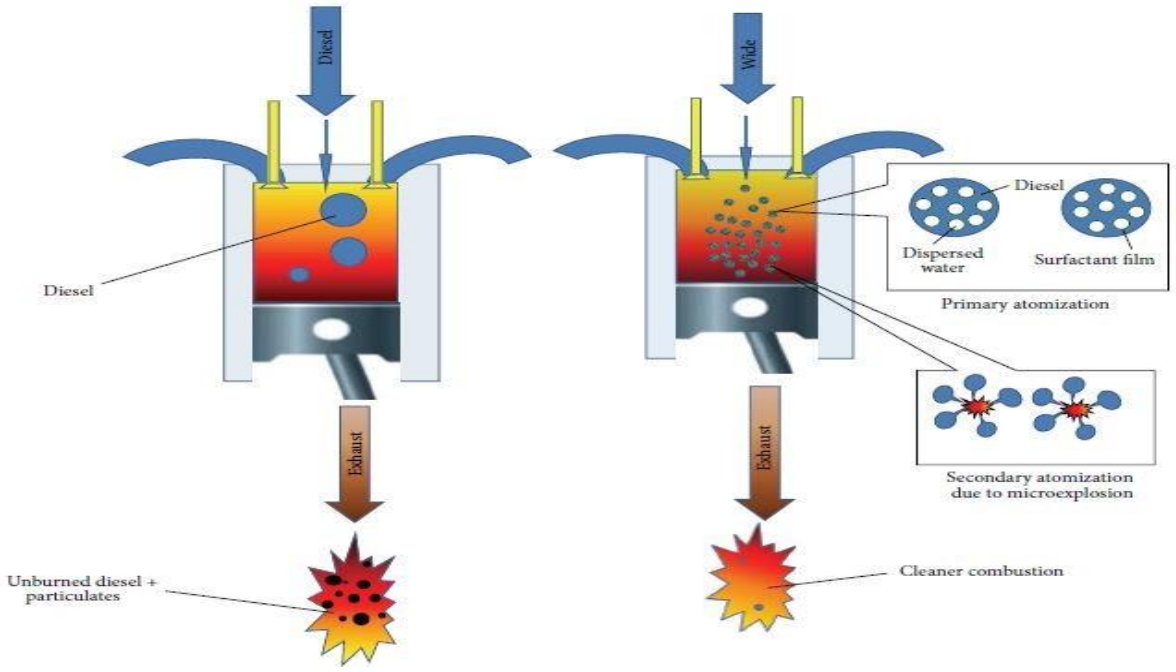

Figure 2: Pictorial View for the Combustion of the Emulsion Fuel [81]

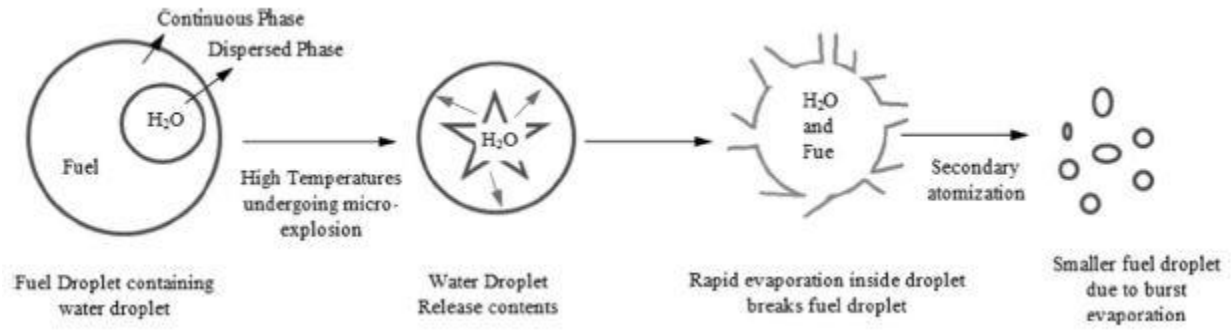

Figure 3: Atomization with Micro-Explosion [71]

Senthil et al. [89] investigated the performance emission of waste cooking oil obtained from palm oil (WCO) and its emulsion fuel on a diesel engine and found that WCO emulsion significantly reduced smoke, HC, and CO when compared with neat WCO and neat diesel. Cheng-Yuan et al. [86] examined the emulsification and fuel properties of biodiesel emulsion and observed that surfactant with HLB 13 had the highest emulsification stability and neat biodiesel had lower kinematic viscosity and carbon residual than biodiesel emulsion. Additionally, two-phase biodiesel emulsion had smaller mean droplet size than three-phase biodiesel emulsion. Zaid et al. [90] tested water-in-Diesel emulsion on a diesel engine to examine the effects of water emulsification on exhaust gas temperature and engine performance and concluded that increase in water content increased BSFC, BTE and decreased EGT.

2.6.2 Neat Glycerine Diesel-Biodiesel Blends / Glycerine Diesel-Biodiesel Blends Emulsion Performance and Emissions

Glycerine is a renewable and biodegradable product which has many advantages even if burnt as a fuel without any purification and can help to eliminate the use of fossil fuel and reduce transportation cost [91]. Therefore, many researchers are focusing their attention to explore the uses of glycerine as a possible alternate fuel.

Oprescu et al. [15] used two glycerine derivatives (methanol and methyl hexanoate diesel blends) as additives in a diesel engine to examine their performance and emissions and noticed that methyl hexanoate gave promising result as an additive by reducing HC, CO, and smoke emissions but slightly increased NOx. Beatrice et al. [17] investigated the effects of a glycerine-derived ethers mixture (GEM) on a CI engine and noticed that due to the oxygen content present in GEM, PM emissions decreased while slightly increasing NOx at medium load, however, at low loads maximum increase was seen in HC and CO. Steinmetz et al. [21] studied acrolein and other volatile organic emissions emitted during the process of combustion of crude glycerine which was measured using SUMMA canister collection and concluded that it produced volatile organic compounds acrolein emissions comparable to those produced during natural gas combustion. Ayoub and Abdulla [92] critically examined the formation and impact of crude glycerine and its current and future utilization and concluded that the vast quantities of glycerine could be used as an additive in different fuels formulations.

Bohon et al. [93] did experiments on prototype refractory burner and furnace to examine the combustion properties and emissions using USP glycerine, methylated and demethylated

glycerine and noted a 100 percent glycerine combustion in the burner and furnace. Roy and Da Silva [94] studied crude glycerine to explore an alternative fuel in Canadian wood pellet industry and observed a reduction of CO_2 and NOx emission in glycerine-soaked pellets during the combustion process as compared to pure wood pellets. Noureddlni et al. [95] investigated the etherification of glycerine with isobutylene and compatibility of glycerine ethers within biodiesel and biodiesel blends and concluded that etherification of glycerine with isobutylene could be achieved using Aberlyst-15 as a catalyst under different reaction conditions. Additionally, it was noted that ethers of glycerine were compatible diesel and biodiesel fuels and can result in reduction cloud point and viscosity by 5℃ and 8% respectively. Eaton et al. [96] examined the glycerine−diesel emulsion system to discover the ideal surfactant systems, its impact on stability and to determine combustion and emission of the emulsion and noted that in case of glycerine-diesel fuel emulsion HLB of 10 surfactants significantly reduced the surface tension and low HLB surfactants showed the longest stability. It was further concluded that NOx and PM (particulate matter) were reduced when glycerine was added whereas BTE and BSFC increased with the increase in glycerine volume.

2.6.3 EGR System

Other than emulsion, EGR has been proven to be very successful in reducing NOx emission in an IC engine [14], [97], [98]. Since high-temperature offer ideal conditions for the formation of NOx, lowering the maximum temperature of the combustion chamber is the perfect solution [99]. EGR reduces the exhaust gases, that is, carbon dioxide and nitrogen by recirculating them back to the combustion chamber where these are displaced by fresh air entering in the chamber which dilutes the oxygen amount needed for combustion, thus reducing peak in-cylinder temperatures [100]. EGR system can be classified into three different categories based on EGR temperature [59].

2.6.3.1 Hot EGR

It involves re-circulating of the exhaust gas without cooling it which results in increased intake charge temperature.

2.6.3.2 Full Cooled EGR

It involves re-circulation of exhaust gas back to the combustion chamber after it has been fully cooled using a water-cooled heat exchanger. This may cause moisture present in the cylinder to condense adversely affecting the inside of the engine cylinder.

2.6.3.3 Partly Cooled EGR

It involves keeping the temperature of the exhaust gas just above the dew point so that water condensation cannot take place.

Various studies have been done on the EGR to study its effects on the reduction of NOx emissions. Hussain et al. [100] tested EGR on a three-cylinder air-cooled diesel engine to examine its effects on engine's performance and emissions and noted reductions in NOx and EGT although, and the increase was seen the emissions of CO, HC, and particulate matters. Yasin et al. [101] experimented with neat palm-biodiesel on a Mitsubishi four stroke, water cooled DI diesel engine using EGR performed under steady state and observed a reduction in brake power output, torque

fuel consumption and NOx while a slight rise was seen in CO, CO_2, and particulate matters. Kumar and Saravanan [102] conducted experiments to study the effects of four pentanol/diesel blends under various EGR rates on the performance and emission of the engine and found that using the combination of pentanol/diesel under EGR conditions decreased NOx emissions 41% at medium load and 33.7% at high load and smoke emissions remained low till 20% EGR rate but increased HC and CO emissions. It was further concluded that 45% pentanol/diesel blends had the potential to be used in diesel engines without any modifications. Chaichan [103] used a duel fuel (Sunflower biodiesel-hydrogen blends) under heavy-EGR conditions to study its effects on engine performance and noted EGR reduced the availability oxygen thus increased HC and CO emissions but reduced NOx emissions.

Thangaraja and Kannan [104] carried out a comprehensive study on the effects of EGR on advanced diesel combustion and concluded that it was advantageous in controlling NOx emissions owing to the low exhaust gas temperatures and oxygen displacement but generated soot, CO, and HC. Pedrozo et al. [105] experimented on a single-cylinder heavy-duty diesel engine under 0% and 25% EGR to investigate the potential of ethanol-diesel dual-fuel combustion and reported that 25% EGR proved effective in reducing NOx emissions by almost 80% but increased HC and CO emissions. Talibi et al. [106] experimented on a DI diesel engine with a H_2-diesel fuel to explore the emission and combustion characteristics using EGR and found that H_2 reduced CO_2 and particulate emissions and at high EGR 75% reductions in exhaust particulate mass were observed. Feng et al. [107] experimented on a modified six-cylinder DI diesel engine to test the effects of EGR on emission and engine performance of a low-temperature combustion engine and observed that combustion was reduced with the increase in EGR rates. It was concluded that HC and CO levels increased with the increase in EGR but opposing trend was seen in the case of NOx which reduced with an increase in EGR. EGR working can be seen in Figure 4.

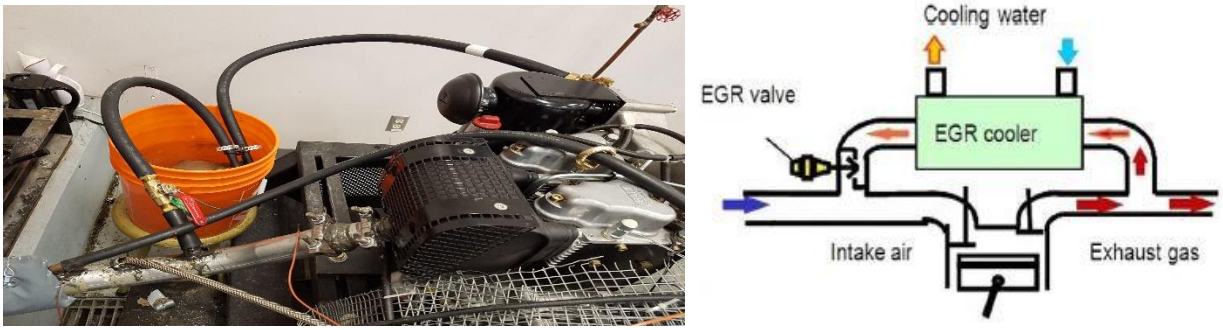

(a) (b)

Figure 4: (a) Pictorial and (b) Schematic Working [108] of the EGR System

2.7 THESIS OBJECTIVE

Most researchers in the past have focused their attention on the use of biodiesel as an alternative fuel which has many benefits to emerge as a possible fuel, but there are certain downsides observed with its usages such as the problem of cold flow and the rise in NOx emissions. It has also raised an environmental concern with the dumping of significant amount of crude glycerine as its by-product and has also adversely affected the prices of glycerine in the

market. However, there have been certain studies done on the utilization of crude glycerine as combustion fuel but due to the impurities present in crude glycerine decrease its solubility and emit harmful emissions and which is why it has eluded to be perceived as an alternate to fossil fuel. In the present study purified glycerine was used to prepare emulsion fuels and its performance and emissions were investigated on two different engines and compared with water emulsion. The blends used were B0, B20, B50, and B100 with 5% and 10% of water and glycerine. Furthermore, partially cooled exhaust gas re-circulation system was installed to control NOx emissions and to see its effects on other emission and engine performance.

CHAPTER 3: METHODOLOGY

3.1 INTRODUCTION

In this chapter, methods and processes used in the experiment are discussed. Firstly, the process of making biodiesel with canola oil through transesterification process and its blends with diesel will be discussed followed by the process of purification of crude glycerine. Furthermore, the process of emulsification will be elaborated which was used to prepare emulsion with water and purified glycerine. Additionally, the use of self-installed EGR will be discussed to test all fuel blends including their emulsion. Lastly, the test engines and the whole procedure of testing will be discussed with measuring apparatus.

3.2 BIODIESEL PRODUCTION

3.2.1 Transesterification

The method used for producing biodiesel (also known as FAME) is known as transesterification method which is most commonly used in everyday life. Presence of glycerides can increase viscosity and its stickiness [23]. This method was used because it is the most efficient method used to reduce the viscosity of the biofuel [10], [23] and also, due to its low production cost and simple process [67], [109]. Triglycerides from the oil were mixed with methanol (alcohol) with the help of the acidic catalysts, sodium hydroxide (NaOH) to form FAME and glycerine as its by-product (BD with sources). Methanol was used, due to its low cost and excellent reaction rate [110]. Minimum of 96.4% esters should be present in the biodiesel w.r.t ASTM D6751 standards [23].

3.2.2 Biodiesel Production Process

Chemicals, such as methanol and sodium hydroxide pellets were taken from the chemistry lab of Lakehead University and Canola oil from the local grocery store. Canola oil was used because of the local produce and high yield in Canada due to the favorable climate present for its production. Biodiesel production started with the process called transesterification, in which vegetable oil was mixed with the solution of methanol and sodium hydroxide (catalysts). There are three types of catalysts which can be used, i.e., alkaline or enzymes [23], [111]. Alkaline catalysts are considered more favorable due to its fast and moderate reaction, but the only problem with using it is that it produces soap which decreases the yield of biodiesel. Ethyl esters can also be formed instead of methyl esters by using ethanol. However, methyl esters are mostly preferred over ethyl esters because of the economical cost and common availability of methanol as compared to other alcohols [112]. Methyl esters were chosen because it generates better engine performance, torque, and power [110] which is because of the fact that methyl esters have a slightly lower viscosity than ethyl esters [112].

Transesterification reaction is summarized in Figure 5 and Figure 6 representing the steps for biodiesel production:

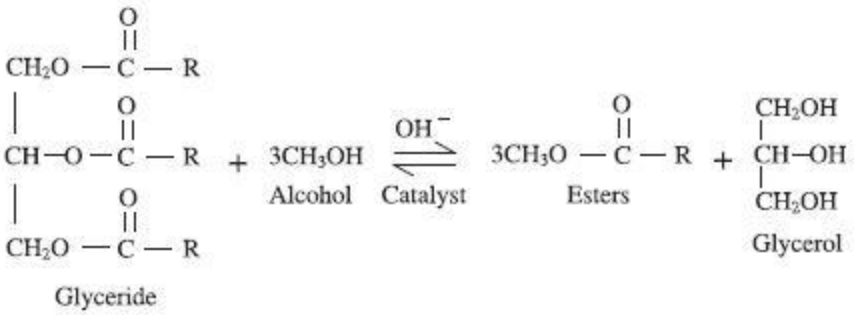

Figure 5: Transesterification Process Reaction [68]

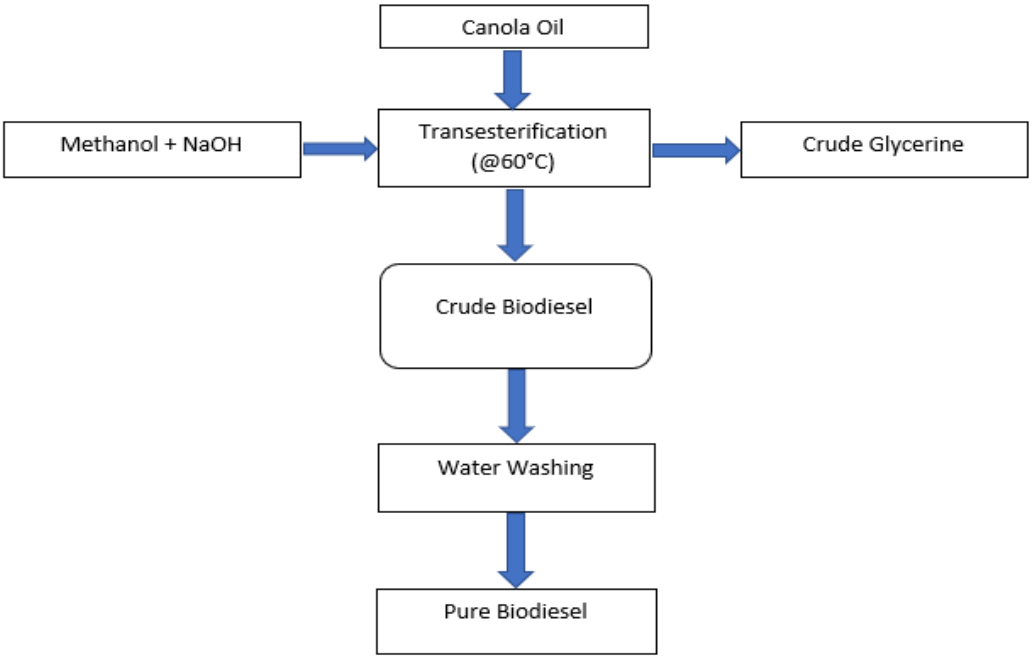

Figure 6: Steps to Produce Biodiesel

Steps for the production:

1. Both chemicals, methanol and sodium hydroxide (alkaline catalysts) were mixed in the proportion of 200 ml and 3.5 gm respectively. These both chemicals were placed in the air-tight container and stirred properly until they were mixed well.
2. Methanol has a boiling point of 65°C, so canola was heated to 60°C and then mixed to the chemical solution. It was heated to activate the molecules of the canola oil which helps in proper mixing.
3. This mixture was placed in the blender at high speed for at least 1 hour, speed is critical for the proper mixing and blender cap should be tight enough to stop the leakage or evaporation of the mixture.
4. After mixing in the blender, single phase yellowish-opaque fluid was obtained.
5. The mixture was placed in a bottle and left for minimum of 12 hours

6. Catalyst breaks the fatty acids of triglycerides of the oil with methanol and to change into methyl ester and glycerine.
7. When kept for 12 hours, 2-phase solution was visible. The upper solution was biodiesel, and lower was glycerine. This difference is due to the difference in their densities, which can be seen in Figure 7 (a).
8. The above solution (biodiesel + little impurities) was poured into another bottle carefully without disturbing the glycerine.
9. The next step was washing the crude biodiesel for its purification which was done twice. Removal of the impurities like soap and other chemicals was done.
10. 500 ml of water was taken for the first washing and was added to the crude biodiesel. The mixture was shaken well for 5-10 minutes. The milky color fluid was observed and left for another day, which can be seen in Figure 7 (b).
11. After a day, 2-phase solution was seen with biodiesel on the top and fatty acids on the bottom due to its high density. Biodiesel was then separated from the fatty acids by pouring it carefully into another bottle.
12. Second washing of the biodiesel was done with 300 ml of water, and the same procedure was employed and left for another day.
13. Afterwards, the purest form of biodiesel was seen along with water and minimal impurities at the bottom (if present any), as seen in Figure 7 (c).
14. Finally, the biodiesel after extraction was heated up to 70-75°C for at least 30-45 minutes, to evaporate impurities like methanol and water to increase its efficiency. And, its final color was reddish-yellow.

The quality of the biodiesel was tested according to the ASTM D6751 standards which can be seen in the Table 1.

Table 1: Properties of Pure Canola Biodiesel

Test name	**Test method**	**ASTM limit**	**Results**
Free Glycerine (mass%)	ASTM D6584	Max. 0.02	0
Total Glycerine (mass%)	ASTM D6584	Max. 0.24	0.112
Flash Point, closed cup (°C)	ASTM D93	Min. 130	169
Water & Sediment (vol.%)	ASTM D2709	Max. 0.050	0
TAN (mg KOH/g)	ASTM D664	Max. 0.5	0.14
Sim. Dist., 50% recovery (°C)	ASTM D2887	N/A	359.8
Cetane Index	ASTM D976 (2 variable formula)	N/A	50
Copper Corrosion 3h @ 50°C (rating)	ASTM D130	Max. 3a	1a

(a)

(b)

(c)

(d)

Figure 7: Various Steps in the Production of Biodiesel (a) Crude Biodiesel with Crude Glycerine (b) Biodiesel on First Wash (c) Separation after Second Wash (d) Pure Biodiesel

3.3 CRUDE GLYCERINE

From the production of biodiesel, it has been noted that approximately $1/10^{th}$ of the total biodiesel production is its by-product i.e. crude glycerine (figure 8). Crude glycerine consists of various impurities like salt, water, alcohol, some chemicals.

Figure 8: Crude Glycerine

Due to expensive purification cost, crude glycerine has been successfully used in its crude form in various areas such as anaerobic digestion, animal feeds, composting and also in combustion due to its heating value [93], [96]. However, glycerine has a low auto-ignition quality, and heating value and high ignition temperature and also its burning can result in the production of carcinogenic acrolein [17], [113], [114] and ash-related problems which makes its use unfeasible in combustion engines. Therefore, there is need to for its purification.

3.4 CRUDE GLYCERINE PURIFICATION

For the emulsion fuel preparation purified glycerine was used as crude glycerine has various impurities, for example, salt, water and alkaline catalyst that can lessen the stability of bio-oil glycerine emulsion to less than an hour [115]. The cleaning of crude glycerine can initiate an increased level of droplet evaporation time and the use of desalting can help in reducing ash-related problems [116].

The method of acidification and desalting was used to purify crude glycerine. In acidification process, 5.85% phosphoric acid (H_3PO_4) solution was added in the crude glycerine until the desired value of pH approximately 5-6 was achieved. The first step was to obtain the phase separation of the impurities and fatty acids from glycerine rich phase and to reach the maximum yield of 81.2% and for this the solution was kept at the temperature of 70°C for 60 mins.

The next step was to further remove the residual impurities from the semi-glycerine product which involved the reaction of glycerine with 0.03% sodium oxalate solution at 80°C for 30 mins to attain the impurities removal rate of 19.8%. Furthermore, by using the process of distillation, the purified glycerine (98.10%) was separated from crude glycerine, while maintaining the temperature between 164°C-200°C. Lastly, the process of decolorization was carried out using 2% activated charcoal twice at 80°C. This process of purification is known as Orthogonal Test Method [117], as shown in Figure 9; and Figure 10 is the pictorial view of the purification process.

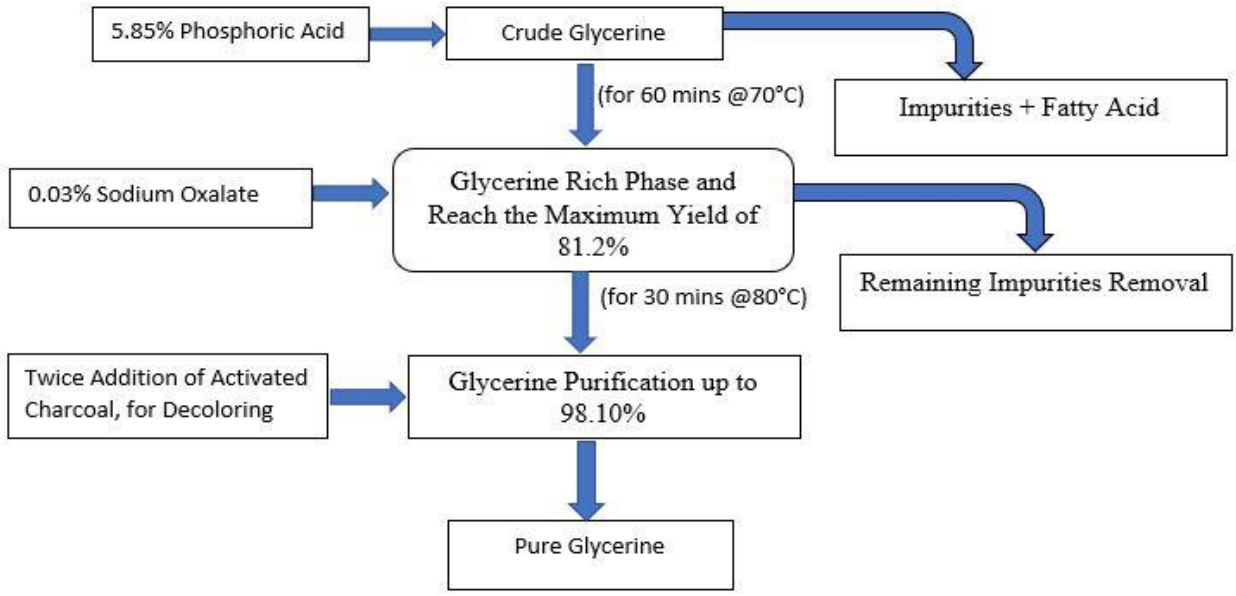

Figure 9: Steps for the Purification of Crude Glycerine

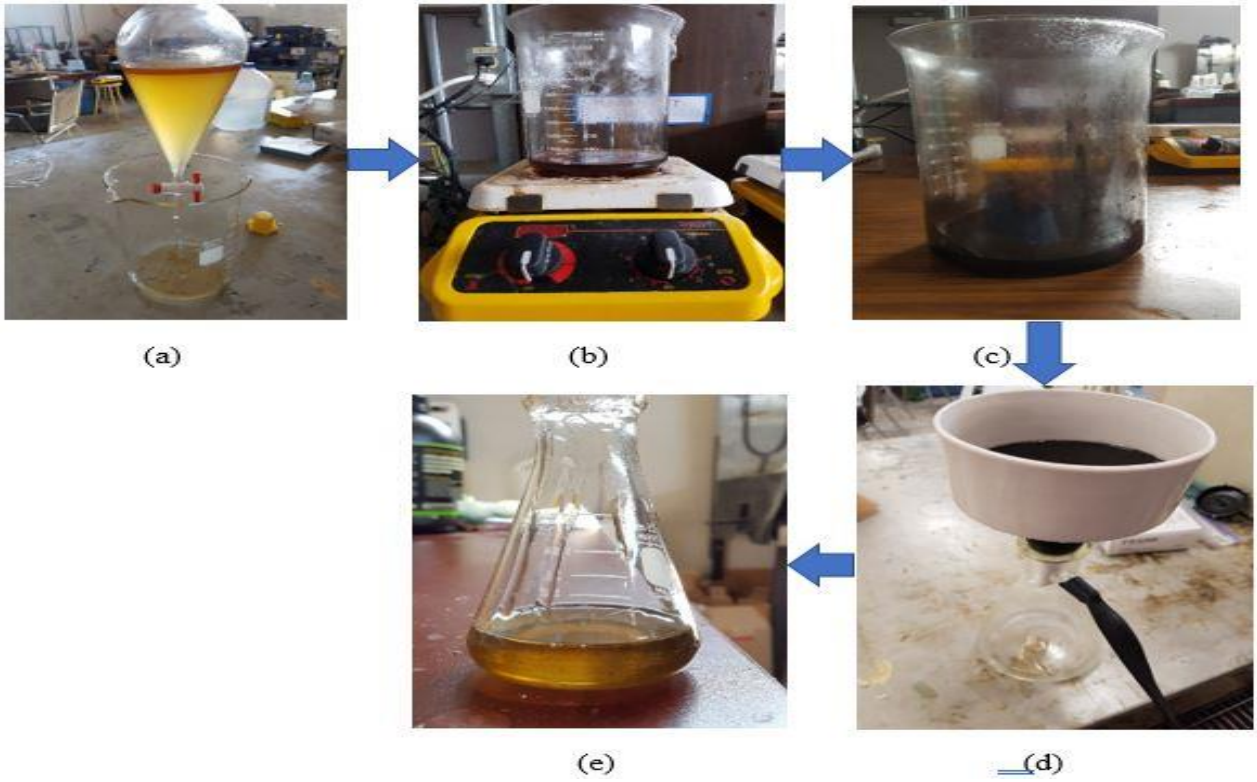

Figure 10: Pictorial View of the Crude Glycerine Purification Steps (a) Separation of Impurities (b) Heating the Glycerine to 80°C (c) Addition of Charcoal (d) Collecting Pure Glycerine (e) Pure Glycerine after 1st Decoloring and it is 98.10% Pure

3.5 EMULSION FUEL PREPARATION

For the preparation of emulsification process different materials were used which were: low sulphur diesel, biodiesel, Tween 80 (Polyoxyethylene Sorbitan Monooleate) and Span 80 (Sorbitan Monooleate), distilled water, purified glycerine and standard blender. A total of 18 emulsions were prepared 9 of which were water emulsion fuels and other nine comprised of glycerine emulsion fuels. To ensure the stability of emulsion fuels a suitable HLB surfactant is required which was identified to be 6.4 for B0, B20, B50 and 5.3 for B100 in case of glycerine emulsion and 8 for B0, B20, B50 and 5.9 for B100 in case of a water emulsion. Two-phase emulsion (Figure 11) was preferred for producing emulsion fuel. All emulsion fuels with their names are shown in Table 2.

The formula used to calculate the HLB value was as follows [79]:

$$\%\text{Tween } 80 = \frac{100(X - \text{HLB}_{\text{Span } 80})}{\text{HLB}_{\text{Tween } 80} - \text{HLB}_{\text{Span } 80}} \quad \ldots\ldots\ldots (3)$$

$$\%\text{ Span } 80 = 100 - \%(\text{Tween } 80) \ldots\ldots\ldots (4)$$

X is the required HLB according to the emulsion.

HLB of the used surfactants was:

Tween 80 = 15, Span 80 = 4.3 [79]

Steps for the emulsification:

1. External force method was used for the preparation of emulsion fuel with the help of a blender.
2. The required amount of fuel was taken in the blender.
3. Distilled water and purified glycerine were added to the fuel at the rate of 50 ml/min -60 ml/min (1 and 49 from my paper).
4. Next step, was to add the surfactant of the required HLB at the rate of 1.25 ml/min.
5. The blender was run for 15 mins, to reduce the droplet size and surface tension which helps to improve the stability of emulsion fuel [74], [118].
6. These steps were used for B0, B20, and B50.
7. For B100 emulsification, biodiesel was heated to 65°C to increase the stability [115] and then added to the blender. Rest of the procedure remained the same.
8. The milky color fluid was prepared which is known as the emulsion fuel.

5% and 10% of the water and glycerine were used for producing emulsion fuels. 2.5% of water and glycerine were also used but only for B100.

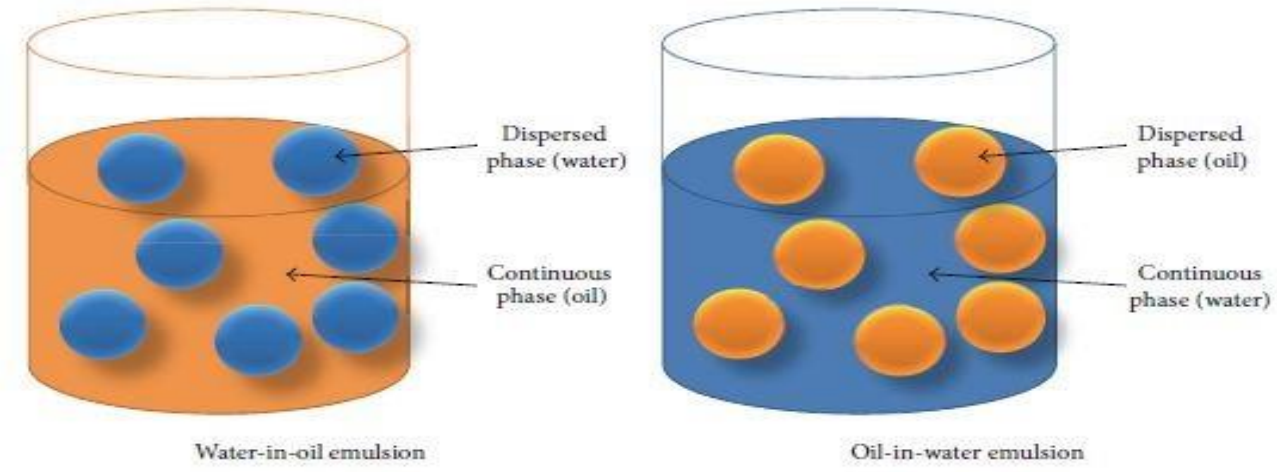

Figure 11: Pictorial View of the Two-Phase Emulsion [119]

Table 2: Fuel Blends with Their Emulsions

Pure Fuel	
B0	Pure 100% diesel
B20	20% biodiesel in diesel-biodiesel blend
B50	50% biodiesel in diesel-biodiesel blend
B100	Pure 100% biodiesel
Water Emulsion	
B0W5%	Pure 100% diesel with 5% water
B0W10%	Pure 100% diesel with 10% water
B20W5%	20% biodiesel in diesel-biodiesel blend with 5% water
B20W10%	20% biodiesel in diesel-biodiesel blend with 10% water
B50W5%	50% biodiesel in diesel-biodiesel blend with 5% water
B50W10%	50% biodiesel in diesel-biodiesel blend with 10% water
B100W2.5%	Pure 100% biodiesel with 2.5% water
B100W5%	Pure 100% biodiesel with 5% water
B100W10%	Pure 100% biodiesel with 10% water
Glycerine Emulsion	
B0G5%	Pure 100% diesel with 5% glycerine
B0G10%	Pure 100% diesel with 10% glycerine
B20G5%	20% biodiesel in diesel-biodiesel blend with 5% glycerine
B20G10%	20% biodiesel in diesel-biodiesel blend with 10% glycerine
B50G5%	50% biodiesel in diesel-biodiesel blend with 5% glycerine
B50G10%	50% biodiesel in diesel-biodiesel blend with 10% glycerine
B100G2.5%	Pure 100% biodiesel with 2.5% glycerine
B100G5%	Pure 100% biodiesel with 5% glycerine
B100G10%	Pure 100% biodiesel with 10% glycerine

3.6 MEASUREMENTS OF THE IMPORTANT PROPERTIES OF FUELS

3.6.1 Viscosity: It is defined as the resistance to the flow of fluid.

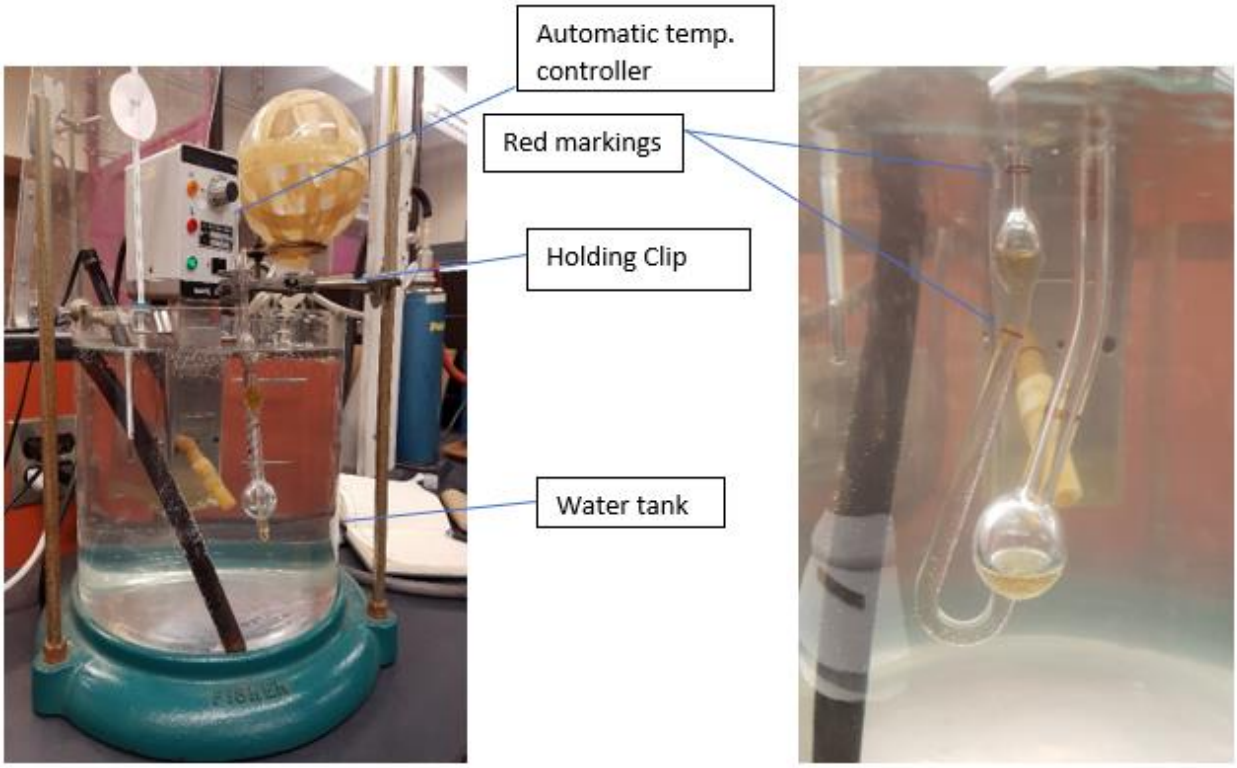

Figure 12: Setup for the Viscosity Test

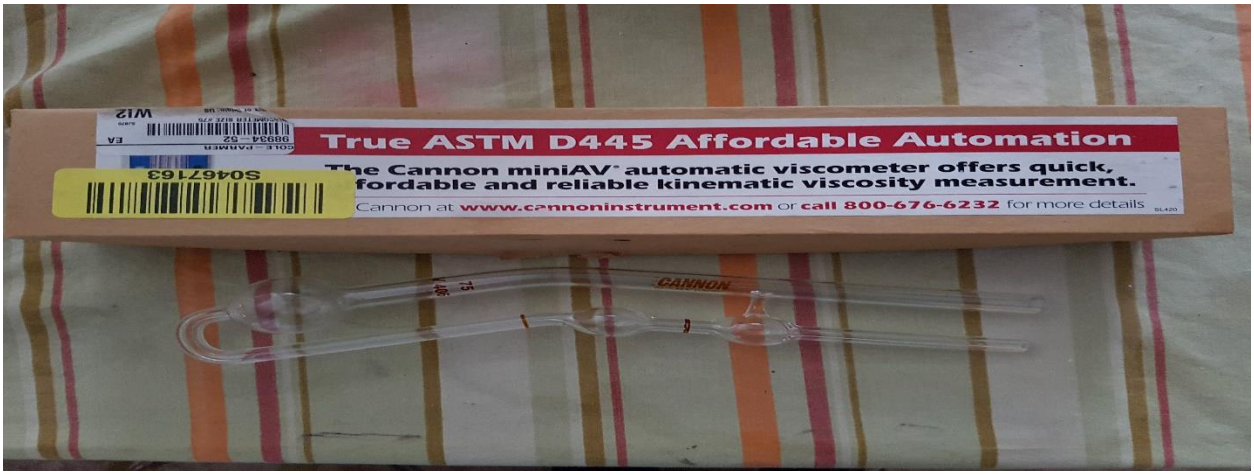

Figure 13: Kinematic Viscometer

The measurement of the viscosity was done with the help of viscometer named Ostwald viscometer, as seen in figure 12 It helps in measuring the kinematic viscosity of the fuel. According to the ASTM D445 standards, the fuels were measured at 40°C [120].

Steps for the measurement:

1. Things required were fuel, stopwatch, Ostwald viscometer, water tank and pump.
2. Firstly, the water tank was taken which had an automatic water heater with temperature reading on it fitted in it, and which helped to heat up the water up to 40°C as required. Moreover, it should be kept constant according to the standards.
3. The viscometer is a u-shaped device, with one side having a wider opening and the other with narrow as shown in Figure 13.
4. The viscometer was fixed in the tank with the help of the holding clip.
5. Around 80-85% of the viscometer should be placed inside the water, with both opening outside.
6. The viscometer was filled with fuel with the help of suction pump for testing its viscosity.
7. Two red line markings were present on the viscometer, on the narrow opening side (one above and one below the bulb).
8. These markings were made to calculate the kinematic viscosity.
9. The fuel was pumped over the lower red mark to a little higher than the top red mark.
10. The pump was removed immediately when it crossed the top red mark, and the fuel was allowed to come down till reached the lower red mark.
11. The stopwatch was turned on when it reached the top red mark (mark above the bulb), and the timing was recorded till it reached the lower red mark (mark below the bulb).
12. Lastly, the kinematic viscosity of the sample fuel was calculated.

3.6.2 Density: It can be stated as the mass per unit volume.

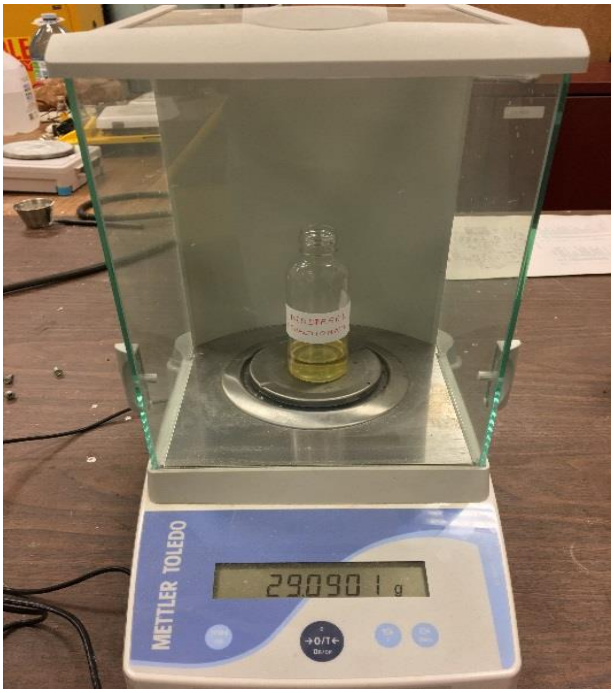

Figure 14: Weighing Machine

Density was another essential property of the fuel to be measured. Below are the steps used to find the density.

1. Materials to be used were collected such as fuel, small empty bottle, weighing machine.
2. Weighing machine was set to 0 at the initial stage. Weighing machine can be seen in Figure14.
3. An empty plastic bottle was placed at the weighing machine, and the weight was set to be zero.
4. For the next step, 100 ml of the fuel was poured into the plastic bottle, and then its weight was recorded.
5. The weight and volume were recorded were used in the formula below, to find the density of the fuel.

$$\text{Density} = \text{mass (g)}/\text{volume}(\text{cm}^3) \quad \ldots\ldots\ldots (5)$$

3.6.3 Heating Value: The quantity of heat produced at the time of the total combustion of the unit mass of fuel. The procedure was completed according to the ASTM standards set for measuring heating value. It was measured with the help of calorimeter which can be seen in Figure 15.

(a)

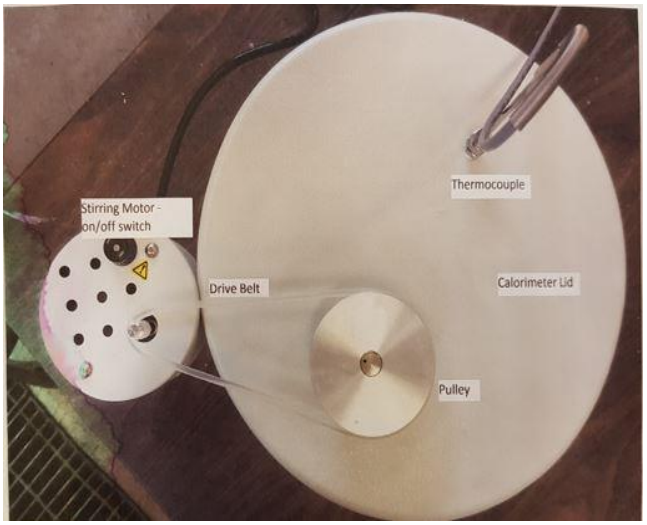

(b) (c)

Figure 15: (a) Bomb Calorimeter (b) Top View of Calorimeter (c) Bomb

Procedure:

1. A bucket was filled with 2L of distilled water and carefully put in the calorimeter without spilling any water.
2. The empty combustion was put on the scale, and tare was pressed to bring the scale to zero.
3. The combustion capsule is filled approximately 0.6 g of the chosen fuel sample.
4. The bomb head was then put on the support stand, and the capsule was placed on the ring.
5. After that, a fuse wire of 10cm was pulled through the eyelets keeping sufficient slack to dip the wire into the chosen fuel or at least touch the surface.
6. The bottom of the bomb was filled with 1 ml of water.
7. The bomb head was carefully put the chosen fuel into the top of the bomb to avoid any spill any of the fuel, and the cap is threaded tightly.
8. The regulator was then set on the oxygen tank to a point to allow enough room for the needle just to move.
9. The oxygen hose was attached to the bomb inlet valve.
10. The bomb was filled with oxygen for 30 seconds before closing the purge valve.
11. The regular was then set to 35 atmospheres, and the large oxygen bottle was closed, and the air in the hose was released using the valve on the regulator.
12. The bomb was then placed into the bucket, which was already set in the calorimeter and the ignition wire was attached to the bomb.
13. The top of the calorimeter was manually closed after removing the tong.
14. The pulley was connected to the stirring motor using the drive belt, and the stirring motor was switched on.
15. The unit was then run was 4-5 minutes before turning on the thermocouple.
16. The starting temperature was noted, and the ignite button was pressed for 5 seconds.
17. The red light would light up for ½ second.
18. The temperature was recorded every minute until it had reached its peak and leveled out.
19. The stirring motor was then turned off, and the drive belt was removed.
20. The lid and the bomb were removed, and the gas was slowly released from the bomb using the exhaust valve.
21. After unscrewing the cap, bomb head was removed and placed on the support stand.
22. The interior of the bomb was examined for any soot of incomplete combustion.
23. Clips were removed to release any unburned wire, and all the unburnt pieces were lined up, and the total length was added.
24. The starting length was subtracted from that length to determine the length of ignition wire that was burnt.
25. The following equation was used to determine the gross heat of the combustion:

$$H_g = \frac{(t*W)-(e*3)}{m} \quad \ldots\ldots\ldots\ldots\ldots (6)$$

t = change in temperature

W = energy equivalent of the calorimeter in calories per degree C

e3 = burned wire length * 2.3 calories per cm

m = mass of fuel tested

3.7 PARTICLE/DROPLET SIZE DISTRIBUTION OF FUEL

The experiment was conducted by using Malvern Mastersizer 2000 instrument which utilizes laser diffraction to measure particle size, shown in Figure 16. The sample was mixed with distilled water and was then poured into the hydro 2000S wet cell attachment where the suspension was used to pump and stir the liquid into the measuring zone, and it was then measured using the v.5.54 software after which the liquid was circulated back for continuous measurement. The obscuration level was measured to be around 15% [121]. The refractive index used in the measurement was 1.4565 [122]. Olympus IX51 inverted microscope was used to take the pictures of the emulsion fuels' droplet size as seen in Figure 17.

Figure 16: Malvern Mastersizer Hydro 2000S to measure the droplet size of the particle

Figure 17: Olympus IX51 Inverted Microscope

Table 3 describes the fuel samples used for the testing along with their fuel properties according to the ASTM standards. Testing was done in the mechanical laboratory of the Lakehead University.

Table 3: Fuel with their Properties

Fuel	Heating Value (kJ/kg)	Density (kg/m^3)	Viscosity (cSt @ 40°C)		
B0	45,124	838	1.87		
B20	44,219	845	2.29		
B50	42,860	856	2.87		
B100	40,597	875	4.23		
Water Emulsion	Heating Value (kJ/kg)	Density (kg/m^3)	Viscosity (cSt @ 40°C)	Stability (days)	Diameter (µm)
B0W5%	41,965	850	2.22	58	4.3
B0W10%	39,709	856	2.59	43	6.3
B20W5%	41,123	857	2.62	46	7.9
B20W10%	38,912	864	3.1	37	9
B50W5%	39,860	867	3.63	73 (hrs)	11.2
B50W10%	37,717	874	4.14	44 (hrs)	13.6
B100W2.5%	38,770	881	4.69	23 (hrs)	9
B100W5%	37,755	884	4.81	20 (hrs)	13.3
B100W10%	35,725	890	5.66	11.5 (hrs)	15.5
Glycerin Emulsion	Heating Value (kJ/kg)	Density (kg/m^3)	Viscosity (cSt @ 40°C)	Stability (hours)	Diameter (µm)
B0G5%	42,948	858	2.43	70	4.6
B0G10%	41,675	874	2.71	58	6.8
B20G5%	42,106	864	3.01	59	8.1
B20G10%	40,878	880	3.33	41	10.1
B50G5%	40,843	875	3.77	29	12.4
B50G10%	39,683	890	4.45	25	16.1
B100G2.5%	39,262	886	4.84	26.5	9.5
B100G5%	38,738	893	5.22	18	16.2
B100G10%	37,691	907	5.86	11	19.2

3.8 WORKING OF PITOT TUBE AND MANOMETER

It is an instrument used to measure the fluid flow velocities using pressure difference, i.e. the difference between the total pressure and the static pressure as shown in Figure 18. From the difference, the velocity pressure is determined which helps to obtain the air velocity.

The tube was inserted into the hole pointing towards the airflow. The hole parallel to the air flow was used to measure the total pressure (p_t) and a small hole on the pitot tube which rested

vertical to air flow measured the static pressure (p_s). The difference in these pressures i.e. the, velocity pressure was indicated by the manometer and then the readings obtained can be converted into velocity.

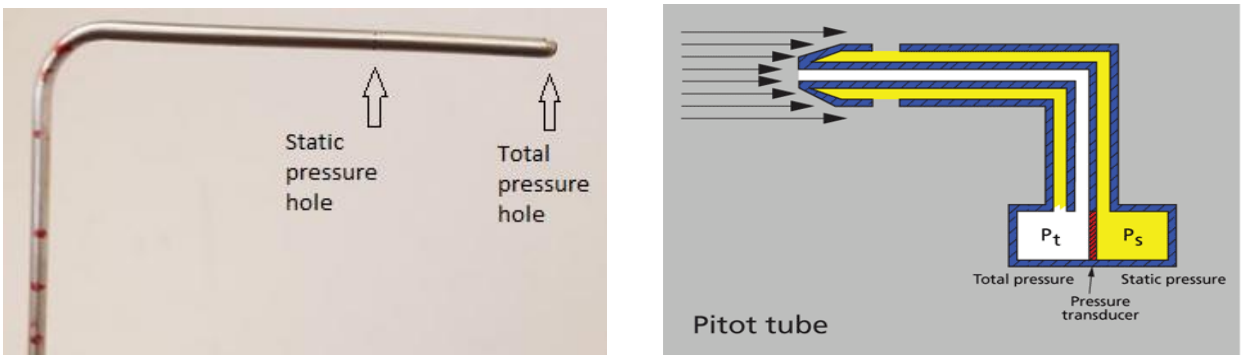

(a) (b)

Figure 18: (a) Marking of two different pressure collecting points (b) Diagram of Pitot Tube

For the measurement of the velocity pressure of the circular duct, log-linear rule shown in Figure 19 was applied. Seven different points were taken from the linear log rule, and the circular duct diameter and the velocity pressure was measured at each point, and later the average was taken using these values. To take accurate reading, it is vital to remove turbulence and for accurate measurement of the flow, pitot tube must be inserted at least 7.5D-10D duct diameters away from the bends and elbows.

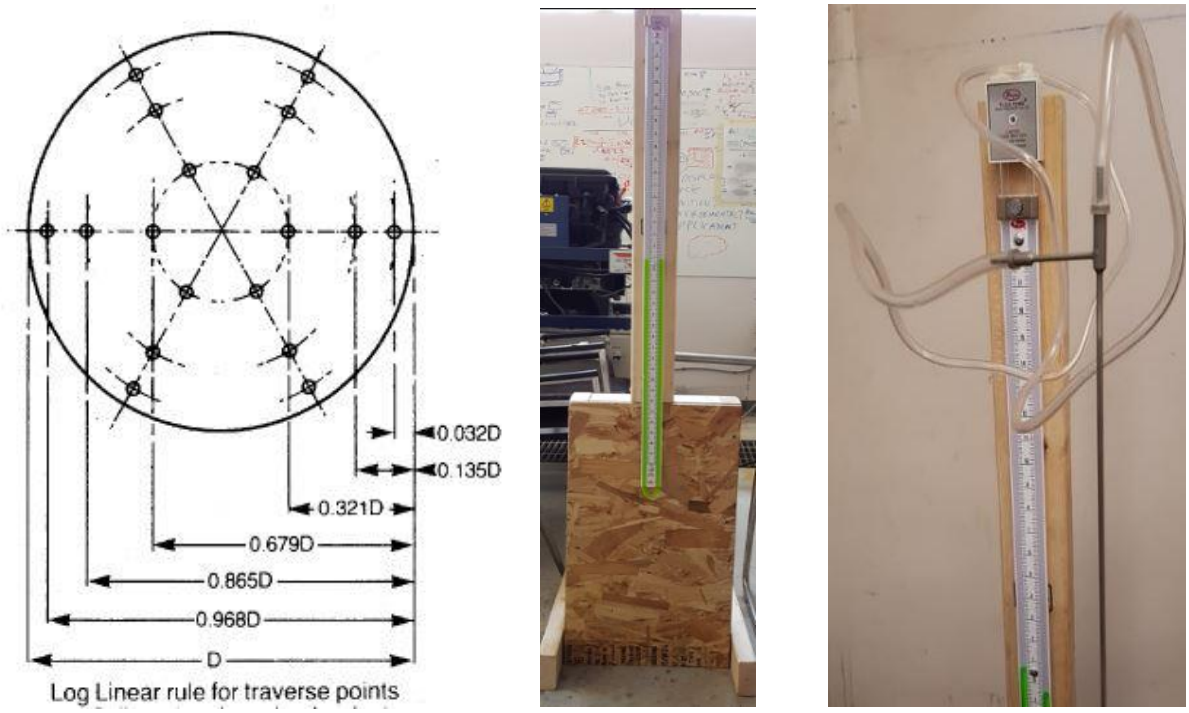

(a) (b) (c)

Figure 19: (a) Log-Linear Rule for Circular Duct (b) Manometer (c) Pitot Tube Working

3.9 EGR CALCULATION

Known things (calculated in lab):

Fuel used is B0, which has a density of (ρ_f)= 838 kg/m^3

Diameter of the air inlet circular duct= 46mm = 0.046m

Area of the circular duct (A) = 0.0016619 m^2

Density of the manometer liquid (ρ_l) = density of the water (ρ_w) = 1000 kg/m^3

Density of the air @ 25°C (ρ_a) = 1.184 kg/m^3

$$\rho = \rho_l/\rho_a$$

Acceleration due to gravity = 9.8 m/s^2

Used equation to calculate EGR%:

$$\text{EGR \%age} = \left(\frac{\text{Mass of air without EGR}_{\text{intake}} - \text{Mass of air with EGR}_{\text{intake}}}{\text{Mass of air without EGR}_{\text{intake}}}\right) * 100 \quad \ldots\ldots. (7)$$

This calculation was taken at 2100 rpm and low load condition:

Calculation 1: Mass of air without $\text{EGR}_{\text{intake}}$:

1. With the help of the manometer, the deflection in height (Δh) was noted at 7 different points, which is due to the pressure difference between static and total pressure, and then the average height is taken. These 7 values are determined as D1, D2, D3, D4, D5, D6, D7. The average deflection height (Δh) noticed was 0.00583 m.
2. The velocity of the inlet air V = $\sqrt{2 * g * \rho * \Delta h}$ = 9.822754 m/s
3. Next is, volumetric flow rate (Q) = V*A = 9.82*0.0016619 = 0.016324 m^3/s
4. mdot of intake air is calculated = Q* ρ = 0.01632*1.184 = 0.019328 kg/s
5. Fuel consumption (F.C) is noted = 11.21 ml/min
6. mdot of F.C in kg/s = ((F.C (ml/min)/60) *10^-6) *ρ_f = ((11.82/60) *10^-6) *838 = .00015657 kg/s
7. Total mdot = 0.019328+0.00016509 = 0.019485 kg/s

Calculation 2: Mass of air with $\text{EGR}_{\text{intake}}$, when the valve is full open:

1. The average deflection height (Δh) observed was 0.0045 m
2. Velocity of inlet air = V = $\sqrt{2 * g * \rho * \Delta h}$ = 8.6309 m/s
3. Q = 8.63*0.0016619 = 0.0143 m^3/s
4. mdot of intake air is calculated = Q* ρ = 0.0143*1.184 = 0.016983 kg/s
5. Fuel consumption (F.C) is noted = 11.84 ml/min
6. mdot of F.C in kg/s = ((F.C (ml/min)/60) *10^-6) *ρ_f = ((11.84/60) *10^-6) *838 = .0001654 kg/s
7. Total mdot = 0.016983+0.0001654 = 0.017148 kg/s

Putting the both total mdot values in the equation above, EGR% was calculated which came out to be 11.99%.

EGR % at each speed and load is calculated through this formula:

Table 4: EGR % of Each Load and rpm

EGR %, when the valve is half open:

Speed	Loads		
	Low Load	Medium Load	High Load
1000 rpm	2.51%	4.13%	5.77%
2100 rpm	7.20%	8.52%	9.75%
3000 rpm	8.08%	10.09%	12.36%

EGR %, when the valve is full open:

Speed	Loads		
	Low Load	Medium Load	High Load
1000 rpm	7.62%	8.72%	9.93%
2100 rpm	11.99%	13.86%	15.58%
3000 rpm	12.77%	15.43%	17.94%

Another method to find the EGR rate [59], [100], [123]:

$$\text{EGR rate} = \frac{CO_{2\,(\text{intake})} - CO_{2\,(\text{atm})}}{CO_{2\,(\text{exhaust})} - CO_{2\,(\text{atm})}} \quad \ldots\ldots\ (8)$$

According to this formula, EGR% was 12.5% at 2100 rpm and low load conditions. The EGR% calculated by both the methods was found to be almost similar.

3.10 ENGINES UNDER STUDY & TEST PROCEDURE

3.10.1 Engines Under Study

Two different types of engines were used for testing.

a. **First Engine (Heavy- Duty Engine):** Cummins 4-cylinder turbocharged diesel engine with a high-pressure common-rail injection system shown in Figure 21. Cooled EGR, diesel particulate filter, diesel oxidation catalyst has already been introduced with this engine. It was also named as a heavy-duty engine because they are used for heavy loads like mining, agricultural purpose, industrial purpose and construction. Testing was done at idling load under cold start conditions at two different rpms, i.e., 1000 rpm and 1500 rpm. For the cold start, the engine was left to cool down than its normal operating temperature (i.e. below 25℃) and the time gap between the two tests was approximately 5-6 hours to facilitate the cold start. The experimental setup was explained in the schematic diagram in

Figure 20. The dual tank was another important installation in the engine for the change of fuel blends with disturbance. Table 5 below presents heavy-duty engine specification:

Table 5: Engine Specifications for Cummins Engine

Engine Make & Model	Cummins QSB 4.5 T4I
Engine Type	Inline 4-Cylinder
Number of Cylinders	4
Bore/Stroke	102mm/138mm
Displacement	4.5L
Compression Ratio	17.3:1
Rated Power	97 kW @ 2300 rpm

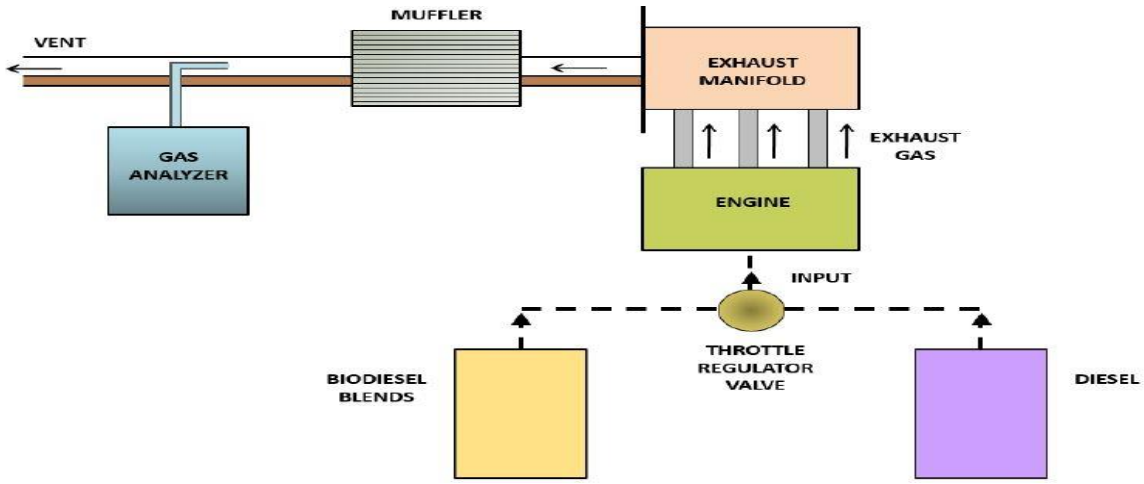

Figure 20: Schematic Diagram of Heavy-Duty Cummins Engine

Figure 21: Cummins Engine Testing Setup

b. **Second Engine (Light-Duty Engine)**: Another engine used for testing the fuel was the air-cooled 2-cylinder, 4-stroke HATZ 2G40 diesel engine. Testing was done on various loads and speeds which were done through the installation of the dyno-meter. Below are the Figures 22 and 23 showing the schematic diagram of the engine setup and light duty test engine, along with the Table 6 telling about the specifications of the engine.

Table 6: Engine Specifications of the HATZ Engine

Engine Make & Model	HATZ 2G40
Engine Type	Four – stroke, air – cooled
Number of Cylinders	2
Bore/Stroke	92mm/75mm
Displacement	997cc
Compression Ratio	20.5:1
Fuel Injection Timing	8°BTDC (≤2250 rpm); 10°BTDC (≥2300 rpm)
Fuel Injection Pressure	26 MPa
Continuous Max. Rated Power	13.7 kW @ 3000 rpm
Maximum Rated Power	17 kW @ 3600 rpm

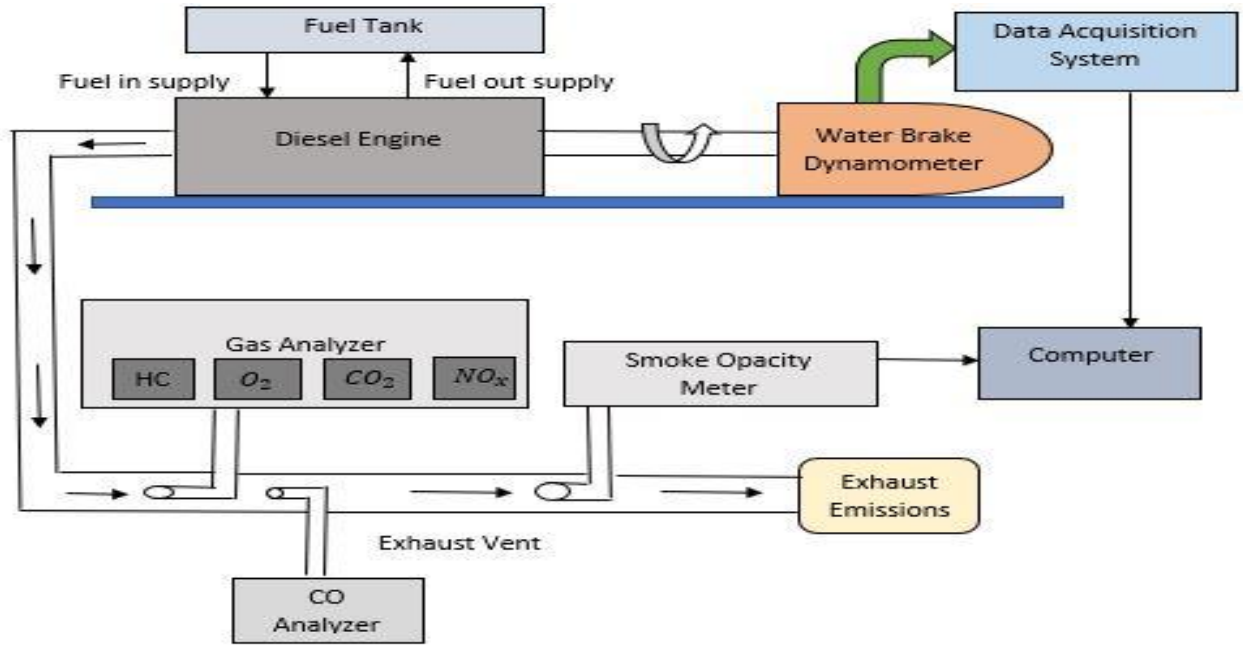

Figure 22: Schematic Diagram of HATZ Engine

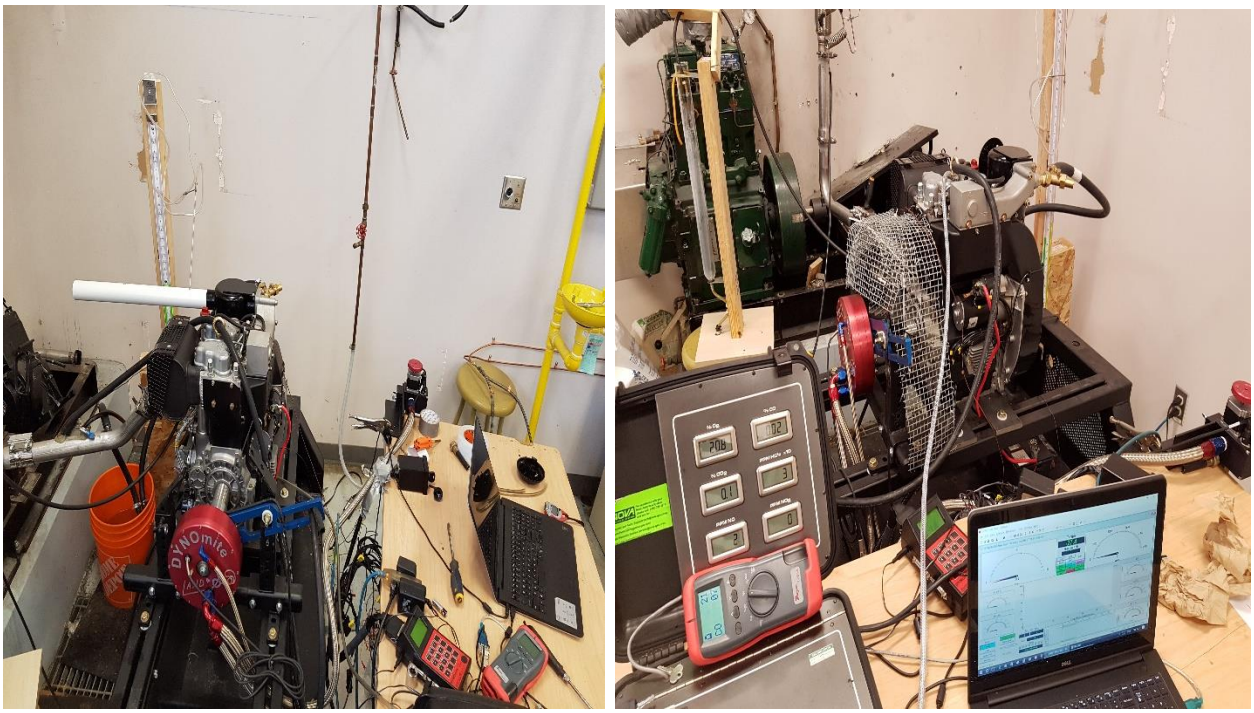

Figure 23: HATZ (Light duty) Engine Test Setup

3.10.2 Test Procedure

Testing was done mainly to perform two tasks, i.e., to know the engine emissions and its performance. This testing was done by using different fuel samples which are the blends of the diesel and biodiesel. Three different sets of fuels were used. First set was the pure fuels B0, B20, B50, B100. Second set was pure fuels with water (water emulsion) with two different water percentages (5% and 10%). Third set was pure fuels with purified glycerine (Glycerine emulsion) with glycerine percentage to be 5% and 10%. The new technique which was introduced and installed on the light-duty diesel engine which is EGR (exhaust gas recirculation) system. EGR technique was divided into two sets (half valve open and full valve open) when tested. Fuel blends tested with this technique were B0, B50 and B100 along with water emulsion and glycerine emulsion. Two extra fuels which were tested are B100W2.5% and B100G2.5% (2.5% water and glycerine emulsion with pure 100% biodiesel)

The first engine used for testing was Cummins 4-cylinder (heavy-duty) diesel engine. Cold start experiments were done on this engine at idling condition, which means no load was applied to it. All the fuels were tested on this engine and done at two different rpms 1000 rpm and 1500 rpm to measure the emissions. The time span of each experiment was 30 minutes. Then the emissions were recorded at the required time interval, i.e., at 1, 2, 4, 6, 8, 10, 15, 20 and 30 minutes after the start of the experiment.

The second engine used for testing was HATZ 2G40 2-cylinder (light-duty) diesel engine. Testing was done at three different speeds (1000, 2100, and 3000 rpm). These rpms were selected because 1000 was the minimum speed, 2100 rpm has the maximum torque, and 3000 rpm has the maximum power of the engine. At each speed, three different loads were also tested (low load

which is 25% of the total torque at the operating speed, medium load, i.e., 50% of total torque at that speed and high load which is 80% of the total torque at that speed), and this load was put to an engine through the dynamometer installed on it. So, the test was done on three different loads at three different speeds. Each test on this experiment took around 60-70 minutes, and warm-up time for this engine was around 10 minutes. All the regulated emissions were measured at each load and speed. Emission readings were taken when the reading gets stable.

Regulated emissions needed to be recorded were CO, NOx, HC, and smoke opacity. For measuring these emissions, a NovaGas 7466 PK gas analyzer was used. Another DWYER 1205A analyzer was used to measure CO in ppm (parts per million). Moreover, the third analyzer smoke opacity meter was used to measure the smoke opacity. The Table 7 shows the specifications of the analyzers used to measure emissions:

Table 7: Emission Analyzers Specification

Method of Detection	Species	Measured Unit	Range	Resolution	Accuracy
NovaGas 7466 PK					
Electrochemical/Infrared Detector	CO	%	0-10%	0.10%	±1%
Infrared Detector	CO_2	%	0-20%	0.10%	±1%
Electrochemical	NO	ppm	0-2000 ppm	1 ppm	±2%
Electrochemical	NO_2	ppm	0-800 ppm	1 ppm	±2%
Electrochemical	O_2	%	0-25%	0.10%	±1%
Infrared Detector	HC	ppm x 10	0-20000 ppm	10 ppm	±1%
Dwyer 1205A Electrochemical	CO	ppm	0-2000	1 ppm	±5%
ExTech EA10	Temp	0.1°C	(-)200°C-1360 °C	0.1°C	±0.3%
Smart 1500	Opacity	%	0-100%	0.1%	±2%
Smart 1500	Soot Density	mg/m^3	0-10	0.00001	±2%

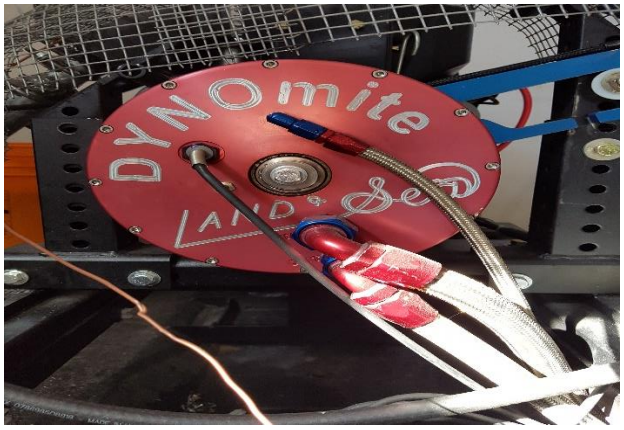

Figure 24: Dynamometer

Dynamometer (Figure 24) is an instrument by which engine's output power can be measured. It was installed on a light-duty diesel engine, which had a wide range of loads (torque), i.e., varying from 2lb/ft to 5000 lb/ft. The load of the dynamometer was controlled using the water-brake load valves. The load can either be controlled manually or with the help of the DYNO-MAX software through computer. The rpm range lay between 1000 rpm to 10000 rpm. The software can be utilized to acquire several parameters of the engine like engine rpm, engine torque, BSFC, BTE, exhaust gas temperature. The formula to calculate BSFC and BTE is discussed below:

BSFC (Brake specific fuel consumption): It is defined as the mass flow rate per unit time. It was represented in g/kWh unit. Fuel consumption was noted manually on the respective load and speed which can be taken from the dyno-max software. The formula of the brake specific fuel consumption is as below:

$$\frac{\text{Fuel Consumption flow rate } \left(\frac{g}{h}\right)}{\text{Brake power (kW)}} = \text{BSFC}\left(\frac{g}{kWh}\right) \quad \ldots\ldots\ldots (9)$$

BTE (Brake thermal efficiency): It is defined as the ratio of heat energy equivalent to 1 kWh to the heat energy produced in fuel per B.P. hour. The formula of brake thermal efficiency is written as:

$$\left(\frac{3600}{\text{BSFC} * \text{H.V}}\right) * 100 = \text{BTE\%} \quad \ldots\ldots (10)$$

CHAPTER 4: RESULTS and DISCUSSION

4.1 INTRODUCTION

In this part of the study, we will discuss the characteristics (such as droplet, stability, viscosity, heating value) of two different kinds of the emulsions prepared through diesel-biodiesel with water and diesel-biodiesel with glycerine. Further, we will discuss the emissions of the heavy-duty engine at two different idling speeds and the performances and emissions of the light-duty diesel engine with and without the EGR system.

4.2 EMULSION FUEL CHARACTERISTICS

4.2.1 Emulsion Fuel Droplet Size

A total of eighteen diesel-biodiesel emulsion blends were tested which were prepared with 5 and 10 percentages of glycerine and water concentration. The particle size of the emulsions is illustrated using graphs obtained from the Malvern Mastersizer 2000 as in Figure 25 (a) for glycerine and Figure 26 (a) for water, and the photos were taken using an Olympus IX51 (figure 17) inverted microscope. The particle size distribution graphs for water and glycerine emulsion show a bimodal distribution where two peaks are formed, signifying the different droplet sizes. The bimodal distribution shows that heavier the oil emulsion the bigger will be the droplet size [124]. From the graphs it was also observed that the emulsion fuels contained several smaller droplets which were below 5 μm in diameter. The difference in sizes can be attributed to that fact that when shear stress is added to the emulsion it results in formation of small droplets which may further cause oil/water phase separation.

It can be seen from Figure 25 (a) that the droplet size continued to increase with the increase in biodiesel percentage. It was further observed that the droplet size also increased with the increase of glycerin the reason of which can be attributed to the fact that the addition of the heavier particle will result in enlarging of the droplet size, which improves combustion efficiency [96]. The same trend in the droplet size was noted in case of water as displayed in Figure 26 (a). The trend for emulsion fuels suggests that higher the water and glycerine levels and heavier the molecules, the larger will be the droplet size. However, glycerine molecules were observed to be heavier than water. The mean particulate size distributions for B0W5%, B0W10%, B0G5% and B0G10% were 4.3 μm, 6.3 μm, 4.6 μm, and 6.8 μm, respectively. B20, B50, and B100 had particle size distribution which ranged from 0.45 μm to 50 μm as seen in Table 3. Higher concentration of smaller particle ranging between 0.45 μm and 8 μm was noted in emulsion fuels containing less water and biodiesel which resulted in lower mean particle size.

The photos of glycerine emulsion and water emulsion fuels were taken from the microscope as seen in Figures 25 (b) and 26 (b) confirms the presences of different size of droplet sizes of molecules. The shear pressure added to the emulsion leads to reduction in the droplet size and increase in water and glycerine percentage cause the formation of droplets with higher diameter as seen in the photos [125]. A continuous increase was seen in the droplet size the increase in biodiesel percentage; the droplet size also appeared to increase with the increase in glycerine

(Figure 25 (b)) and water (Figure 26 (b)). The droplet size of glycerine molecules was observed to be bigger than the droplet size of water molecules. Therefore, water emulsion stability is more than glycerine emulsion as observed from photos because the droplet size distribution of water had maximum sharply defined and low diameter droplets that are representative of emulsion stability [126]. Coalescence was also observed in the photos of emulsions with higher concentrations of glycerine and water which results in the formation of droplets with higher average diameters. Coalescence can occur because of weak repulsive forces between the droplets which leads to droplet collision, thus reducing the thin-film separating them which finally breaks to form larger droplets[127]. Use of surplus surfactants in emulsion fuels result in the formation of double layer spherical micelle around a membrane of aqueous molecules wrapped around heavy compounds of bio-oil resulting in coalescence and later resulting in breaking up of the micelle due to difference in the densities [115]. In the present experiment the same reason can be attributed to the presence of coalescence where the heavier densities of water and glycerine wrapped under membrane of diesel-biodiesel blends which may result in droplet collision resulting in breaking of the membrane to form larger droplets.

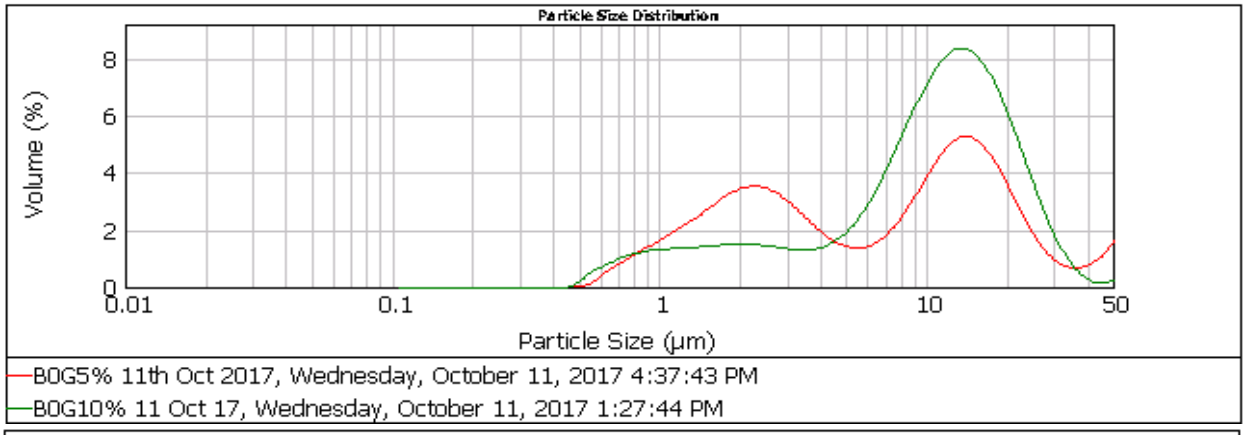

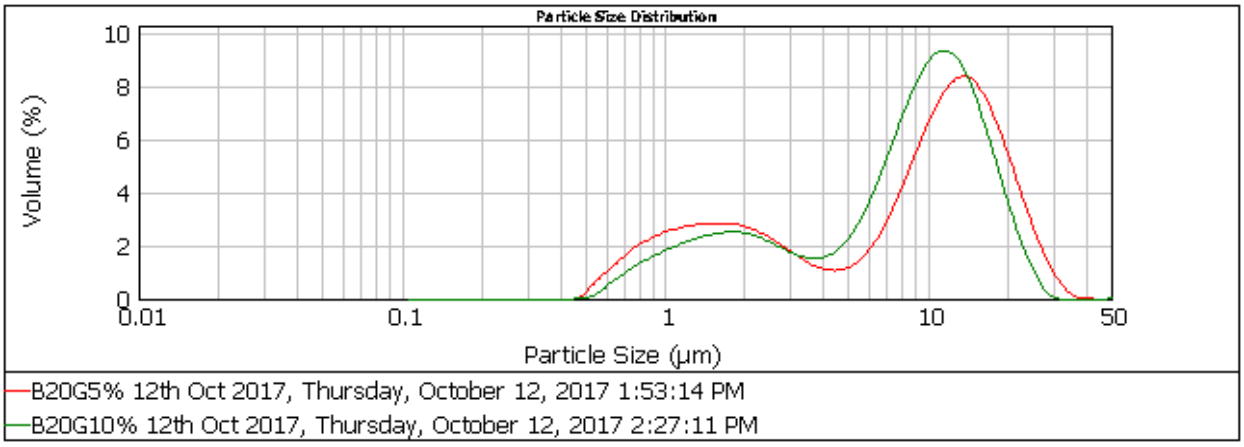

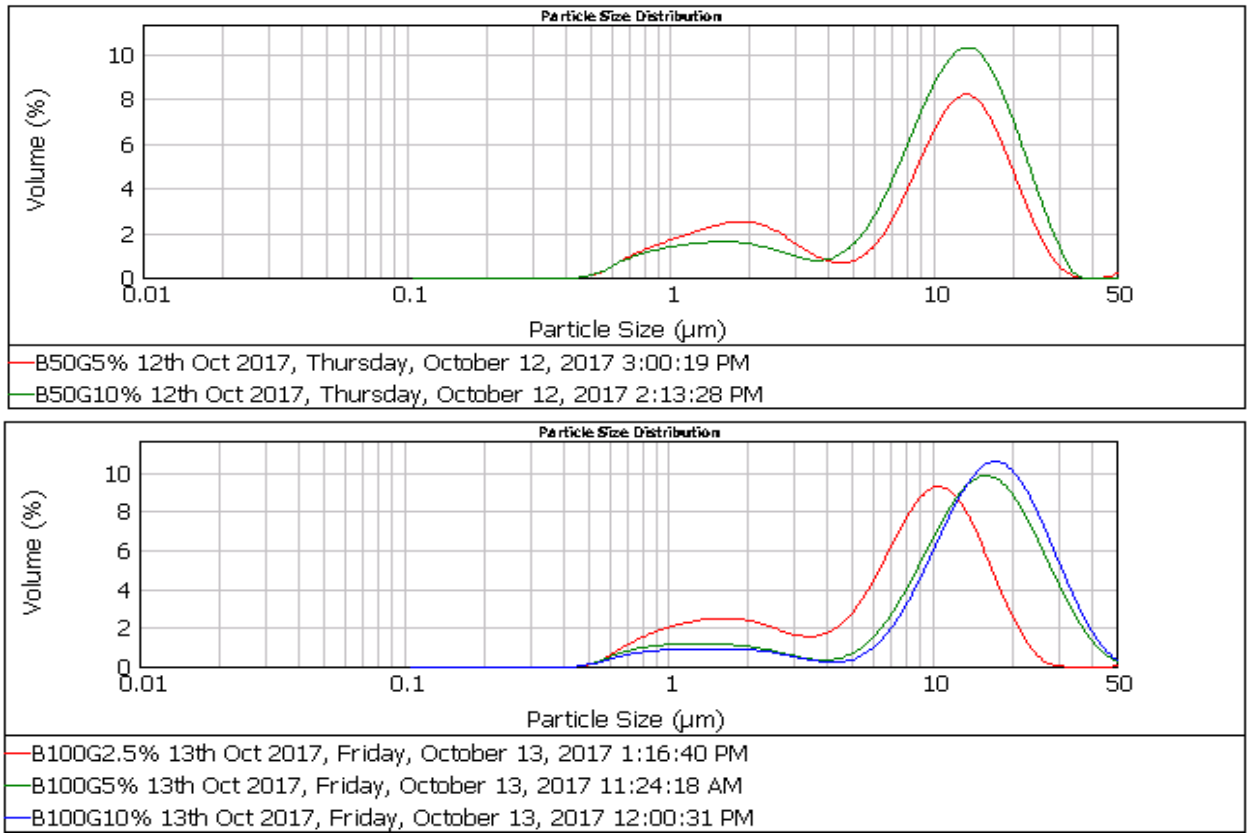

(a)

	B0	B20	B50	B100
G. %				
2.5%				
5%				
10%				

(b)

Figure 25: (a) Bimodal Particle Size Distribution Graphs and (b) Microscopic Pictures of the Glycerine Emulsion Fuels

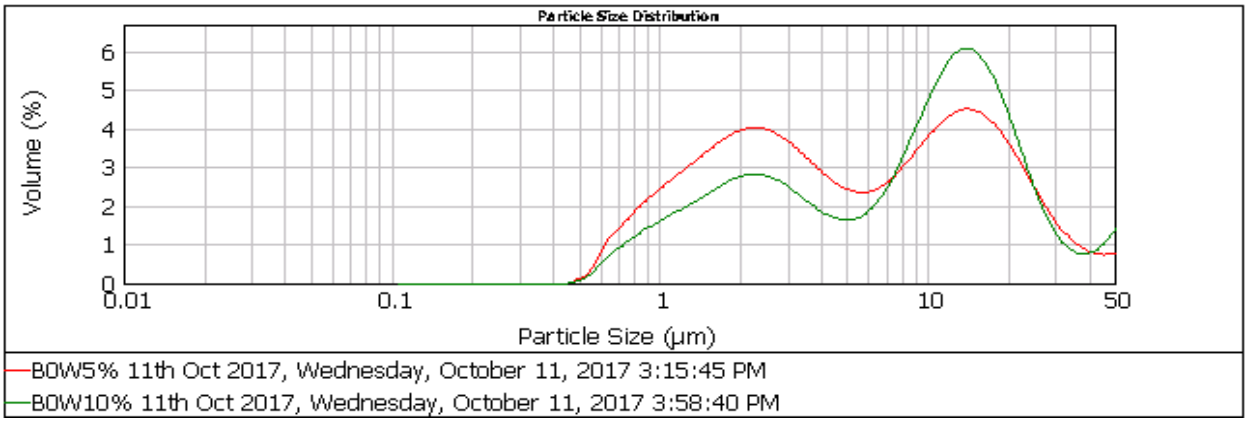
Particle Size Distribution
Volume (%)
0
1
2
3
4
5
6
0.01
0.1
1
10
50
Particle Size (µm)
B0W5% 11th Oct 2017, Wednesday, October 11, 2017 3:15:45 PM
B0W10% 11th Oct 2017, Wednesday, October 11, 2017 3:58:40 PM

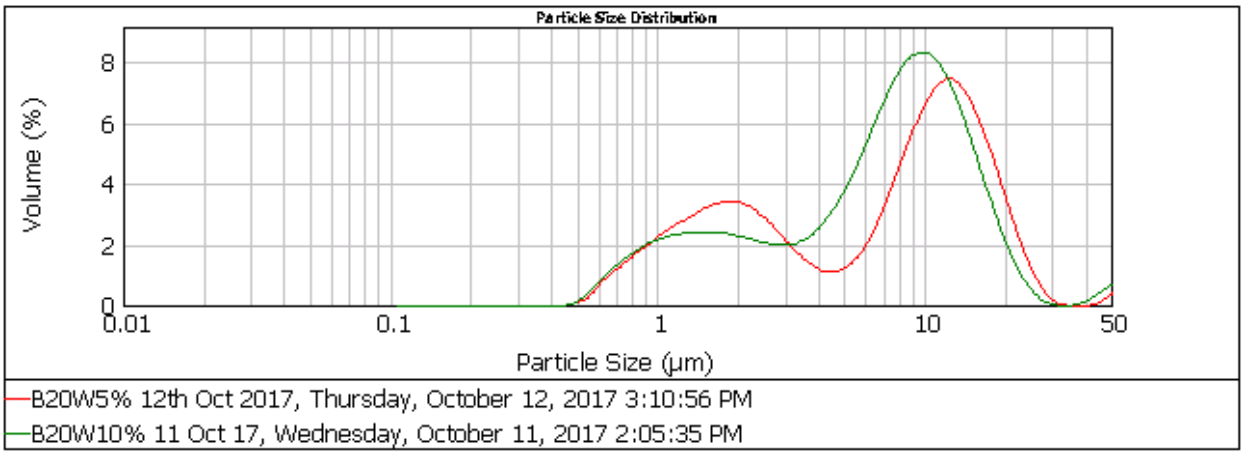
Particle Size Distribution
Volume (%)
0
2
4
6
8
0.01
0.1
1
10
50
Particle Size (µm)
B20W5% 12th Oct 2017, Thursday, October 12, 2017 3:10:56 PM
B20W10% 11 Oct 17, Wednesday, October 11, 2017 2:05:35 PM

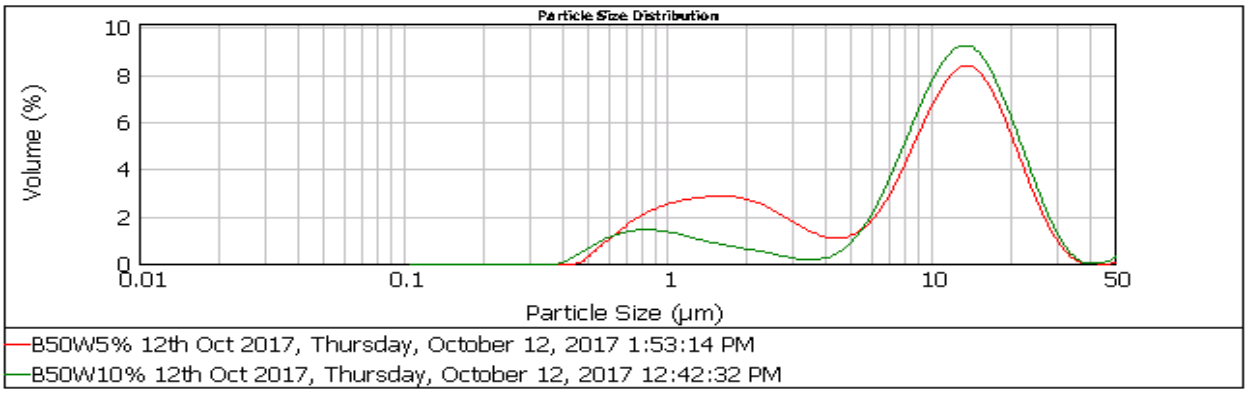
Particle Size Distribution
Volume (%)
0
2
4
6
8
10
0.01
0.1
1
10
50
Particle Size (µm)
B50W5% 12th Oct 2017, Thursday, October 12, 2017 1:53:14 PM
B50W10% 12th Oct 2017, Thursday, October 12, 2017 12:42:32 PM

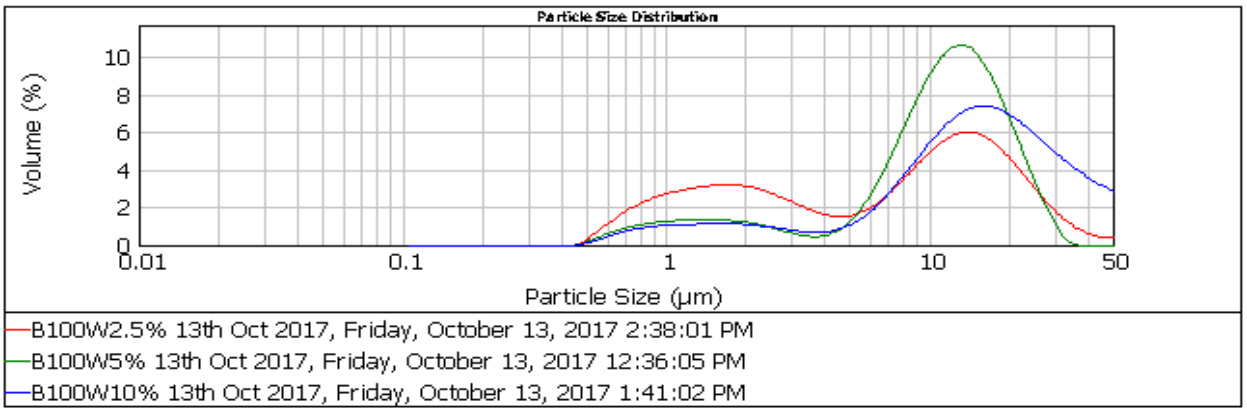
Particle Size Distribution
Volume (%)
0
2
4
6
8
10
0.01
0.1
1
10
50
Particle Size (µm)
B100W2.5% 13th Oct 2017, Friday, October 13, 2017 2:38:01 PM
B100W5% 13th Oct 2017, Friday, October 13, 2017 12:36:05 PM
B100W10% 13th Oct 2017, Friday, October 13, 2017 1:41:02 PM

(a)

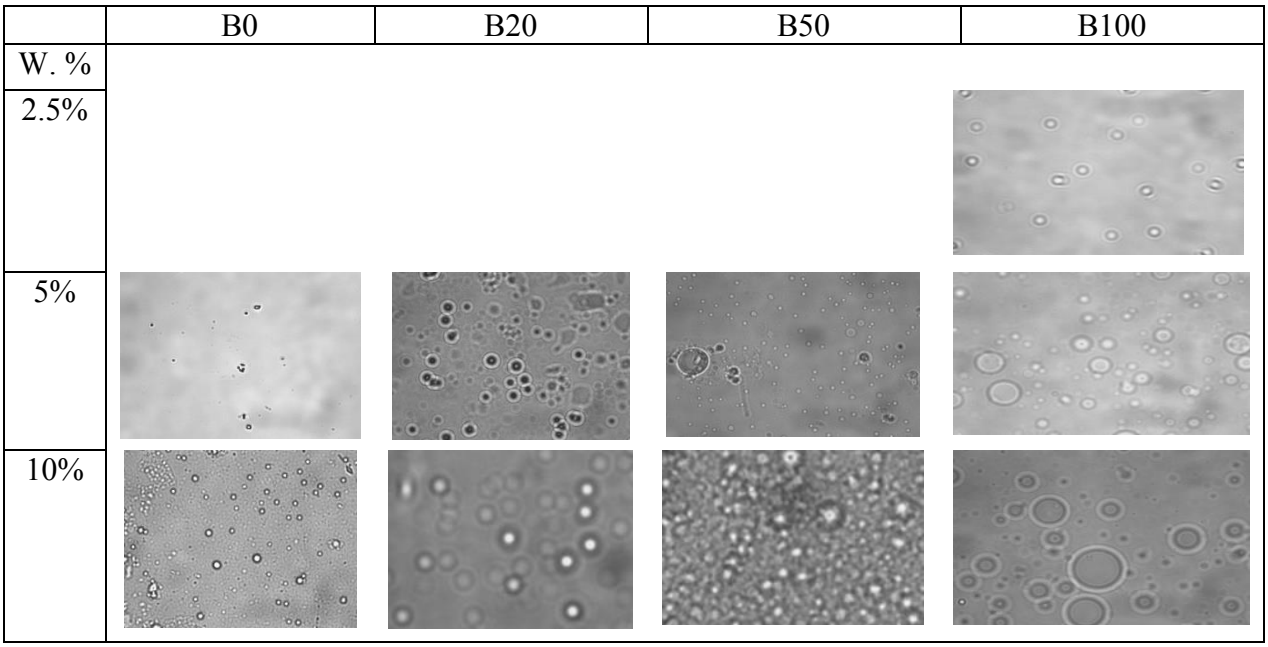

(b)

Figure 26: (a) Bimodal Particle Size Distribution Graphs and (b) Microscopic Pictures of the Water Emulsion Fuels

4.2.2 Emulsion Fuel Viscosity

Figure 27, shows an increase in fuel kinematic viscosity with the increase in glycerine concentration. The kinematic viscosity of B100 was observed to be about 4.2 cSt without glycerine but increased to a nearly 6 cSt with the addition of 10% glycerine, which resulted in an estimated increase of 40%. Kinematic viscosity also increased with the addition of biodiesel. Kinematic viscosity for B0 was observed to be about 1.85 cSt, whereas for B100 it was noted to be about 4.2 cSt, which was about 225% of B0. The increase was seen due to a high percentage of oxygen present in the glycerine [96], as well as in biodiesel. In case of water emulsion, the fuel viscosity was increased with the increase of water content. The viscosity of B100 with 10% of water was noted to be 5.66 cSt. The difference in the distribution size of emulsion particles and surface contact contributes to an increase in friction [71].

From Figure 28 it was observed that kinematic viscosity decreased with the increase in temperature in case of both diesel and biodiesel. Kinematic viscosity was measured in the temperature range of 25°C to 90°C. Kinematic viscosity for biodiesel (B100) at 25°C was nearly twice as higher than that of diesel (B0). However, kinematic viscosity was noted to decrease considerably as the temperature increased [128]–[130]. This is due to the fact that the molecules in liquid are loosely packed and have a strong intermolecular attraction and at higher temperature these molecules strongly oppose intermolecular forces and start to move more freely thus decreasing the viscosity [131]. The reduction in the kinematic viscosity for diesel and biodiesel at 90°C was observed to be 63.5% and 69% respectively. Although, the kinematic viscosity of diesel is much lower than that of the biodiesel but the change in the kinematic viscosity with temperature is similar.

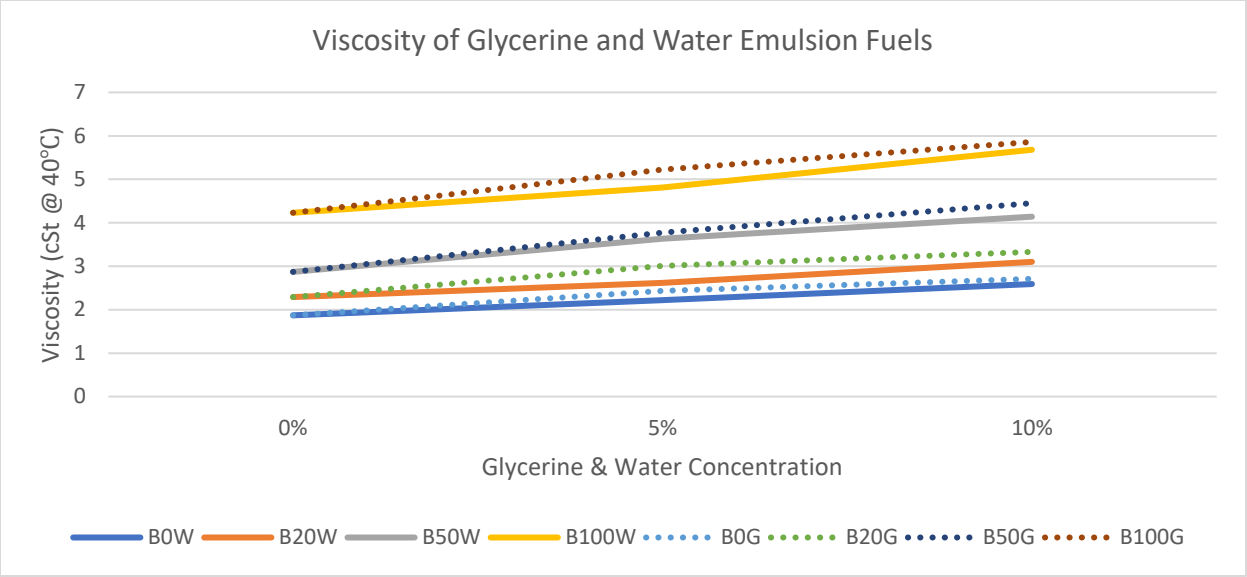

Figure 27: Kinematic Viscosity of Emulsion Fuels

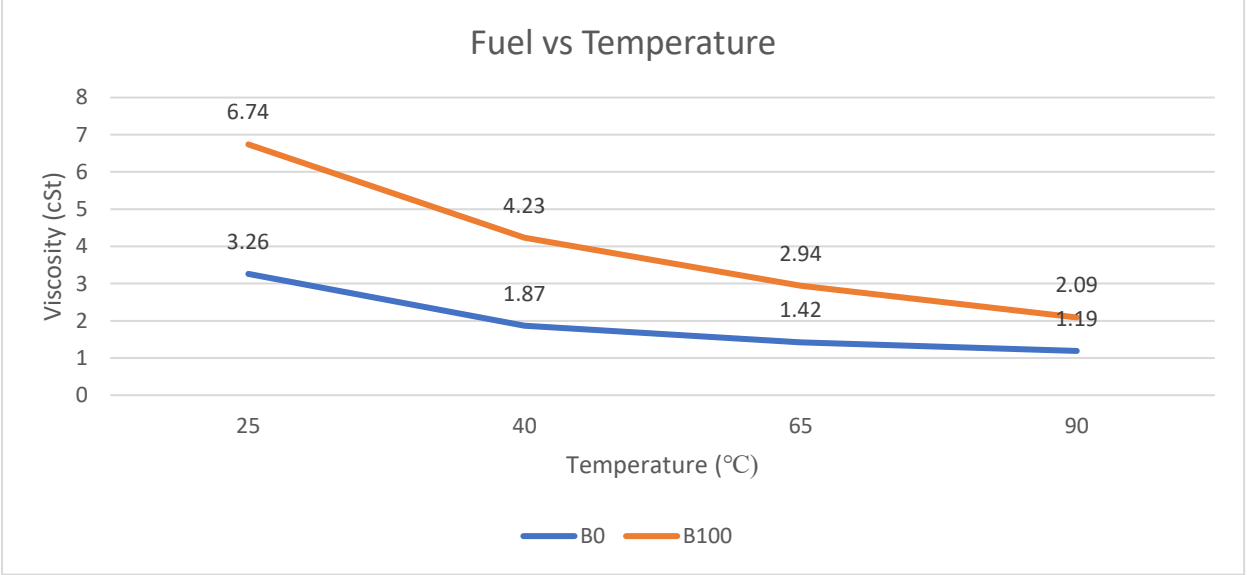

Figure 28: Kinematic Viscosity of Diesel and Biodiesel at Various Temperatures

4.2.3 Emulsion Fuel Stability

Emulsion stability refers to an emulsion's capacity to preserve the emulsifying layer when kept in a stationary position over time [71]. Stability was primarily investigated at normal room temperature (25°C). The emulsion's stability depends on various factors such as the stirring rpm, the concentration and type of surfactant used, the techniques used, the duration of the emulsification, and the viscosity of the continuous phase [81]. The stability of the emulsion fuel also relies on its HLB value which operates by activating the surface and maximizing its contact area [132]. Two emulsifiers (Tween 80 and Span 80) were used in order to achieve the desired stability. It was observed that the stability decreased with the increase of biodiesel, water and glycerin concentration which is due to the increase in the droplet size. The salts present in the

crude glycerine lead to phase separation, thus, reducing its stability [115] and in order to increase its stability there is a need to purify it [133]. B0G5% demonstrated the greatest stability for up to 70 hours in case of glycerine emulsion, and for water emulsion, the best stability was seen in B0W5% for up to 58 days. However, the stability of B50 and 100 at 10% of glycerine and water was noted to be quite less which was probably due to coalescence. The time span is an important factor responsible for the coalescence of droplets which is caused as a result of the processes involved in emulsification [134]. The increase in water percentage increases the size of droplets which with the time swell up resulting in coalescence [134]. The duration of stability is represented in Table 3.

4.2.4 Heating Value

The heating value reduced with the increase in biodiesel, water, and glycerine. The significant amount of oxygen present in glycerine reduces its heating value. In pure glycerine, oxygen weighs up to 52% [96]; therefore with the increase in the percentage of glycerine heating value reduces. As glycerine has a heating value of its own, due to which the heating values of the glycerine emulsions are higher than that of their respective water emulsion fuels. From the results, it was noted that B100G10% displayed the lowest heating value which was 37,691 kJ/kg. B100G10% displayed a reduction of 16.47% and 7.15%, respectively, in the heating value when compared to that of neat diesel and biodiesel, as illustrated in Table 3.

4.3 Heavy-Duty Engine Emissions

Experiments were done with B0, B50 and B100 along with their water and glycerine emulsions at idling condition at two different rpms, i.e. 1000 rpm and 1500 rpm. The exhaust emission (NOx, CO, HC and Smoke Opacity) were measured. The trends for the emissions were similar at both rpms that is why only the graphs for 1000 rpm were included in results of this study. The results for all the emissions at both rpm are shown in appendix A.

NOx Emission

Figure 29, displays that the average NOx emission increases with the increase of biodiesel due to the presence of oxygen in the biodiesel. An increase of 14.26% was noted in B1005 as compared to B0. Two different emulsions were formed using glycerine and water (5% and 10%). NOx was seen to reduce in case of both emulsions when compared to biodiesel but was even lower in case of a water emulsion. Average NOx emissions for B0W10% and B0G10% was 24.63% and 19.09% respectively lower than B0 due to the low heating values of water and glycerine emulsion. A similar trend was seen in case B50 and B100.

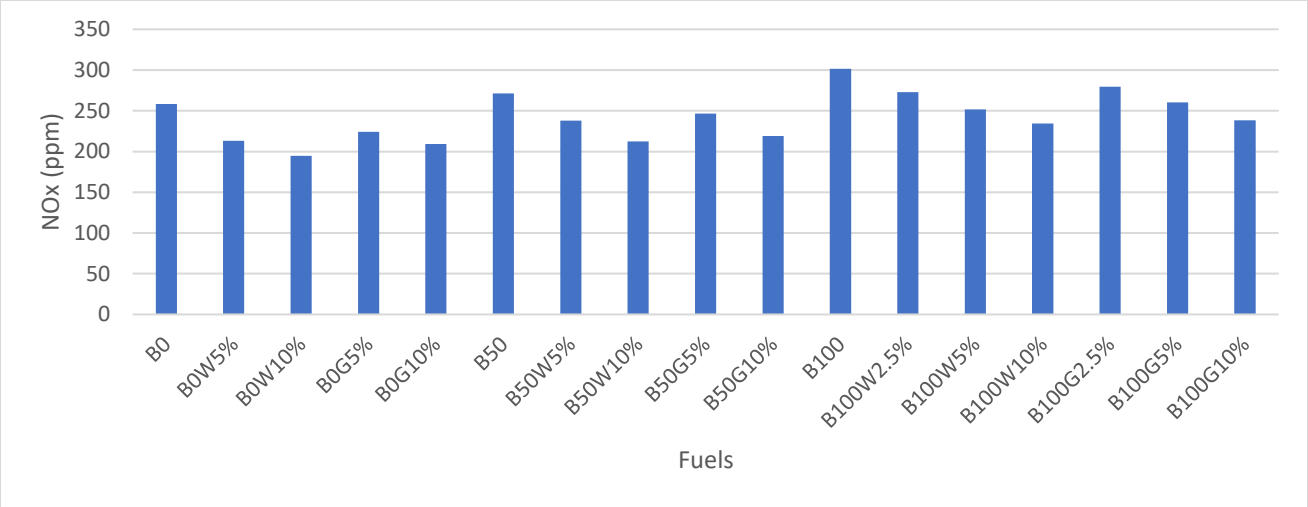

Figure 29: NOx Emission in Heavy-Duty Engine at 1000 rpm

CO Emission

It can be seen from Figure 30 that with the increase of biodiesel concentration CO reduces due to the presence of oxygen which helps in the complete combustion of the fuel. CO was seen to increase in case of emulsions. Water emulsion has a higher average of CO emissions because of the lower combustion temperature which results in incomplete combustion which forms more CO instead of CO_2 [135]. A reduction of 26.5% was seen for B100 as compared to B0 in case of CO emissions. An increase of 23.48% in average CO emission for B100G10% compared to B100, which increased 3% more for B100W10%. It was observed that with the increase of water and glycerine percentage CO increased.

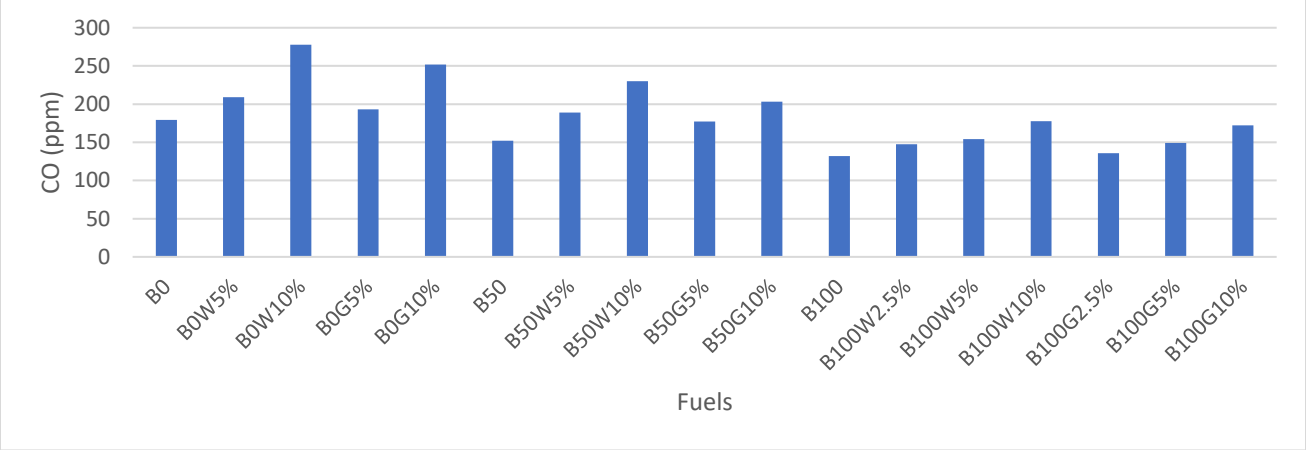

Figure 30: CO Emission in Heavy-Duty Engine at 1000 rpm

HC Emission

Figure 31 illustrates that the HC emission at 1000 rpm decreased with increase in biodiesel concentration but increased with glycerine and water content. HC emissions for B0G10% were approximately five times more than B0, and a similar trend was seen in B50 and B100. For W10% emulsion fuels HC emissions increased about 4 times more than its base fuel. These trends were

seen as a result of inbuilt cold EGR which reduces the amount of oxygen and decreases the flame temperature of the combustion chamber resulting in improper combustion (incomplete combustion).

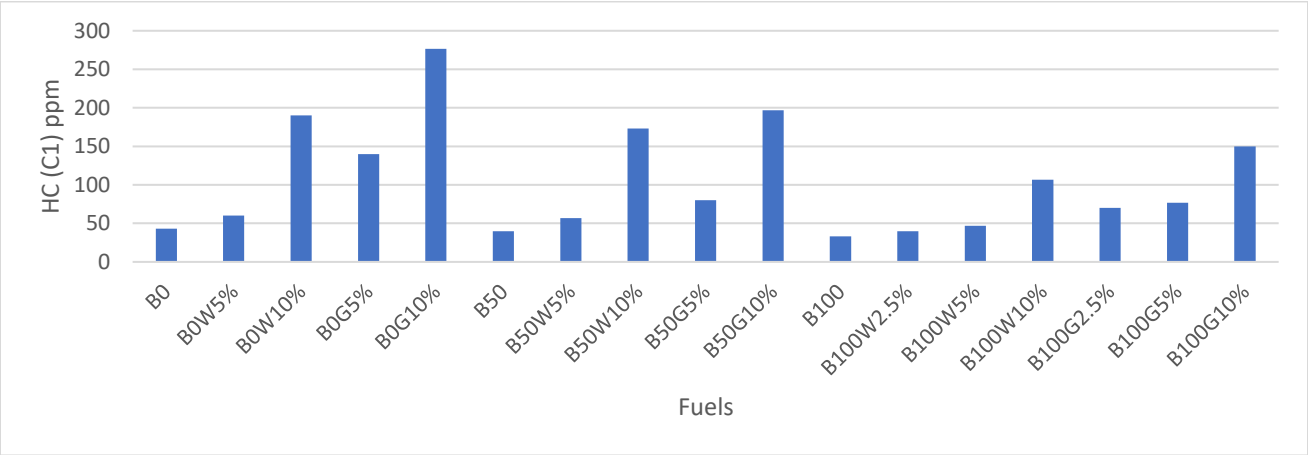

Figure 31: HC Emission in Heavy-Duty Engine at 1000 rpm

Smoke Opacity

Figure 32 demonstrates that smoke emissions at 1000 rpm decreased with the emulsion fuels. The minimum smoke emissions were noted in the case of glycerine emulsion fuels followed by water emulsion fuels and its base fuel. The smoke emissions increased with the increase in biodiesel concentration which can be due to the increase in viscosity. Smoke decreases with the increase of water and glycerine concentration. Nearly 31% decrease was noted in smoke emissions for B0W10% and about 50% decrease for B0G10% when compared to B0.

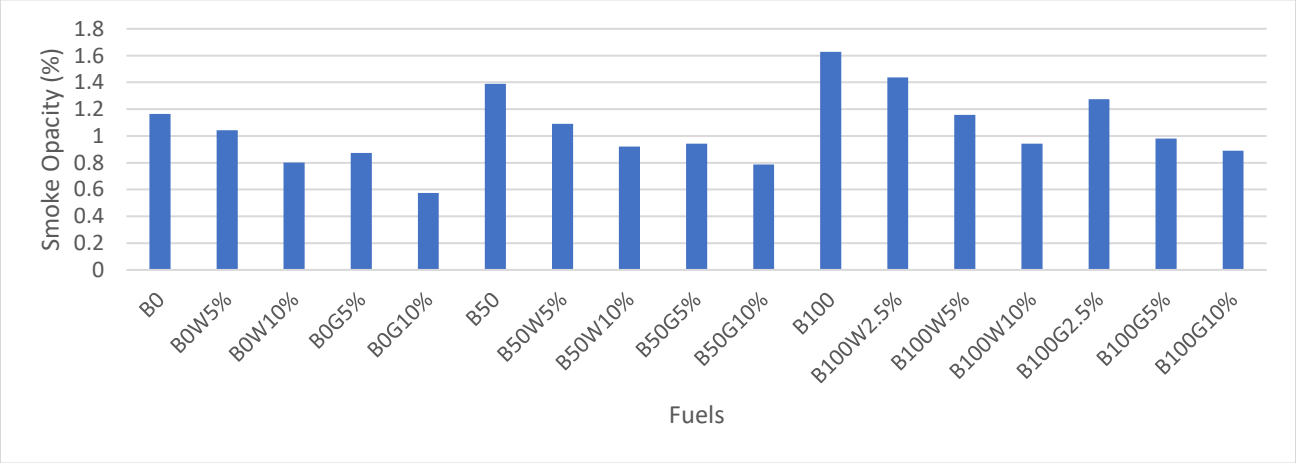

Figure 32: Smoke Opacity Emission in Heavy-Duty Engine at 1000 rpm

4.4 Light Duty Engine

4.4.1 Without EGR Technology

The experiments were done for B0, B20, B50 and B100 and with their water and glycerine emulsion (5% and 10%) at three different rpms and three different loads. The rpms selected for

testing were 1000 rpm (lowest engine speed), 2100 rpm (speed with the maximum torque) and 3000 rpm (speed with maximum power for continuous working). Furthermore, the three loads selected were low load (20%), medium load (50%) and high load (80%) of the maximum toques at the selected speed. All the results can be seen in Appendix 3. The power, torque and BSFC curve of the light-duty engine are shown in Appendix E.

4.4.1.1 Base Fuels

Performance

BSFC

From the results as in Figure 33, it was observed that BSFC increases with the increase in diesel-biodiesel blends. The increase of 4.68% was seen at 2100 rpm and low load condition of B100 as compared to B0. Higher BSFC of diesel-biodiesel blends is due to the lower heating value as compared pure diesel [63]. BSFC decrease with the increase in the load due to the increase in the burning efficiency of the fuel. The highest BSFC was noticed at 1000 rpm and low load condition. BSFC was seen to be decreasing at 2100 rpm, but it again increased at 3000 rpm due to the increase in friction losses. Out of all 3 speeds, the lowest BSFC was noticed at 2100 rpm high load condition which was 229.95 g/kWh.

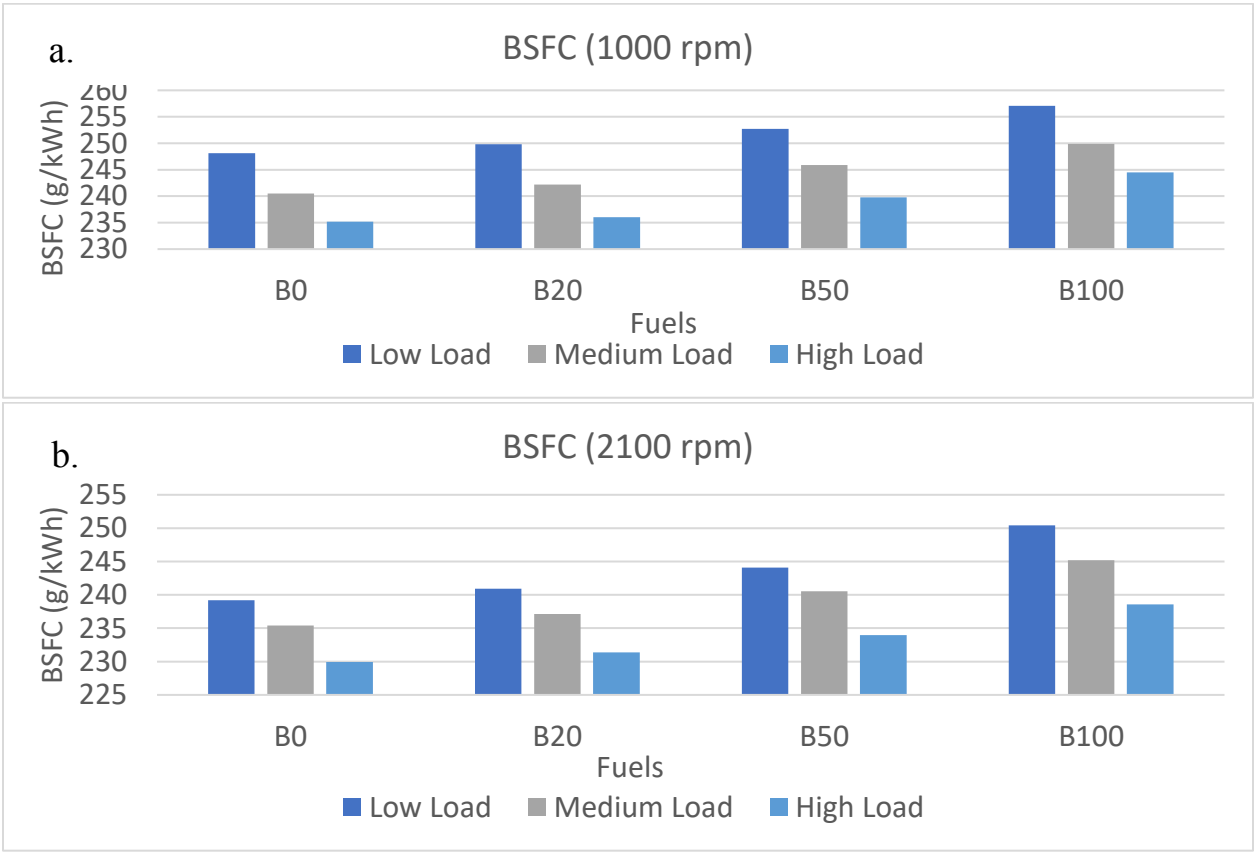

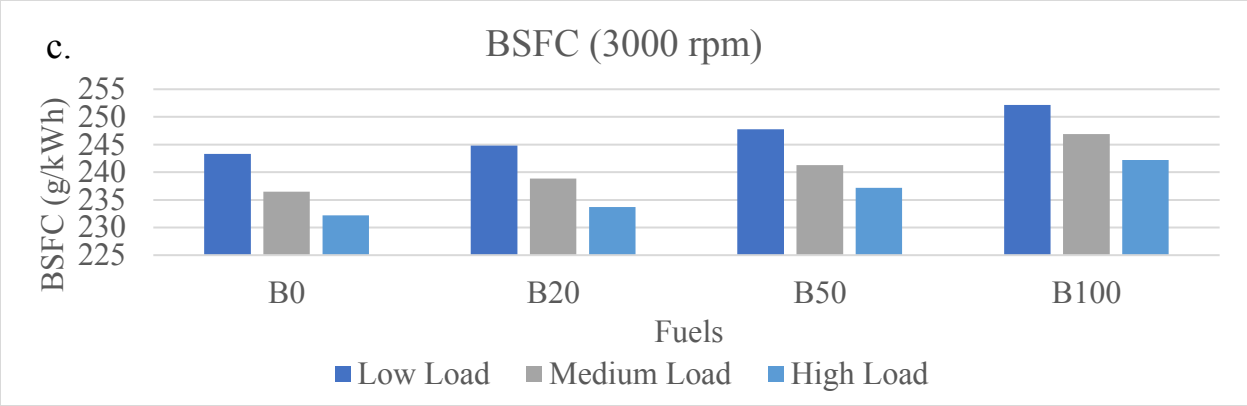

Figure 33: BSFC of a Light-Duty Engine at Different Loads at (a) 1000 rpm (b) 2100 rpm and (c) 3000 rpm

BTE

Figure 34 shows that BTE increases with the increase of biodiesel which can be attributed to the significant amount of oxygen present in it which helps in the proper combustion of fuel and increases the thermal efficiency. BTE increases with the increase in the load at all operating speeds. BTE increased with speed at 2100 rpm due to proper air-fuel mixing but decreased at 3000 rpm. The maximum BTE was observed for B100 at 2100 rpm on high load condition as 37.17%. The increase in BTE for B100 was 6.48%, 6.67% and 6.14% on high load condition at 1000 rpm, 2100 rpm, and 3000 rpm respectively.

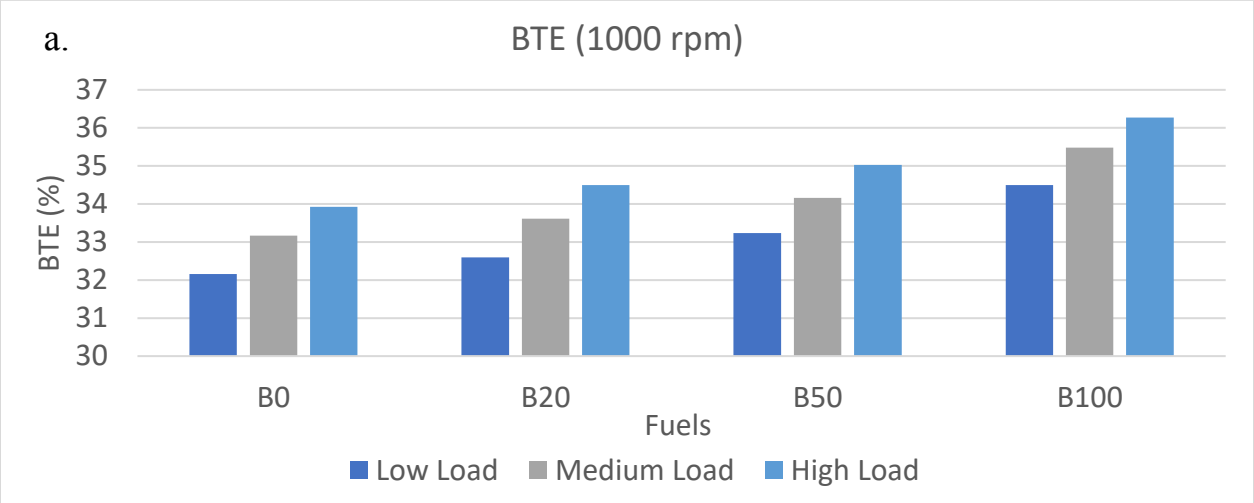

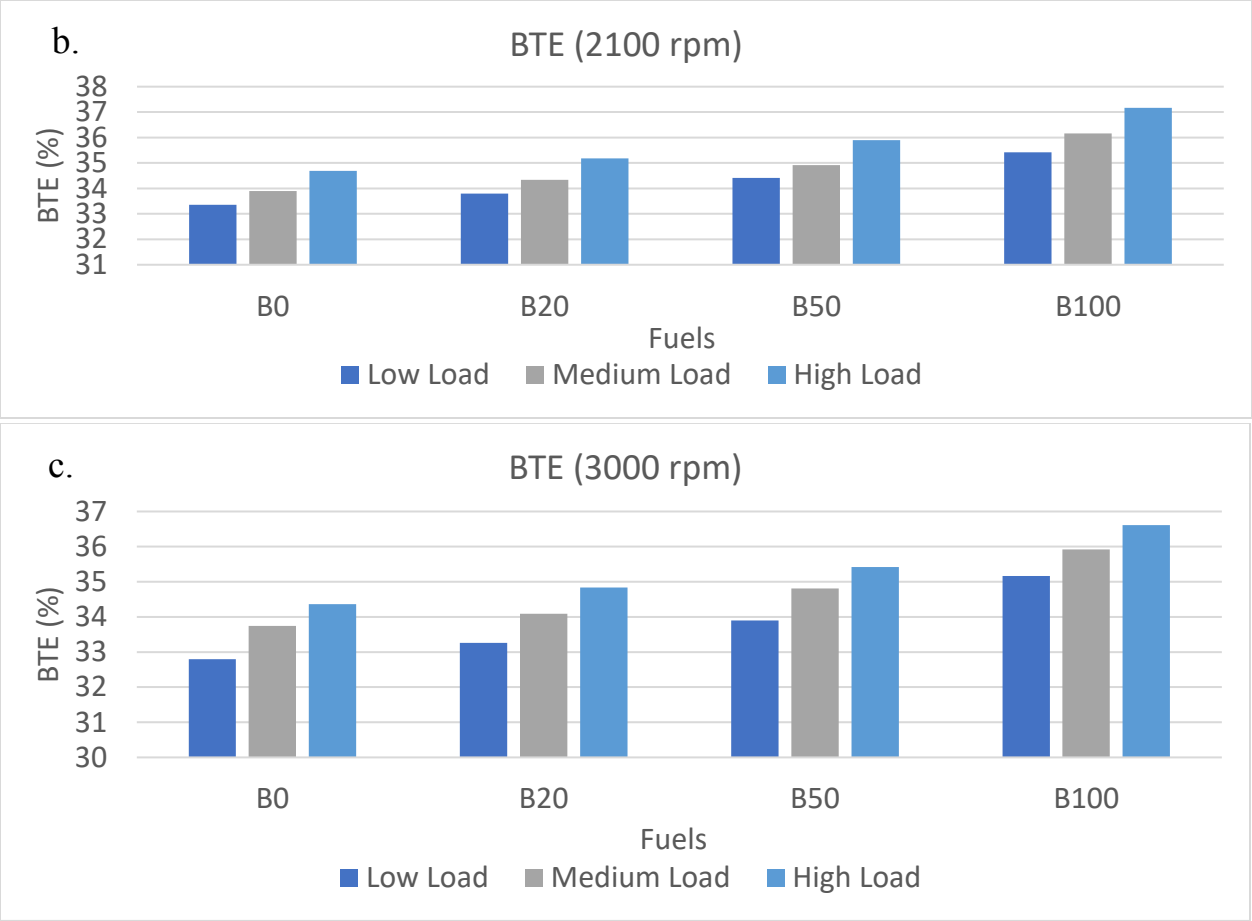

Figure 34: BTE of a Light-Duty Engine at Different Loads at (a) 1000 rpm (b) 2100 rpm and (c) 3000 rpm

Emissions

NOx Emission

From the Figure 35, we can see that with the increase of biodiesel concentration the level of NOx emission increases due to the presence of oxygen which helps in the proper burning of the fuel and increases the combustion chamber temperature. It was noticed that with the increase in the load NOx emissions increased regarding ppm, due to the increase in the combustion temperature. However, when converted into g/kWh a decrease in NOx is seen with the increase in load because the rate at which ppm increases is lower than the rate at which power increases with load. NOx also reduces with the increase in speed due to shorter ignition delay which occurs because of the increase in volumetric efficiency and inlet air motion, leading to better air-fuel mixing at a higher speed. On an average NOx emission of B0 was noted to be 4.34 g/kWh and for B100 was 4.78 g/kWh, which is 9% more than B0.

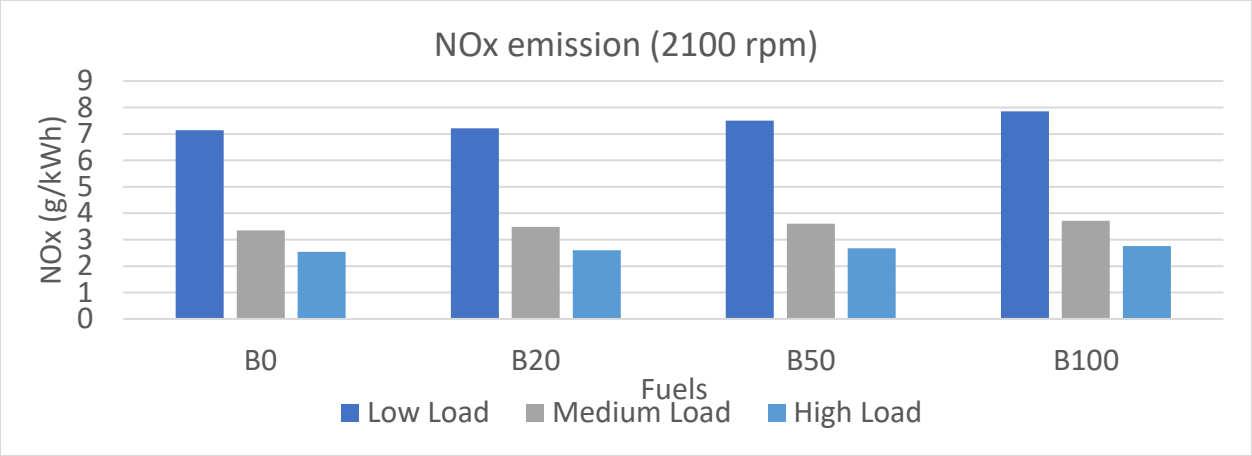

Figure 35: NOx Emission of a Light-Duty Engine at Different Loads 2100 rpm

CO Emission

It can be noted from the graphs shown in Figure 36 that average CO decreases with the increase of biodiesel in the diesel-biodiesel blends as the presence of oxygen facilitates in the complete combustion of the fuel. Moreover, CO also decreases with the increase in load and speed as these result in the higher temperature of the combustion chamber which results in the complete combustion of the fuel [13] and converts CO to CO_2. The average CO decrease for B100 was 16.43% as compared to B0. CO emission for high load 1000 rpm was 2.559 g/kWh which reduced by 51.46% at 3000 rpm high load and was noted as 1.242 g/kWh for B100.

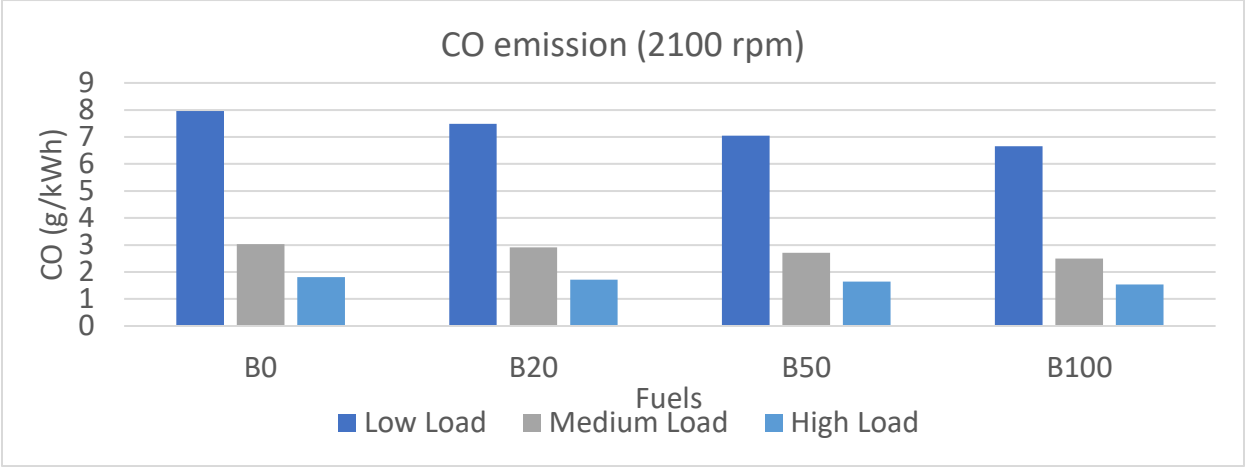

Figure 36: CO Emission of a Light-Duty Engine at Different Loads at 2100 rpm

HC Emission

From Figure 37, it was observed that HC emission decreases with the increase of speed, load, and biodiesel content. The reasons for the cause of HC can be attributed to low-temperature bulk quenching, incomplete burning of fuel, the improper stochiometric ratio (over-rich or over-lean burning), liquid wall films for excessive spray impingement and the fuel trapping in the crevice volumes of the combustion chamber [57]. In case of biodiesel CO was reduced due to the

presence of oxygenated compounds in biodiesel which aided in the proper burning of the fuel resulting in the lower formulation of unburnt hydrocarbons. Increase in engine load decreases HC because of the lean combustion process. HC emissions for B0 and B100 were noted to be 10.32 and 6.02 respectively, and a decrease of approximately 40% was seen. A decrease of 64.6% was seen in HC emissions for B100 working between 1000 rpm and 3000 rpm at high load. HC emission for B100 at 1000 rpm high load condition witnessed a decrease of 64.6% for B100 at 3000 rpm high load condition which was calculated as 1.788. a decrease of 64.6% was seen in HC emissions

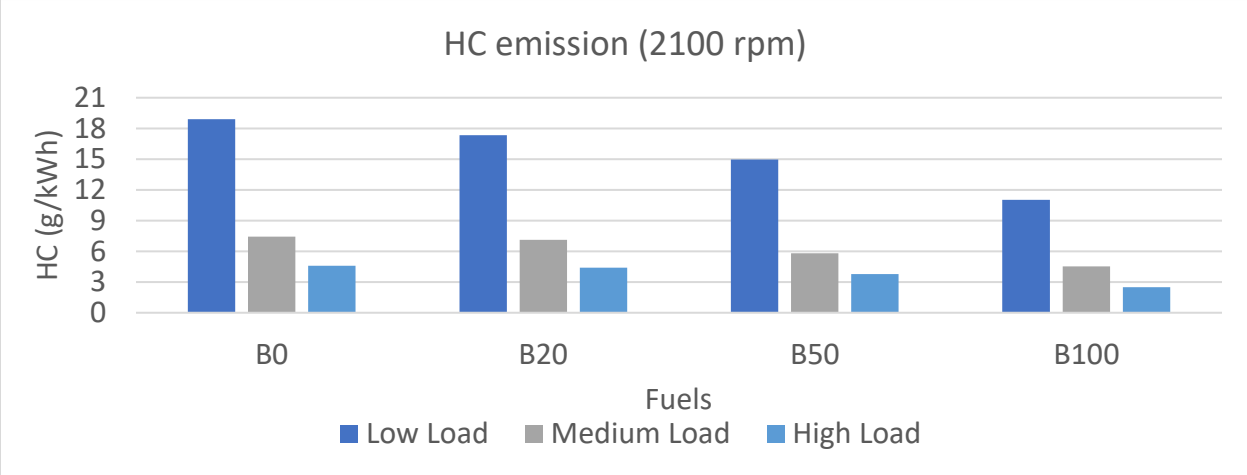

Figure 37: HC Emission of a Light-Duty Engine at Different Loads at 2100 rpm

Smoke Opacity

Smoke opacity is the measure of formation of smoke or soot in the engine and is dependent on the collision of molecules (primarily carbon and oxygen) and the concentrations of fuel fragments [136]. Smoke emissions increased with the increase in biodiesel in the biodiesel-diesel blend which can be due to the higher viscosity and density of biodiesel fuel which worsens atomization and combustion of the fuel [137]. The increase in smoke with the addition of biodiesel, however, shows a contrary trend and a cause of which can be attributed to the occurrence of wall-quenching resulting from over penetration of the fuel through the increase in the injection pressure [74]. The average smoke opacity of B0 was measured as 4.36% which increased with biodiesel and was noted as 7.80% in case of B100 as seen in Figure 38. Smoke emissions were seen to increase with the increase in loads but decreased with the increase in speed. 65.18% and 75.88% reduction in smoke emission was observed at high load at 2100 and 3000 rpm respectively on comparing with 1000 rpm high load condition in B100 fuel.

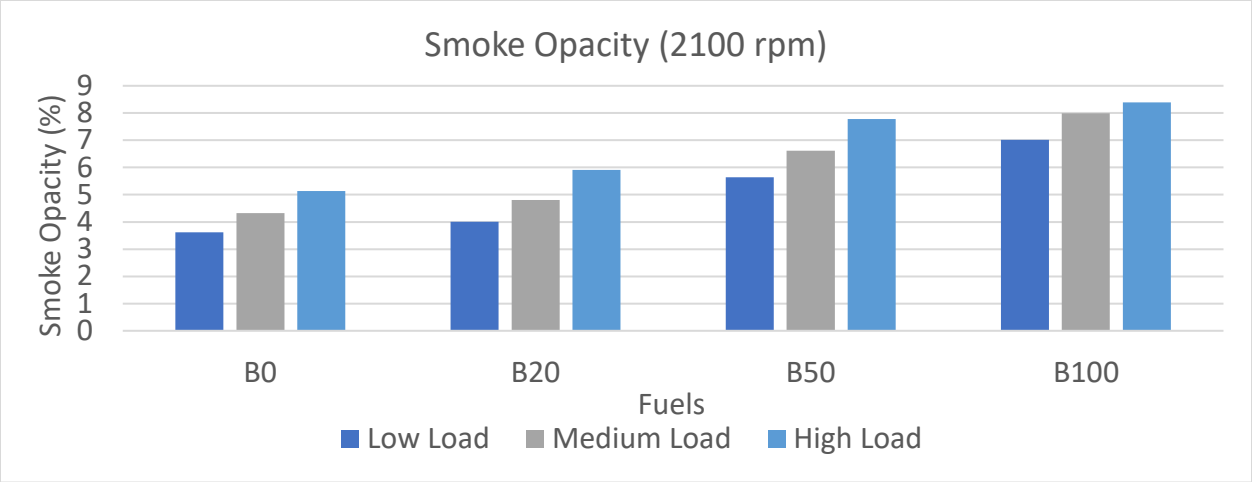

Figure 38: Smoke Opacity of a Light-Duty Engine at Different Loads at 2100 rpm

EGT

Exhaust gas temperature (EGT) illustrated in Figure 39 shows that average EGT was slightly more (approx. 7°C) in case of B100 than pure diesel which was due to the presence of oxygen molecules in biodiesel which increases the burning efficiency of the fuel and the combustion chamber temperature. EGT increases with the load and speed. A rise of 51% was seen in average EGT on changing the speed to 3000 rpm from 1000 rpm.

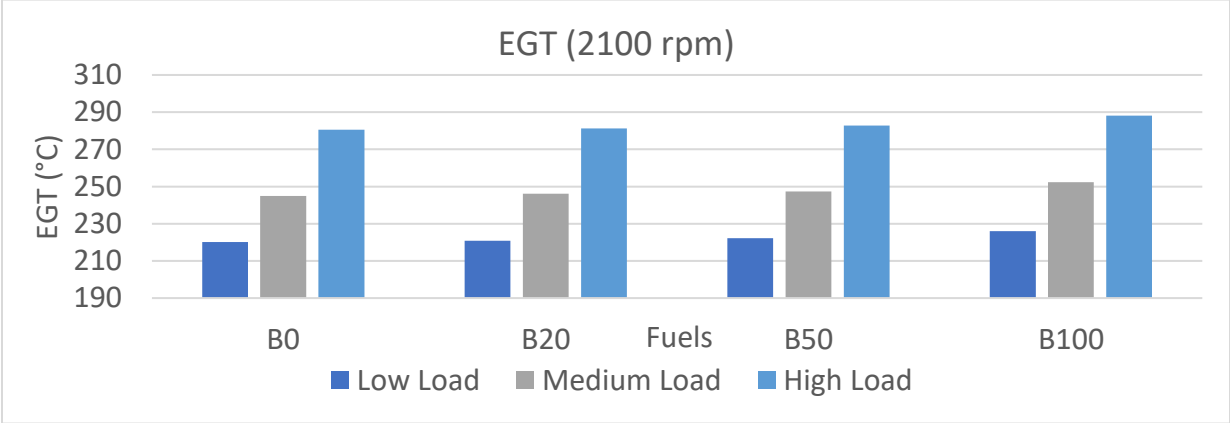

Figure 39: EGT of a Light-Duty Engine at Different Loads at 2100 rpm

4.4.1.2 Emulsions

All the performances and emissions done from this part ahead were done at 2100 rpm for water and glycerine emulsions (5% and 10% for both) of diesel-biodiesel blends. This rpm was selected because it has the maximum torque.

Performance

BSFC

On comparing the results of different fuels and their emulsions, it was noted that BSFC increased with the increase in water, glycerine and biodiesel concentration at a specific load, as shown in Figure 40 and 41.

From Figure 40 it can be observed that BSFC increase for the water emulsion fuels with respect to their base fuels. The BSFC was seen to be more in the emulsion fuels having 10% water present in them. The maximum average BSFC was noted to be 248.09 g/kWh for B100W10% w.r.t. all water emulsion fuels. There was an increase 1.70% in BSFC for B0W10% and 5.64% for B100W10% as compared to B0.

Figure 41 illustrates the BSFC of glycerine emulsion fuel. B100G10% on an average displayed nearly 5% increase in BSFC as compared to B0 which was due to the reduction in the heating value or the emulsion energy density of the glycerine emulsions [77], [96]. BSFC was noted to be affected by the engine load; that is, it decreased with the increase in load due to its higher burning efficiency [74]. The BSFC was more in case of water emulsions as compared to glycerine emulsions because of its lower heating value, though the average BSFC difference was a mere 0.85 g/kWh.

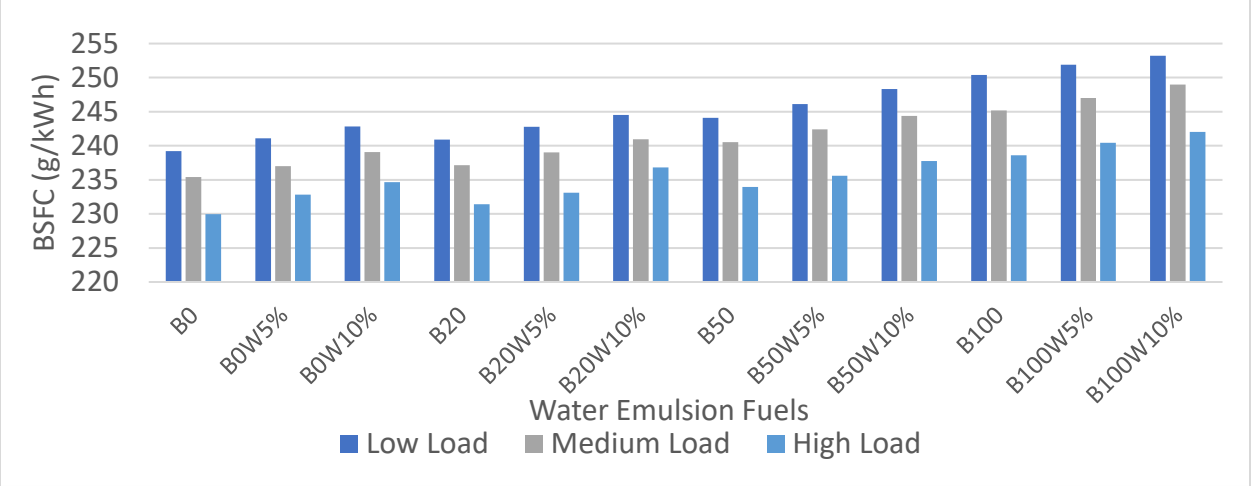

Figure 40: BSFC of a Light-Duty Engine at Different Loads at 2100 rpm when Operated with Water Emulsion Fuel

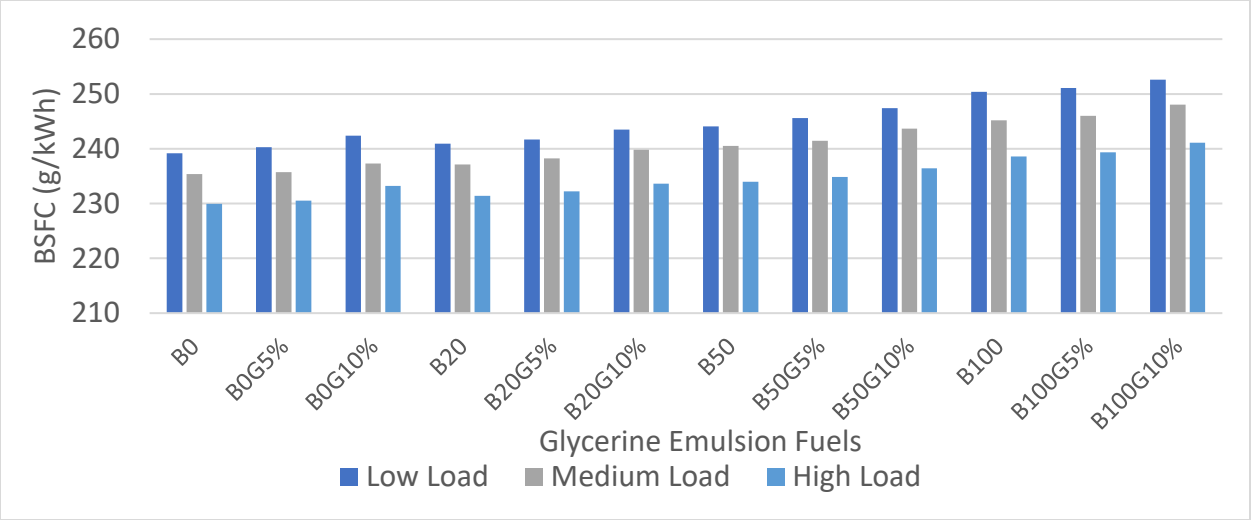

Figure 41: BSFC of a Light-Duty Engine at Different Loads at 2100 rpm when Operated with Glycerine Emulsion Fuel

BTE

BTE for all the base fuels and their emulsions was observed at different loads as seen in Figures 42 and 43. BTE implies better and efficient combustion of fuels [13]. BTE for the emulsion fuels was found greater than their base fuels because of the presence of oxygen which increases combustion efficiency. BTE increase with the increase of glycerine or water percentage and from which water emulsion has better bake thermal efficiency.

BTE for water emulsions increased with the increase in water percentage and with biodiesel in biodiesel-diesel blends due to the presence of oxygen which facilitates the better combustion of the fuel as seen in Figure 42. BTE increased with the load. The maximum BTE was noted for B100W10% to be 40.63% which was 6.66% and 4.38% more than B0 and B100 respectively.

BTE for glycerine emulsion witnessed an increase between 0.8% - 1.1% at medium load and 1.7% - 2 % at high load as compared to low load for all fuel blends as seen in Figure 43. Brake-thermal efficiency was seen to improve with the addition of biodiesel and glycerine, because of the oxygen molecules present in them that assist in the proper burning of the fuel leading to increased burning efficiency. The average BTE for B100G10% was observed to be about 38%. However, average BTE of B0 was about 34%. The increase in the BTE for B100G10% was noted as 4.65% and 2.4% w.r.t B0 and B100 respectively.

On comparing water and glycerine emulsion fuels, water emulsion was found to have better thermal efficiency because glycerine emulsion has the higher viscosity which reduces/worsens the fuel atomization and results in poor BTE. The BTE for B100w10% was about 2% more than B100G10%.

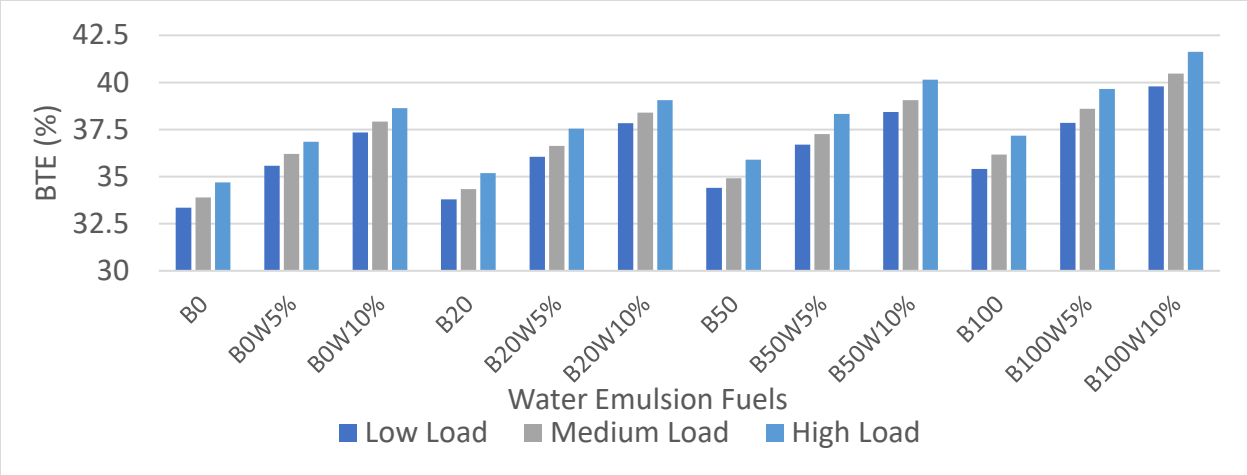

Figure 42: BTE of a Light-Duty Engine at Different Loads at 2100 rpm when Operated with Water Emulsion Fuel

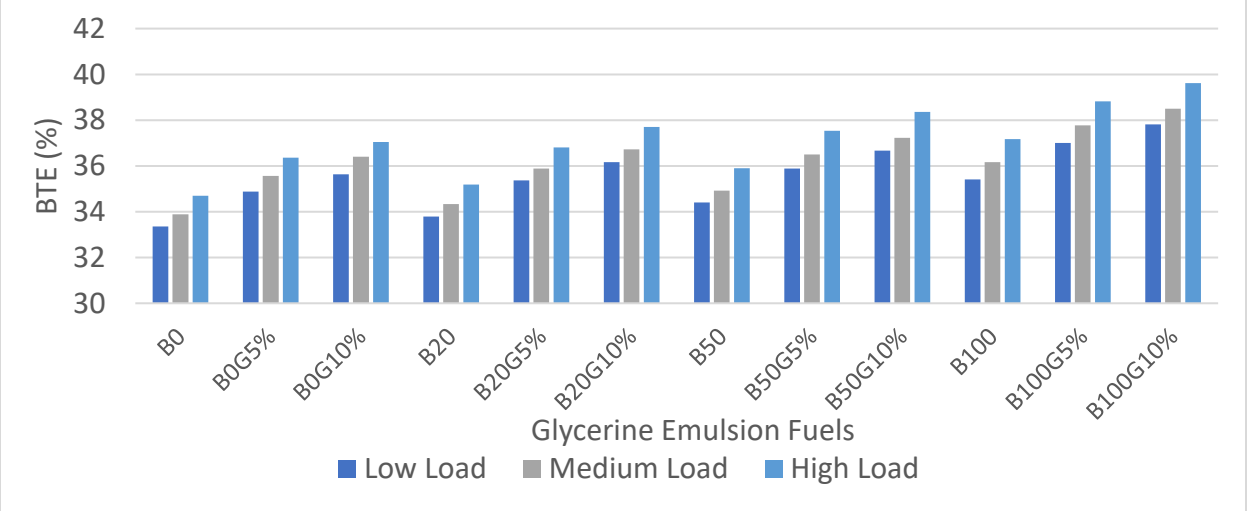

Figure 43: BTE of a Light-duty Engine at Different Loads at 2100 rpm when Operated with Glycerine Emulsion Fuel

Emissions

NOx Emission

Figure 44 and 45 present NO_x emissions for different fuel blends along with their water and glycerine emulsions at various engine loads. Reduction in NOx emission was observed with the use of emulsification technique, which helps decrease the combustion temperature by reducing the flame temperature of the combustion chamber. NOx emissions were found to be the least at 3000 rpm high load condition.

From Figure 44 demonstrated that with the increase of water percentage the level NOx emission reduced. In case of water emulsion, fuel reduction in NOx can be attributed to the lower calorific value and high latent heat of vaporization of water which results in a decrease of adiabatic

flame temperature [132]. NOx emission for B0 was 4.34%, and it reduced to 3.48% for B0W10% which was observed to be the lowest.

Upon investigation of NOx emissions for glycerine emulsion as shown in Figure 45 it was noted that NOx slightly increased with the addition of the biodiesel because of the additional oxygen present in biodiesel. The NO_x level for glycerine emulsion was noted to decrease due to the lower flame temperature of the glycerine emulsion and its high heat of vaporization, and also due to the improved atomization of the emulsion fuel [96], [138], [139]. The highest reduction was seen in the fuels blended with the maximum amount of glycerine, in all cases. The average NOx of B100 was 4.77 g/kWh, and it reduced to 3.91 g/kWh for B100G10%, which is 18% lower than B100.

The reduction in NOx emission was more for water emulsion than glycerine emulsion because water has higher latent heat of vaporization as compared to glycerine and moreover, its calorific value is also lower which lowers the in-cylinder flame temperature more as compared to glycerine emulsion. Additionally, the atomization of water emulsion was better due to its less viscosity. Average NOx for B100W10% was noted as 3.81 g/kWh and for B100G10% was 3.91 g/kWh.

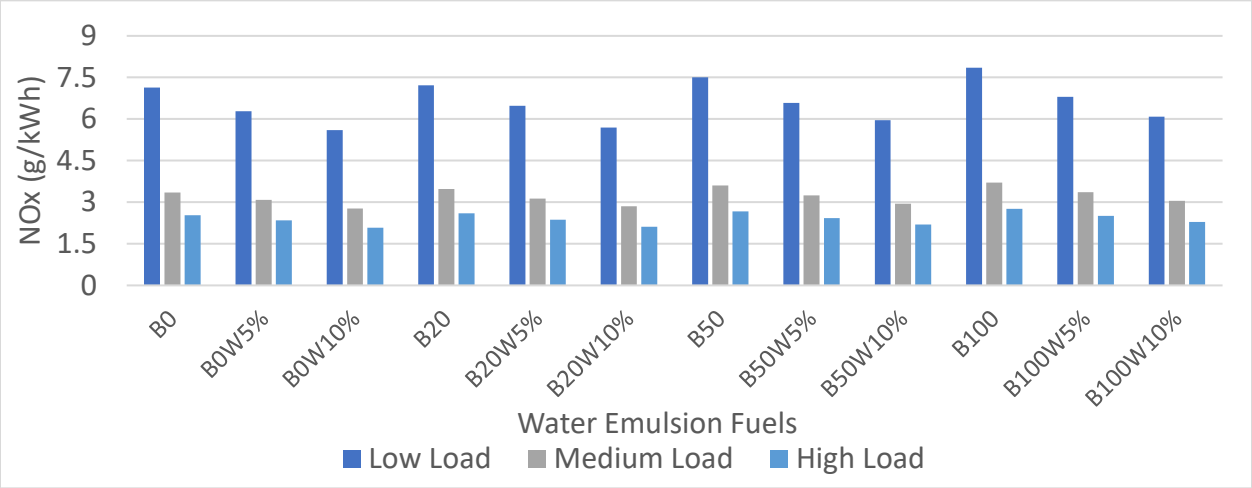

Figure 44: NOx Emission of a Light-Duty Engine at Different Loads at 2100 rpm when Operated with Water Emulsion Fuel

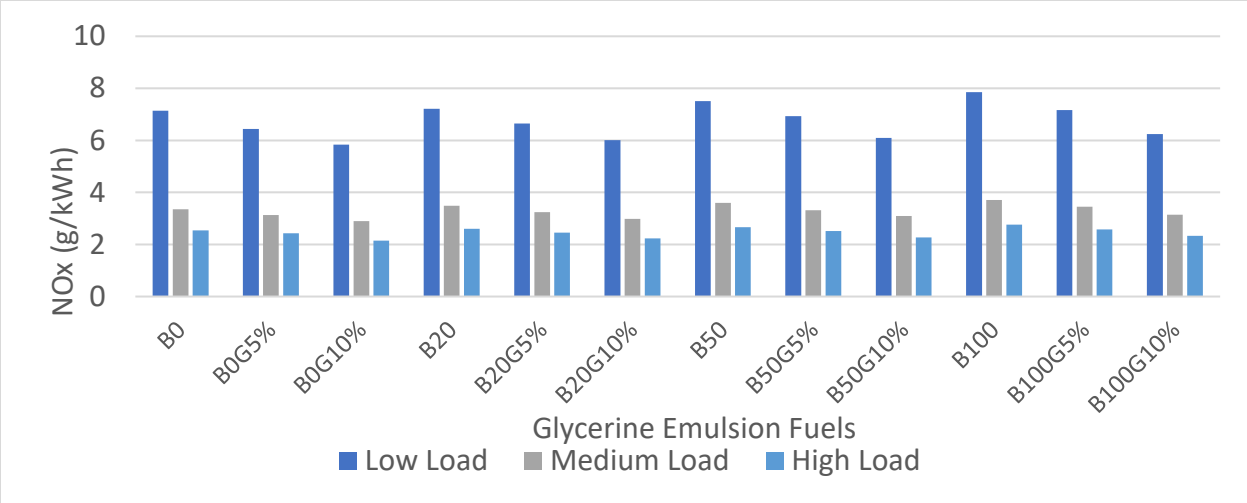

Figure 45: NOx Emission of a Light-Duty Engine at Different Loads at 2100 rpm when Operated with Glycerine Emulsion Fuel

CO Emission

CO is formed due to insufficient oxygen present in the combustion chamber which is not sufficient to oxidize CO to form CO_2. CO increases with the increase in water and glycerine percentage in emulsion fuels which leads to a reduced flame temperature in the combustion chamber resulting in incomplete combustion.

On observing Figure 46, it can be noted that CO increased with the increase in water emulsion due to the presence of water inside the emulsion fuel which decreases the combustion temperature resulting in increased formation of CO [140]. B100W5% demonstrated the lowest average CO emission among all the tested water emulsion fuels and was measured to be 4.56 g/kWh which was 1 g/kWh more than B100 and slightly more than the CO produced by pure diesel which was 4.02 g/kWh.

In case of glycerine emulsion fuel, it was seen that CO emissions increased for all the emulsion fuels when compared to their neat base fuels as seen in Figure 47. It was found that the addition of glycerin increased CO emissions because it lowers down the flame temperature which results in incomplete combustion which further weakens the higher oxygen content present in glycerine. The average CO emissions noted for B100G5% was 4.29 g/kWh which was the lowest whereas maximum CO was measured in case of B0G10% which was 6.04 g/kWh.

The CO emission for glycerine emulsion was observed to be lower than those recorded for water emulsion fuels because of the oxygen content present in glycerine which improves its combustion efficiency as compared to water emulsion fuels.

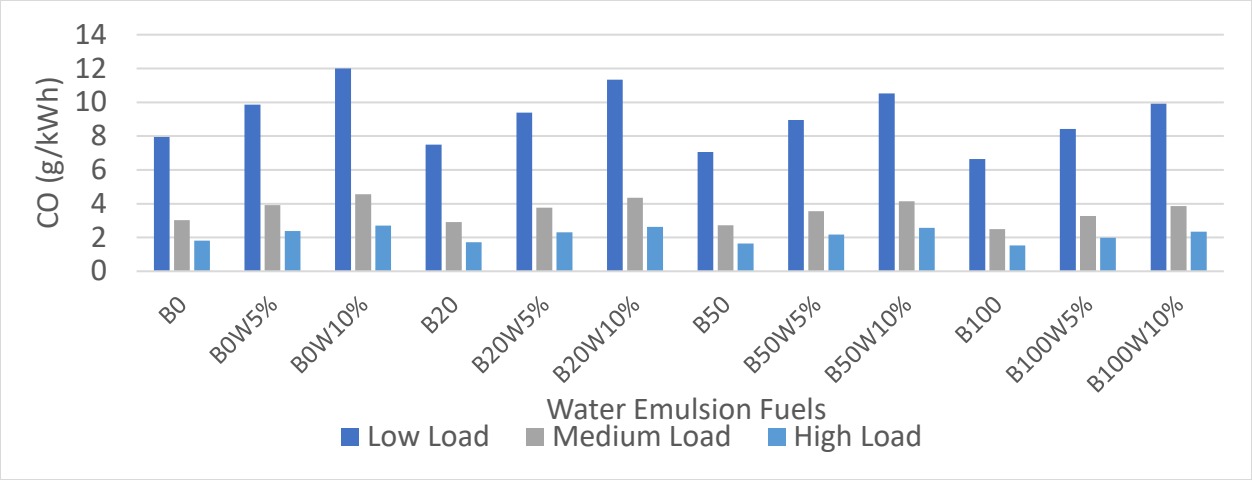

Figure 46: CO Emission of a Light-Duty Engine at Different Loads at 2100 rpm when Operated with Water Emulsion Fuel

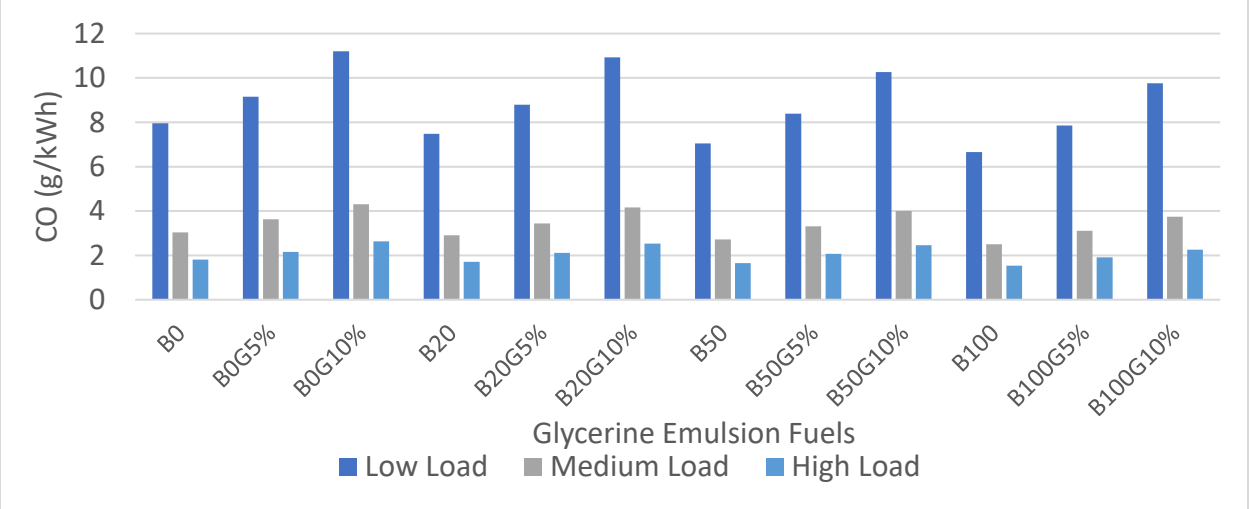

Figure 47: CO Emission of a Light-Duty Engine at Different Loads at 2100 rpm when Operated with Glycerine Emulsion Fuel

HC Emission

HC emissions of emulsion fuels were noted to increase with an increase in the water and glycerine percentage. HC emissions depend on air-fuel mixing which is improved with emulsion due to the presence of micro-explosions however, these micro-explosions also result in local flame quenching causing combustion temperature to reduce thus increasing formation HC [71].

Figure 48 depicts that HC increased with the increase in the level of water in case of water emulsion fuels because of the latent heat of vaporization of water which lowers the flame temperature of the combustion chamber. The HC emission for B100 was noted to be 6.02 g/kWh which increased to 11.08 g/kWh with the addition of 10% water in B100.

Figure 49 demonstrates that HC emissions increased with the increase of glycerine in glycerine emulsion as it contains a high heat of vaporization that lowers the combustion

temperature thus, producing high HC emissions. Also, the high viscosity of the glycerine emulsion fuels results in increased HC formation due to poor atomization. HC emission for B100 was 6.022 g/kWh, increased with the addition of 5% and 10% glycerine in B100 to 9.19 g/kWh and 12.18 g/kWh respectively. HC emission of B100G10% was approximately 20% higher than B0.

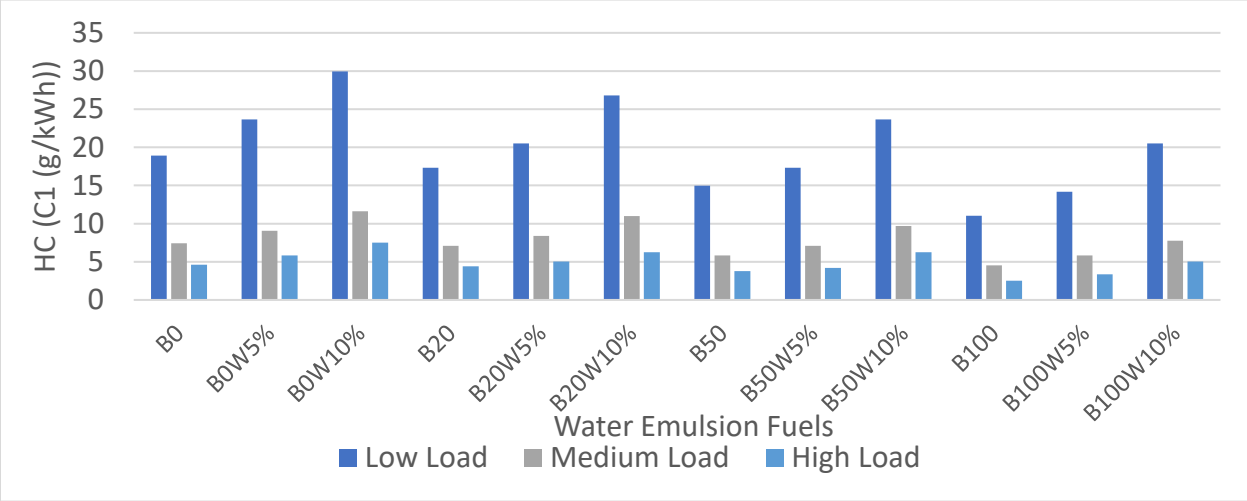

Figure 48: HC Emission of a Light-Duty Engine at Different Loads at 2100 rpm when Operated with Water Emulsion Fuel

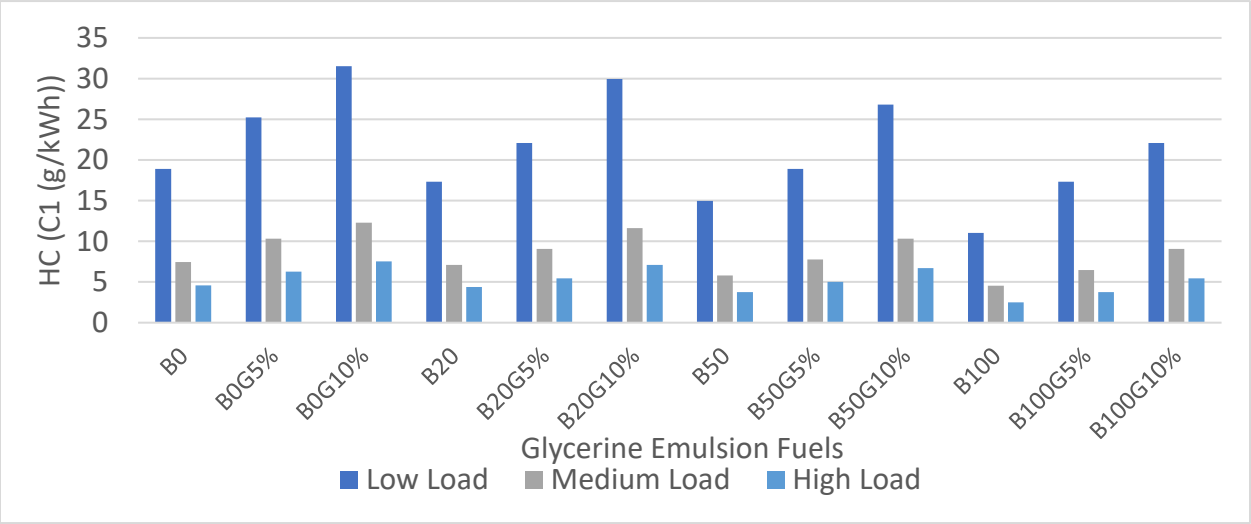

Figure 49: HC Emission of a Light-Duty Engine at Different Loads at 2100 rpm when Operated with Glycerine Emulsion Fuel

Smoke Opacity

Upon investigation of smoke emissions, it was observed that smoke opacity decreased with the increase of water and glycerine concentration.

Smoke opacity in case of water emulsion was seen to decrease (as seen in Figure 50) which was due to the micro-explosion of water droplets leading to enhanced air-fuel mixing, better fuel atomization by the injectors and reduction in burning rate constant which resulted in lower combustion temperature and lesser formation of smoke or soot. The least average smoke opacity was measured for B0W10% which was 1.87%. The smoke opacity for B100, B100W5%, and B100W10% was measured as 7.80%, 5.34% and 3.94% respectively. 50% reduction was seen in B100W10% when compared to B100.

Smoke levels were seen to reduce significantly with the increase in glycerine concentration as seen in Figure 51. Smoke emissions for B0G10% were recorded to be the lowest in case of all glycerine fuel blends. The smoke reduction for B0G10% and B100G10% was observed as 66% and 53%, respectively as compared to their base fuels. B100G10% displayed an average smoke reduction of nearly 20% w.r.t. B0. The main reason for the reduction in smoke attributed to the presence of oxygen in the emulsified fuel [141].

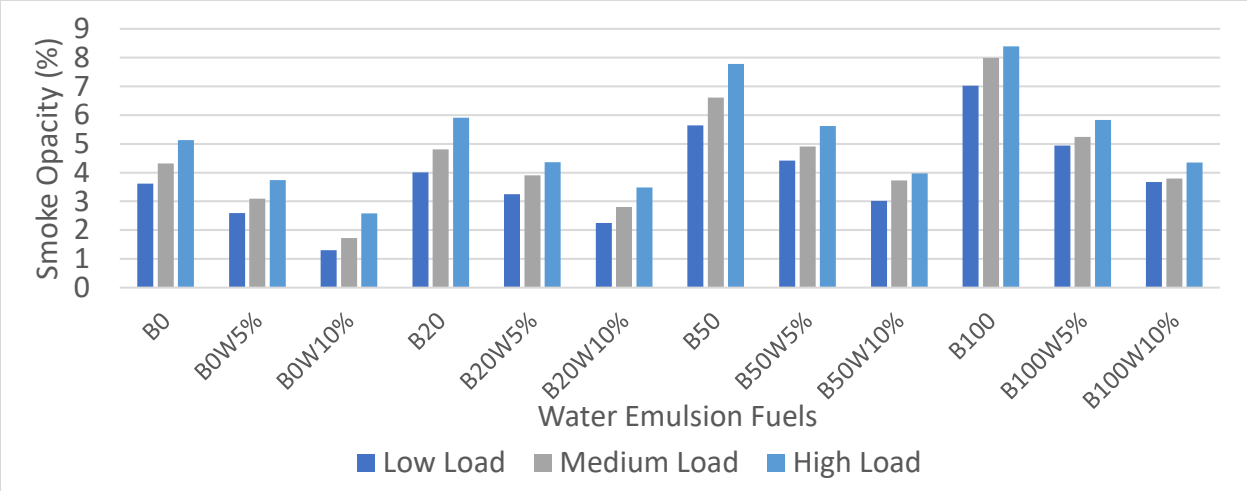

Figure 50: Smoke Opacity of a Light-Duty Engine at Different Loads at 2100 rpm when Operated with Water Emulsion Fuel

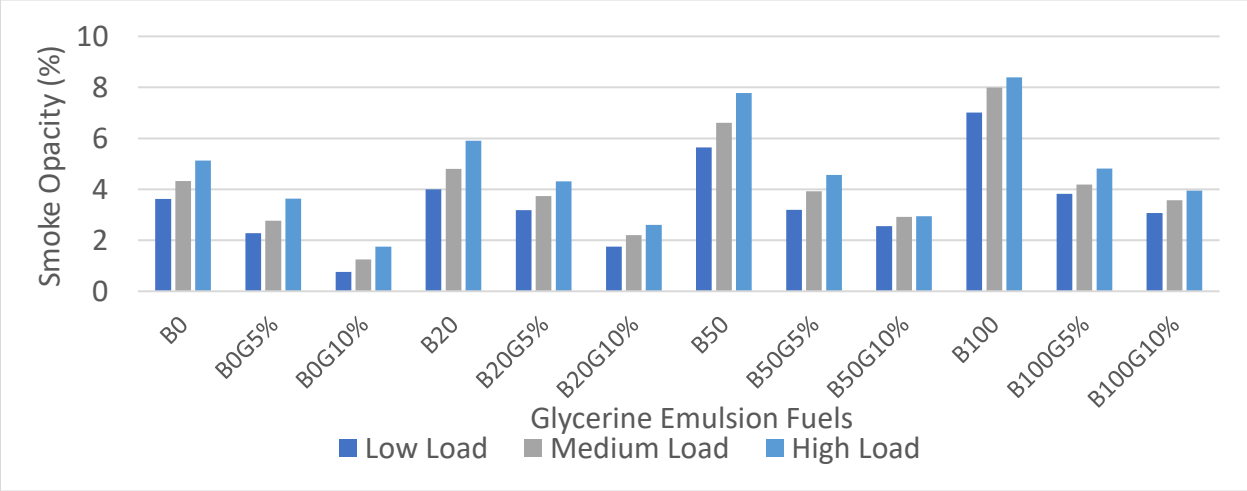

Figure 51: Smoke Opacity of a Light-Duty Engine at Different Loads at 2100 rpm when Operated with Glycerine Emulsion Fuel

EGT

The exhaust gas temperature decreased with the increase of the emulsion fuels (as shown in Figure 52 and 53) due the existence of latent heat of vaporization of water and glycerine in their emulsion fuels which reduces adiabatic flame temperature more than diesel and gasoline resulting in the cooling of exhaust gas temperature [96], [139]. EGT for B0 was found to be 220.1℃, 245℃ and 280.6℃ but it reduced to 188.5℃, 210℃ and 244.4℃ in B0W10%. EGT for glycerine emulsion fuel B0G10% was recorded as 193.6℃, 213.1℃ and 248.2℃ for low load, medium load and high load condition respectively. EGT was less in water emulsion fuels as compared to glycerine emulsion fuels because the water has higher latent heat of vaporization and low calorific value which reduces the in-cylinder temperature more than glycerine.

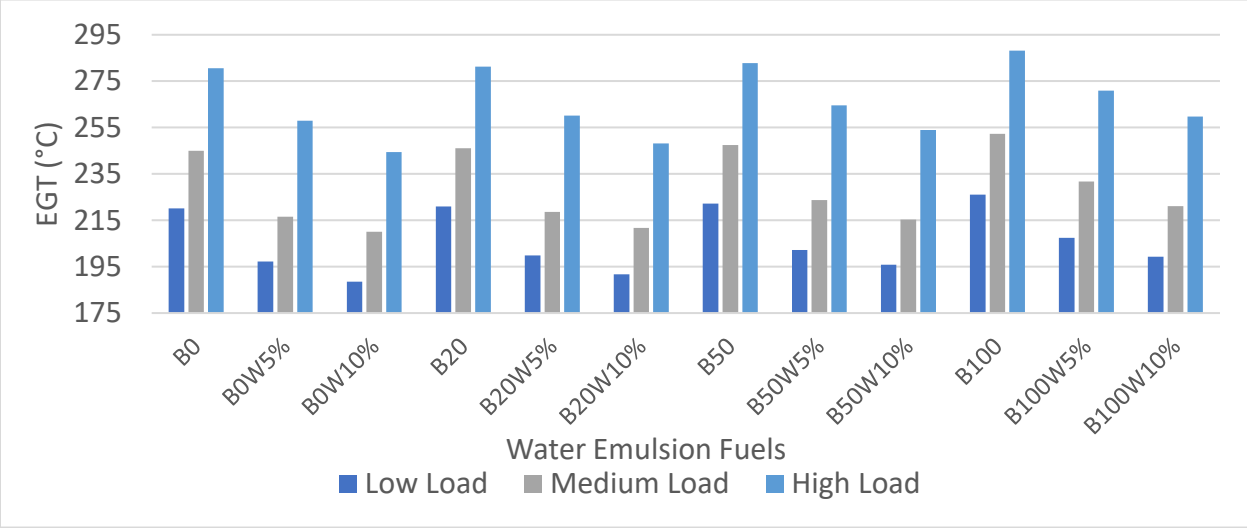

Figure 52: EGT of a Light-Duty Engine at Different Loads at 2100 rpm when Operated with Water Emulsion Fuel

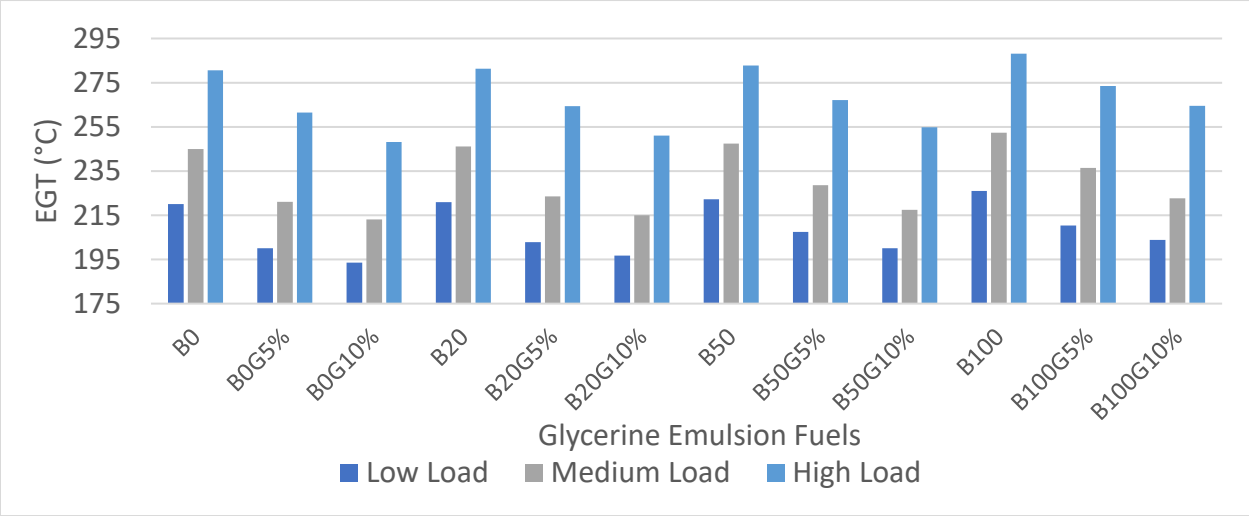

Figure 53: EGT of a Light-Duty Engine at Different Loads at 2100 rpm when Operated with Glycerine Emulsion Fuel

4.4.2 With EGR Technology

Exhaust gas recirculation (EGR) is a technique used to reduce NOx emissions which works by recirculating a small portion of the engine's the exhaust gas (inert gas- already burnt) back to engine combustion chamber which reduces the amount of oxygen present in the chamber to reduce the cylinder temperature and hence, reducing the NOx. Cold EGR technique was preferred. Base fuels like B0, B50 and B100 were tested with their water and glycerine emulsion fuels (5% and 10% content). In B100 water 2.5% and G2.5% was also tested in EGR conditions. Testing shown below was done at 2100 rpm at various load conditions. Half open valve and full open valve EGR testing was done and the EGR percentages were calculated at these points for each rpm and load conditions. All results of EGR tested at various rpms, and load conditions were included in Appendix C.

Performance

BSFC

From the investigation of graphs shown in Figures 54, 55 and 56 it was seen that BSFC increased with the use of EGR for all diesel-biodiesel fuel blends and their emulsions. The increase of BSFC with EGR may be attributed to a dilution effect, altering of air-fuel ratio and reduced oxygen and burning rate resulting in reduced combustion efficiency [108]. Furthermore, EGR requires more fuel to generate the same power output, as engine working without EGR which increases BSFC [142]. The highest increase was perceived for the water emulsion due to its lower calorific value. The increase was not as significant, but the overall increase was seen to be in the range of 0.8 g/kWh to 1.2 g/kWh for no EGR to maximum EGR percentage for all fuel blends and with their fuel emulsions.

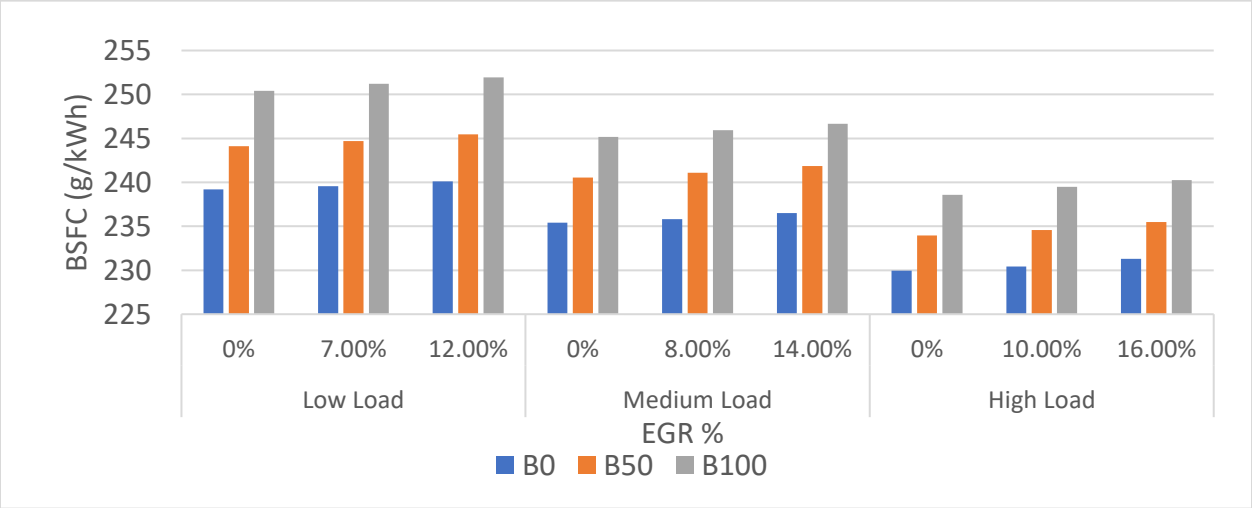

Figure 54: BSFC of a Light-Duty Engine at Different Loads with their EGR % at 2100 rpm

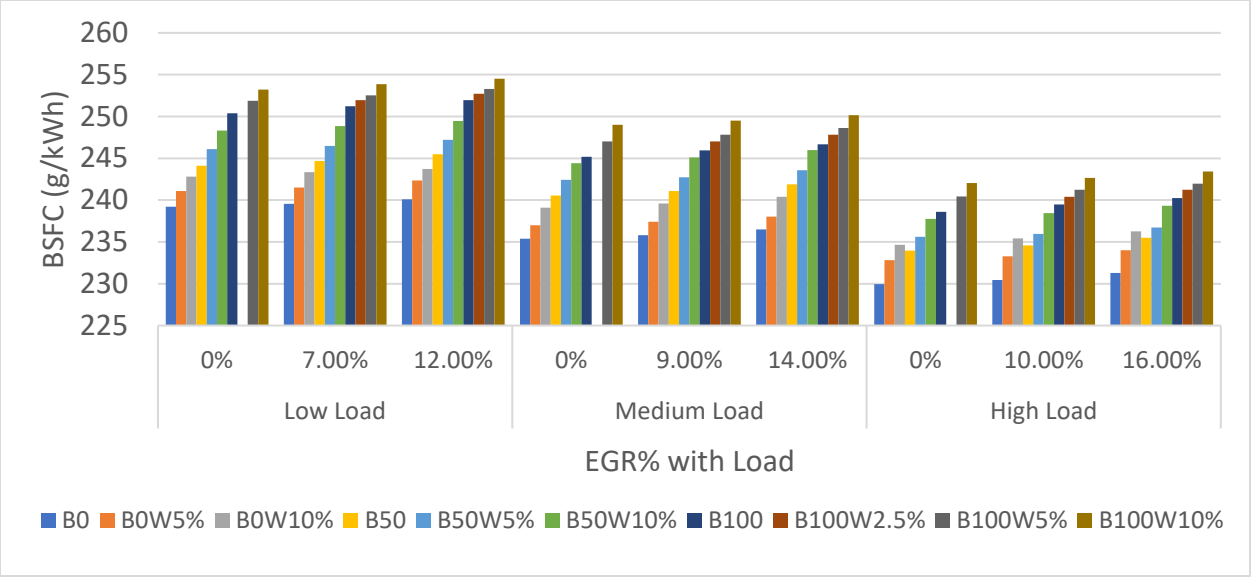

Figure 55: BSFC of a Light-Duty Engine at Different Loads with their EGR% at 2100 rpm when Operated with Water Emulsion Fuel

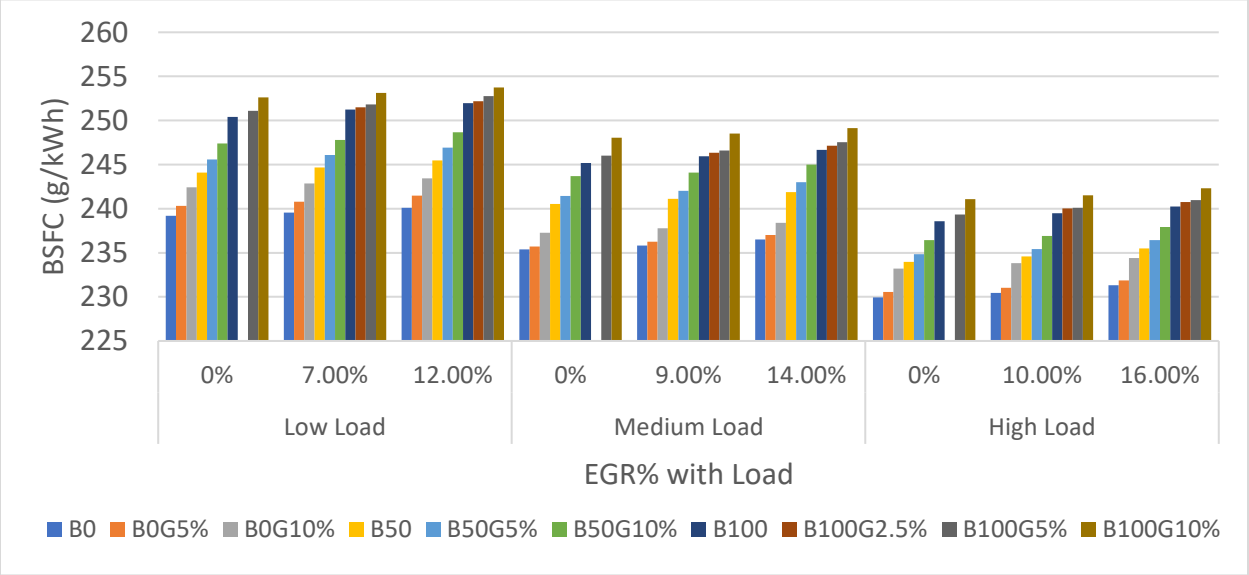

Figure 56: BSFC of a Light-Duty Engine at Different Loads with their EGR% at 2100 rpm when Operated with Glycerine Emulsion Fuel

BTE

It was observed from the results illustrated in Figures 57, 58 and 59 that BTE decreased with the increase of EGR percentage for all diesel-biodiesel fuel blends and their emulsions as EGR as creates obstruction for normal combustion process to take place due to the reduced availability of oxygen which worsens the burning rate of fuel [143]. The BTE for B100 with no EGR at 2100 rpm medium load was 36.17%, but it reduced to 35.95% when the EGR condition was maximum.

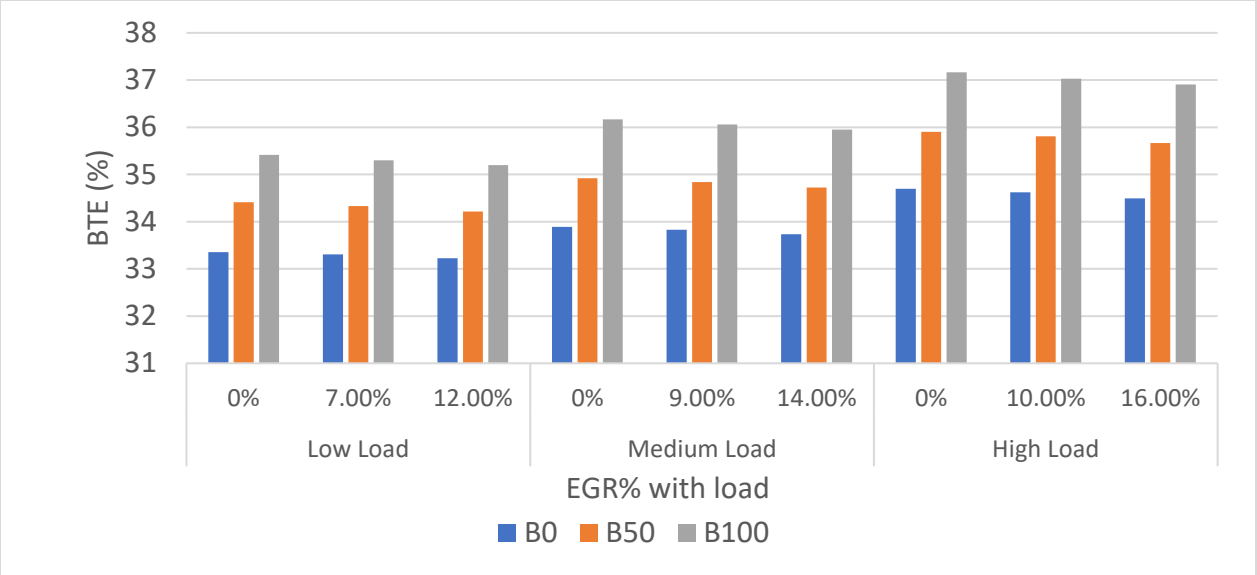

Figure 57: BTE of a Light-Duty Engine at Different Loads with their EGR % at 2100 rpm

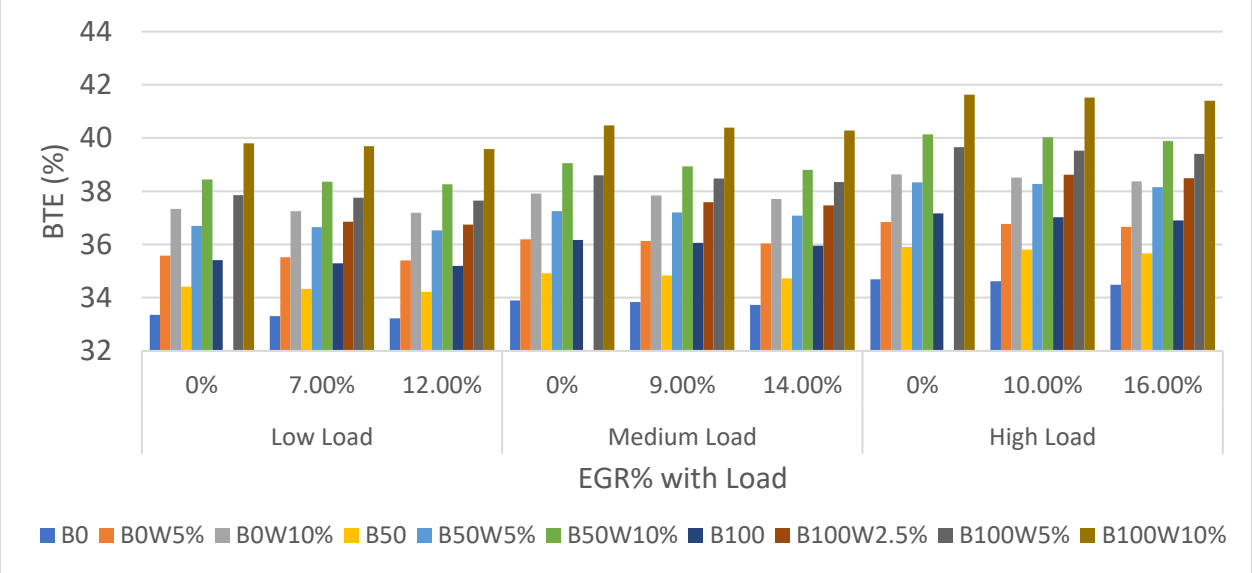

Figure 58: BTE of a Light-Duty Engine at Different Loads with their EGR% at 2100 rpm when Operated with Water Emulsion Fuel

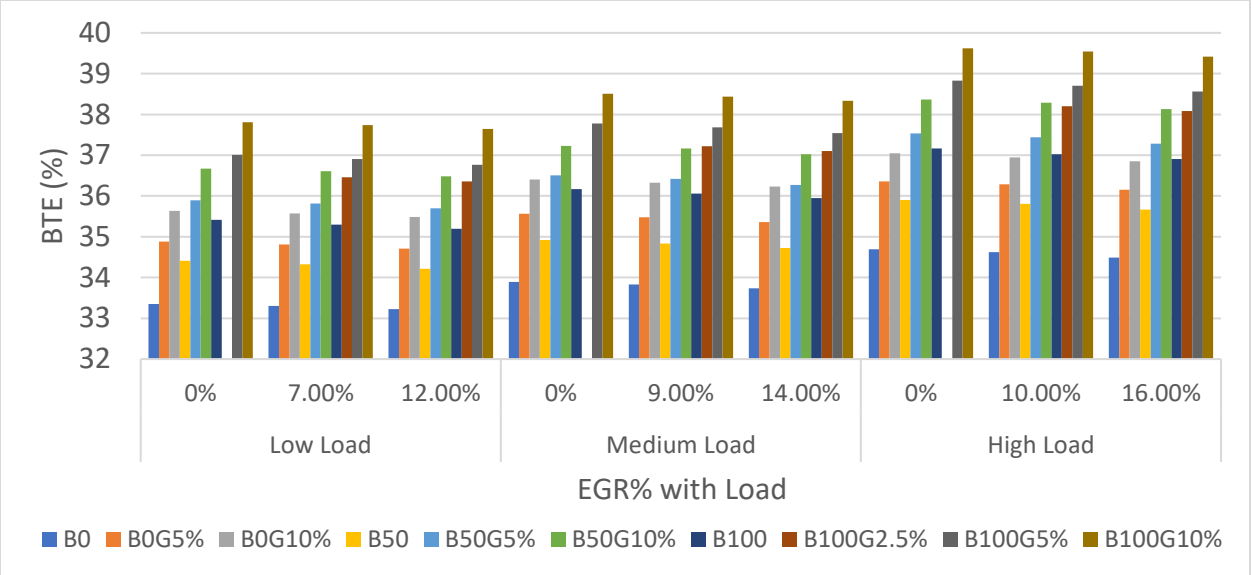

Figure 59: BTE of a Light-Duty Engine at Different Loads with their EGR% at 2100 rpm when Operated with Glycerine Emulsion Fuel

Emissions

NOx Emission

As can be seen from Figures 60, 61 and 62 it was examined that NOx emissions declined with the increase of the EGR percentage for all diesel-biodiesel fuel blends and their emulsions which is due to the fact that the recirculated exhaust gases are primarily composed of CO_2, water vapor and nitrogen (inert gases) which act as a heat sink and reduces oxygen availability and delays the combustion process thus decreasing the in-cylinder temperature and restricting NOx emissions [103]. The reduction recorded for NOx was approximately 30% for low, medium and high load for B0 at 2100 rpm on reaching the maximum EGR percentage respective to their load. B100 shows an approximate average reduction of 27%. EGR used with emulsion fuels showed a reduction of about 32% and 30% for B100W10% and B100G10% respectively at 2100 rpm and medium load condition at maximum EGR percentage.

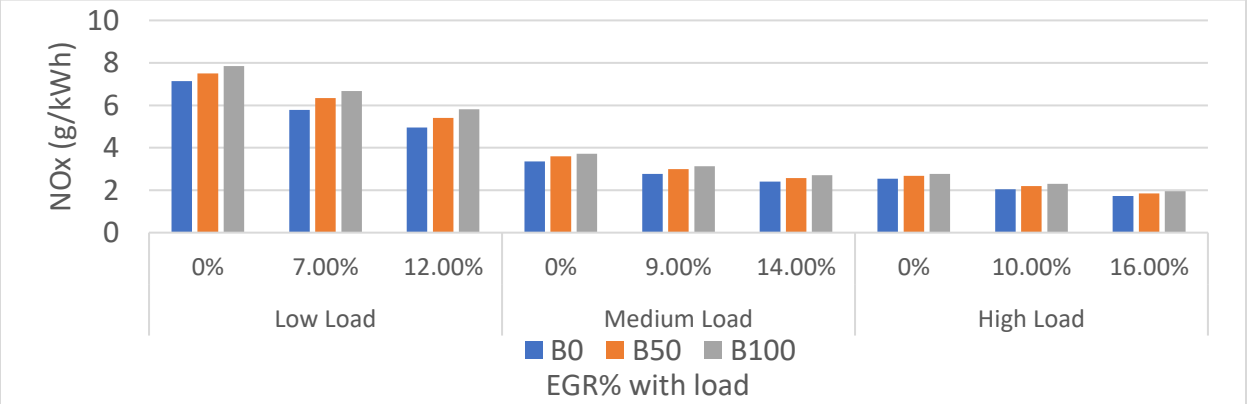

Figure 60: NOx Emission of a Light-Duty Engine at Different Loads with their EGR % at 2100 rpm

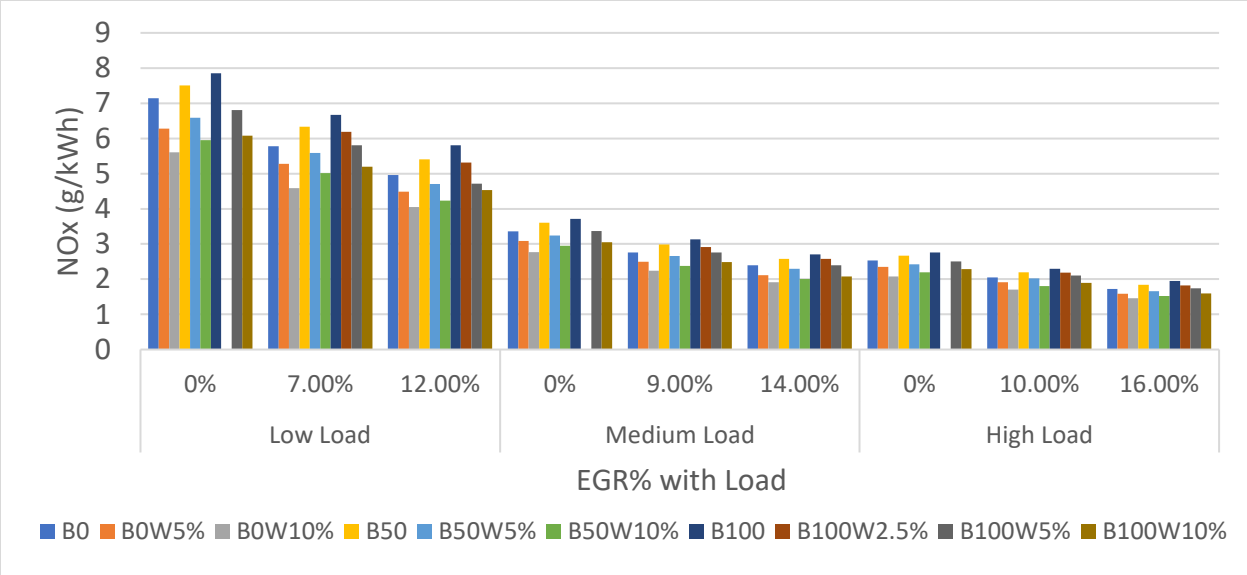

Figure 61: NOx Emission of a Light-Duty Engine at Different Loads with their EGR% at 2100 rpm when Operated with Water Emulsion Fuel

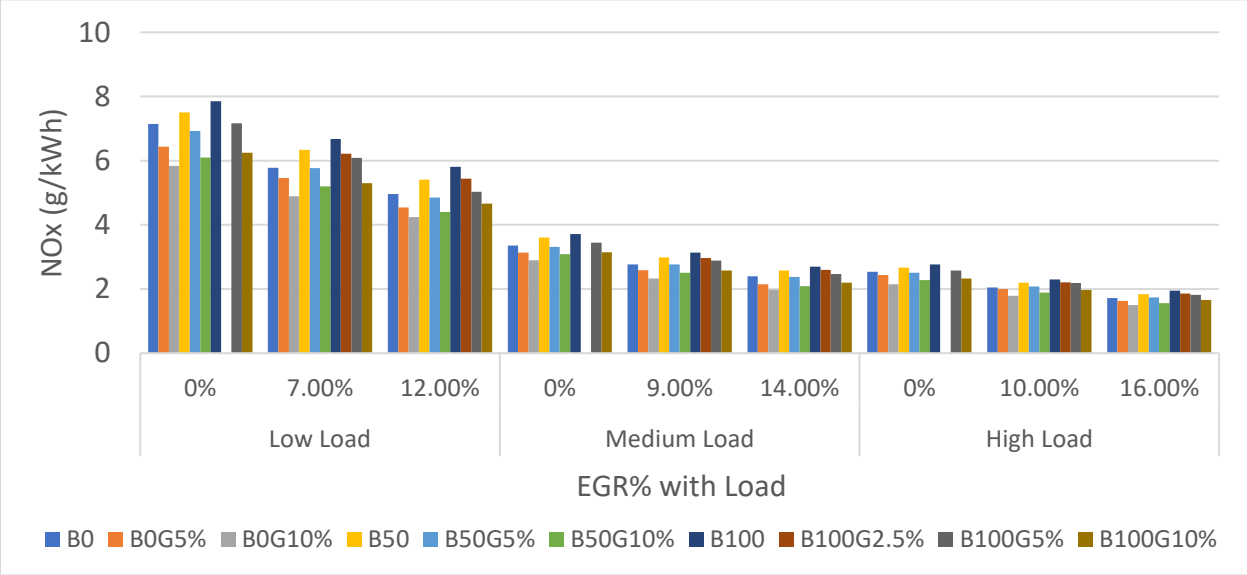

Figure 62: NOx Emission of a Light-Duty Engine at Different Loads with their EGR% at 2100 rpm when Operated with Glycerine Emulsion Fuel

CO Emission

Figures 63, 64 and 65 indicate that CO increased with the increase of EGR percentage for all diesel-biodiesel fuel blends and their emulsions as it reduces the speed and temperature of reaction in the combustion chamber which weakens the oxidation reaction and results in increased CO formation [103]. CO emissions of B100 were low in case of emulsions and EGR than B0. CO in B100, B100W10%, and B100G10% increased by approximately 33%, 45% and 39% respectively at 2100 rpm medium load condition at maximum EGR. The CO was measured to be

maximum in case of water emulsions due to its low calorific value. B100G10% (at 0% EGR) had almost equal CO emission to B0 (at maximum EGR percentage).

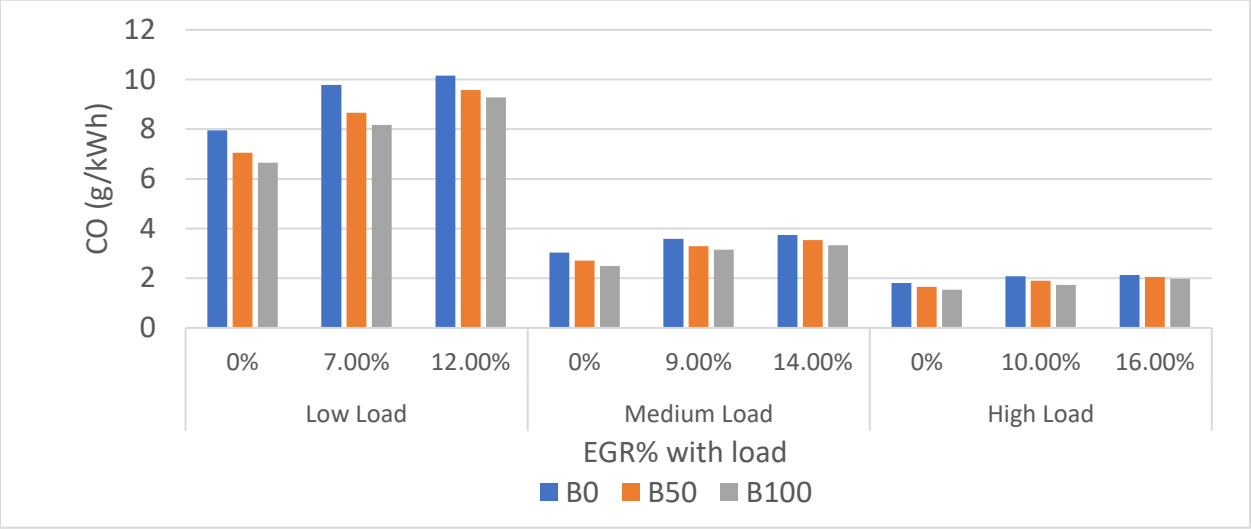

Figure 63: CO Emission of a Light-Duty Engine at Different Loads with their EGR % at 2100 rpm

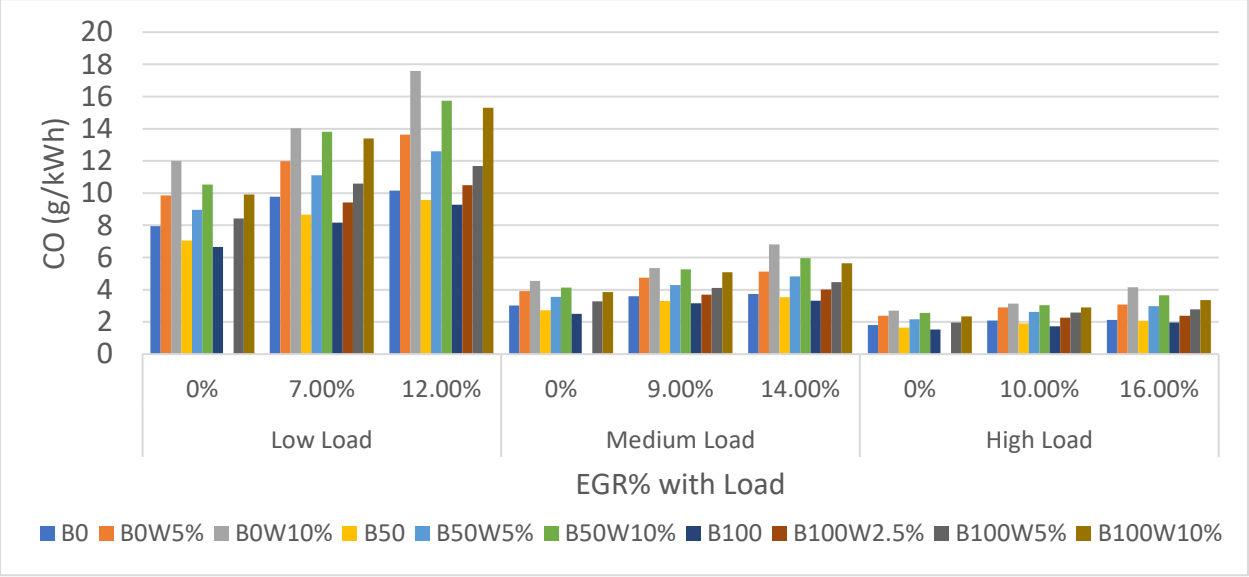

Figure 64: CO Emission of a Light-Duty Engine at Different Loads with their EGR% at 2100 rpm when Operated with Water Emulsion Fuel

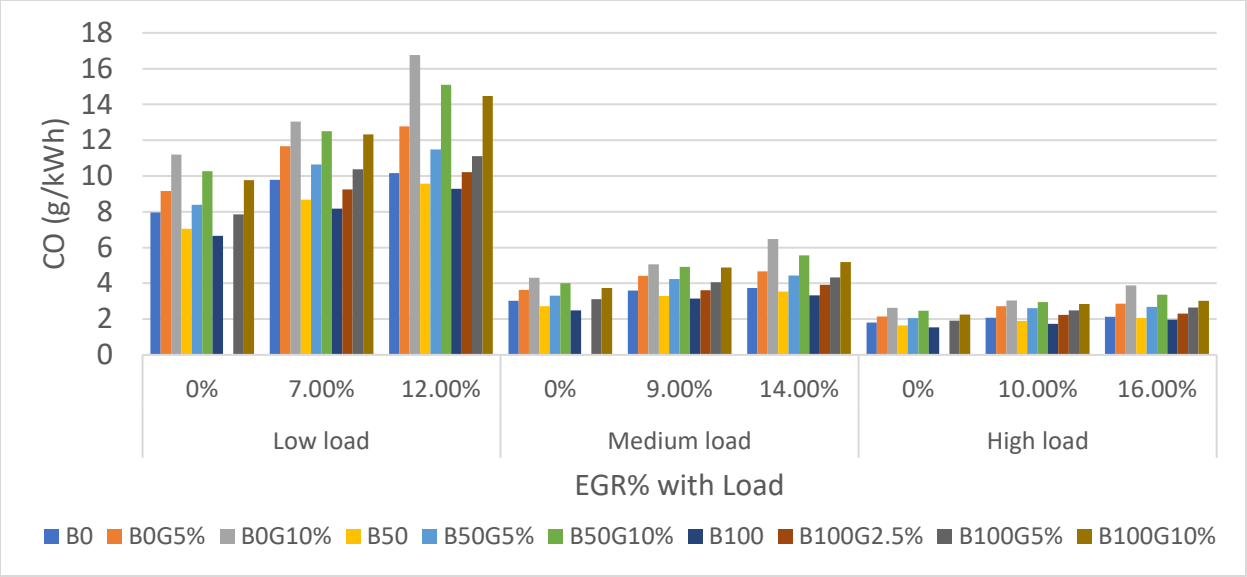

Figure 65: CO Emission of a Light-Duty Engine at Different Loads with their EGR% at 2100 rpm when Operated with Glycerine Emulsion Fuel

HC Emission

HC emissions were observed to increase with the increase of EGR percentage for all diesel-biodiesel fuel blends and their emulsions (as seen in Figures 66, 67 and 68) which can be because of the addition of exhaust gas to the inlet air that leads to improper fuel-gas mixing which reduces the combustion temperature resulting in incomplete combustion and production of unburnt hydrocarbons [144]. The increase in HC emission for B0 and B100 was 9.418 g/kWh and 7.756 g/kWh (at maximum EGR percentage) from 7.435 g/kWh and 4.525 g/kWh (at 0% EGR condition) at 2100 rpm and medium load condition. For 2100 rpm highest HC emission was recorded at low load condition and maximum EGR% as 37.393 g/kWh for B0G10%.

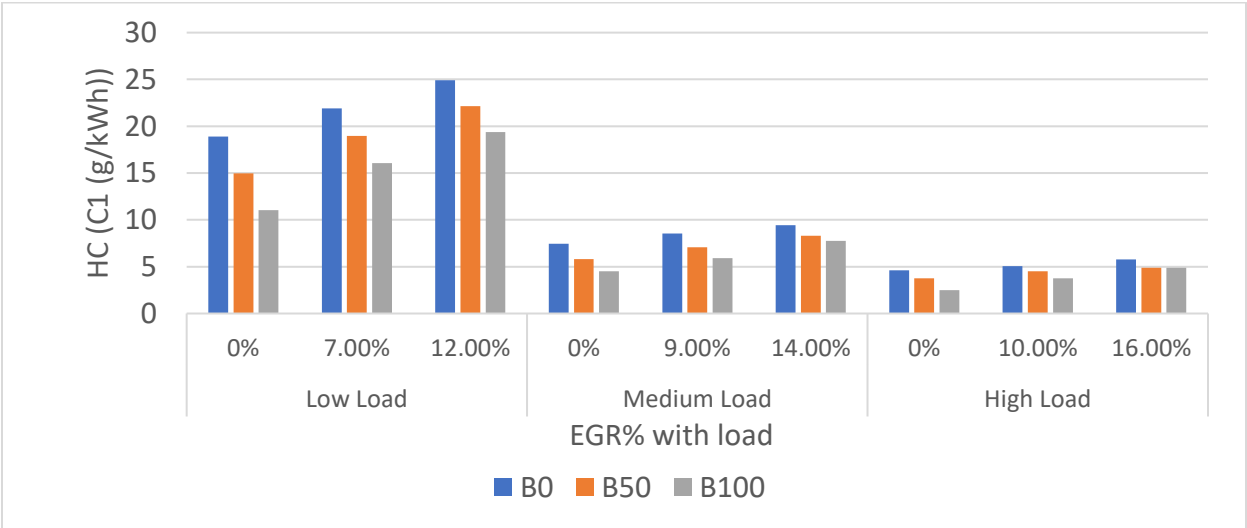

Figure 66: HC Emission of a Light-Duty Engine at Different Loads with their EGR % at 2100 rpm

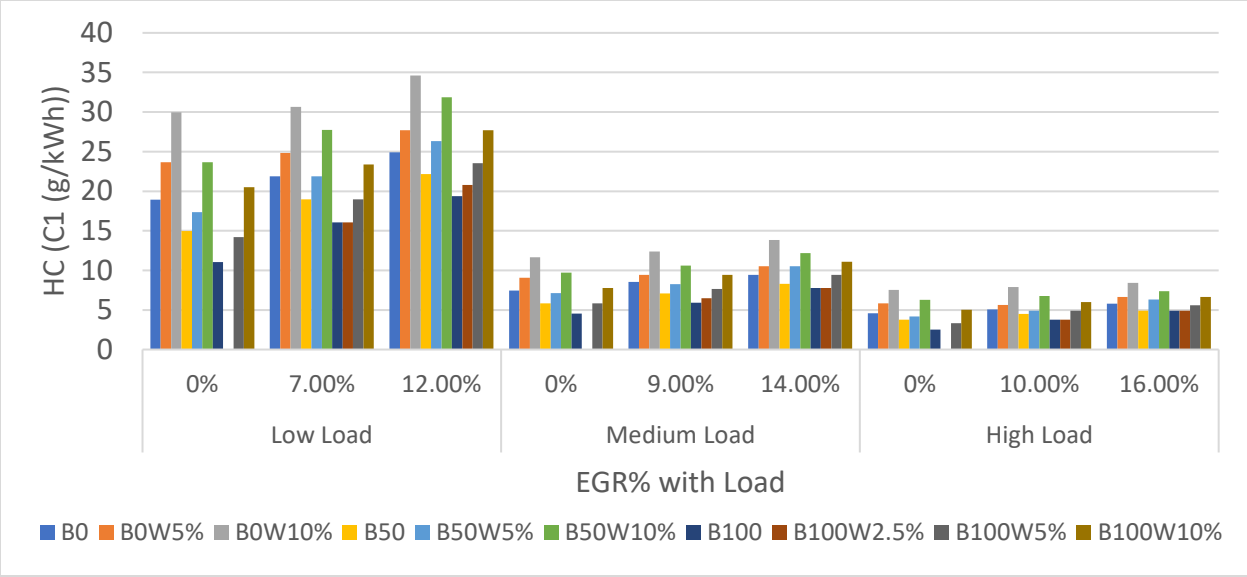

Figure 67: HC Emission of a Light-Duty Engine at Different Loads with their EGR% at 2100 rpm when Operated with Water Emulsion Fuel

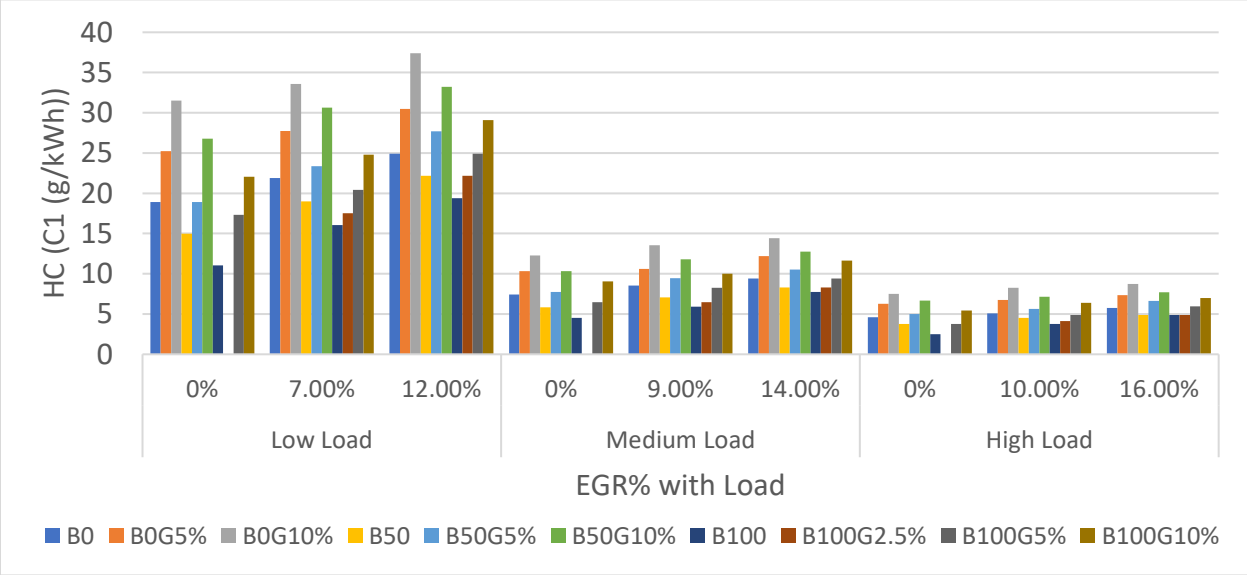

Figure 68: HC Emission of a Light-Duty Engine at Different Loads with their EGR% at 2100 rpm when Operated with Glycerine Emulsion Fuel

Smoke Opacity

On examining the results, as shown in Figure 69, 70 and 71 it was observed that with the increase of the EGR% the smoke level increased for all diesel-biodiesel fuel blends and their emulsions. Increased EGR rate reduces the oxygen quantity which leads to the reduction of the cylinder temperature causing the soot oxidation rate to decline resulting in incomplete combustion and soot/smoke formation. [58], [143]. Smoke opacity decrease with speed but increases with load and the same pattern is followed by EGR. Overall increase rate was recorded to be around 30%

for all fuels tested at 2100 rpm and medium load as depicted in the EGR graphs below. The least smoke was recorded for B0G10% which was 1.86% for 2100 rpm medium load at maximum EGR%.

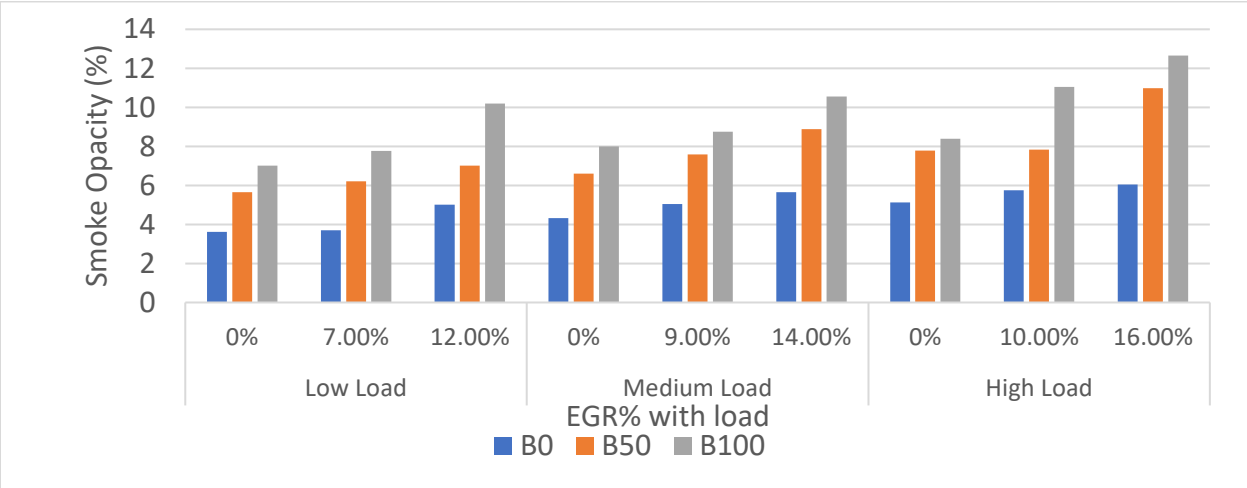

Figure 69: Smoke Opacity of a Light-Duty Engine at Different Loads with their EGR % at 2100 rpm

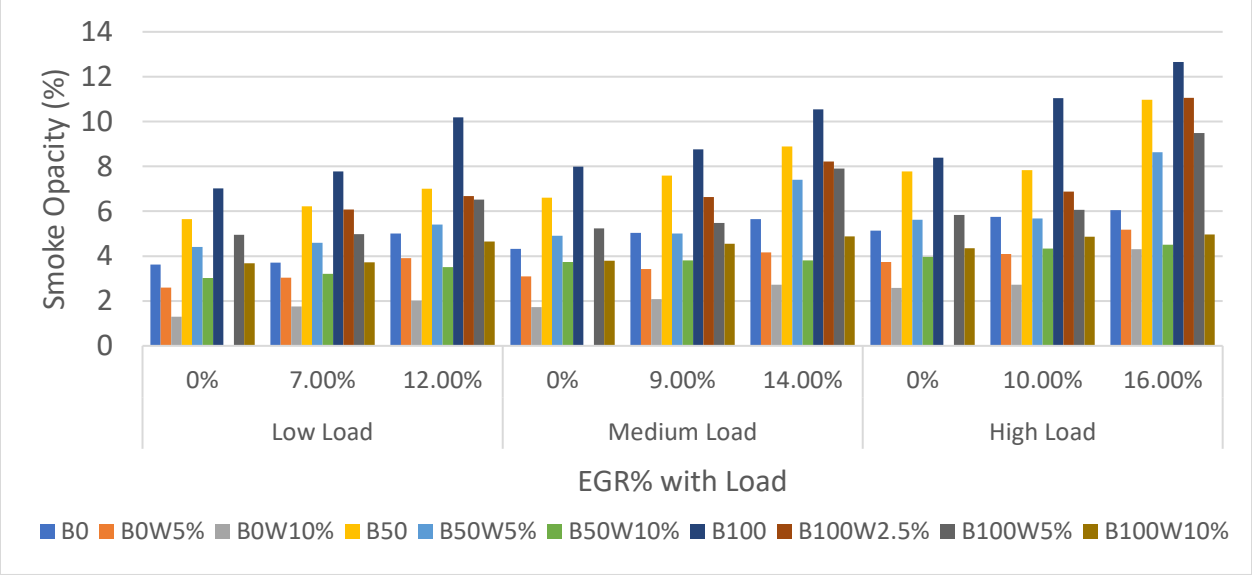

Figure 70: Smoke Opacity of a Light-Duty Engine at Different Loads with their EGR% at 2100 rpm when Operated with Water Emulsion Fuel

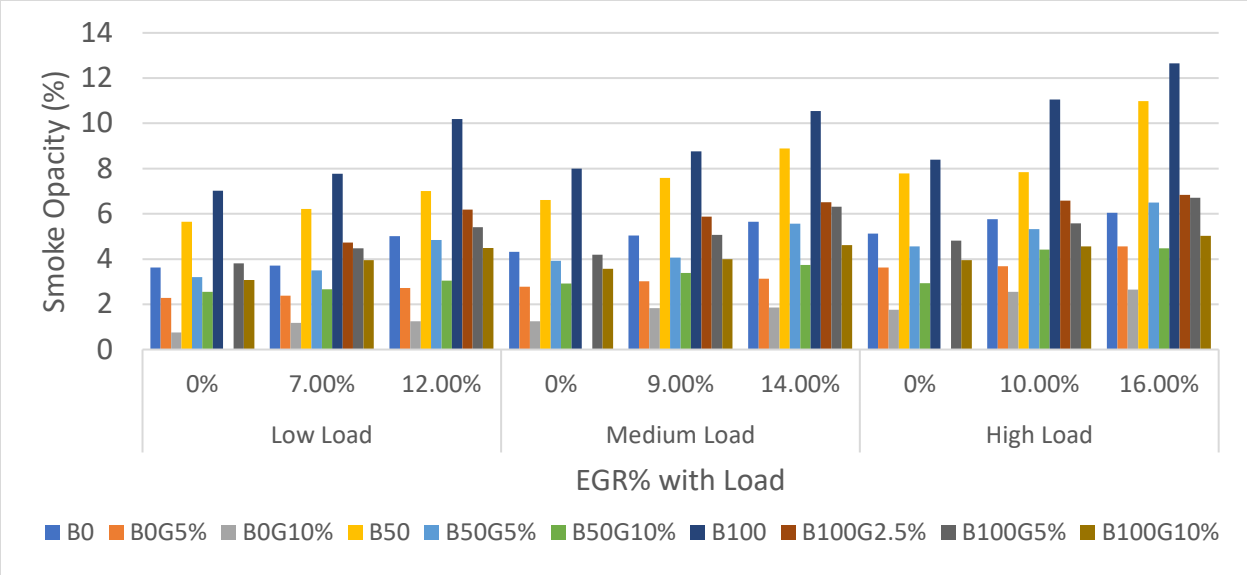

Figure 71: Smoke Opacity of a Light-Duty Engine at Different Loads with their EGR% at 2100 rpm when Operated with Glycerine Emulsion Fuel

EGT

Figures 72, 73 and 74 illustrates that with the increase of the EGR%, the exhaust gas temperature decreases because the inert gases which combine with fresh air reduces the amount of oxygen in the combustion chamber which lowers the burning efficiency of fuel and the incomplete combustion occurs resulting in the reduction of in-cylinder temperature [142]. EGT was minimum in case of water emulsions which was followed by glycerine emulsions and base fuels as water emulsions have the lowest calorific value and water has the high latent heat of vaporization which decreases the cylinder temperature. From the figures below, it can be observed that the reduction in EGT varies between 3.75% to 5.5%. The maximum EGT and minimum EGT were recorded as 242.3℃ and 200.1℃ for B100 and B0W10% at maximum EGR%.

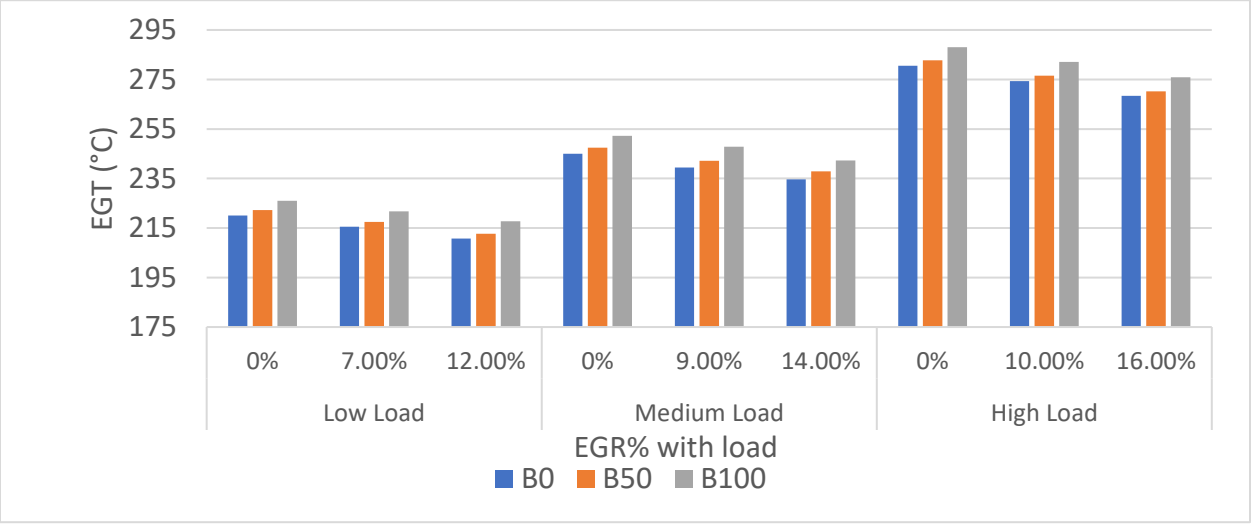

Figure 72: EGT of a Light-Duty Engine at Different Loads with their EGR % at 2100 rpm

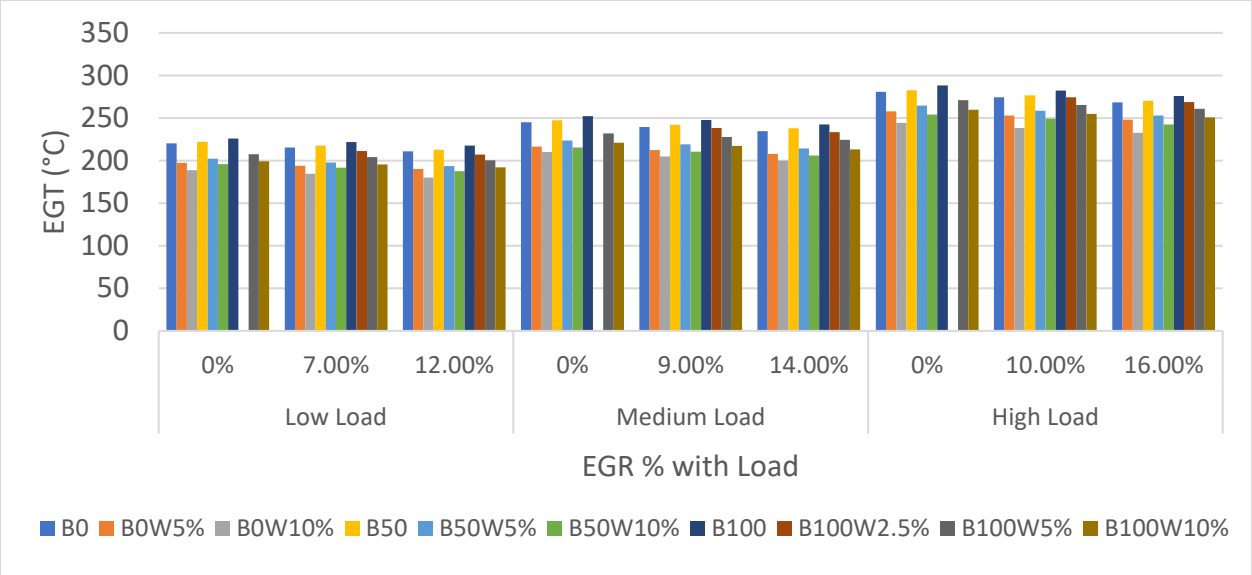

Figure 73: EGT of a Light-Duty Engine at Different Loads with their EGR% at 2100 rpm when Operated with Water Emulsion Fuel

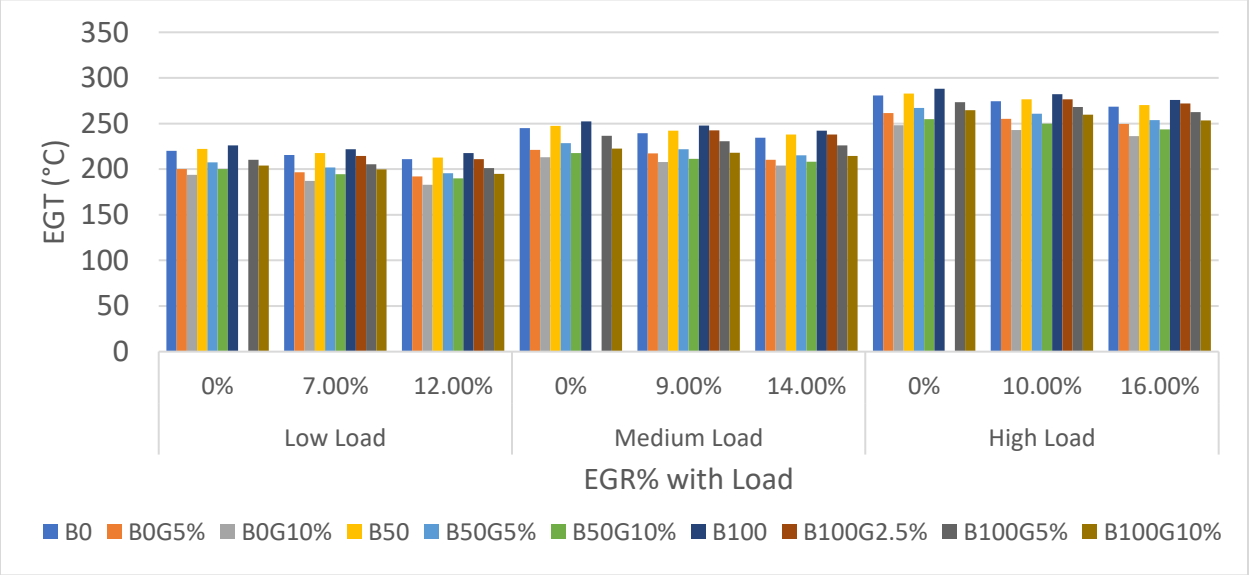

Figure 74: EGT of a Light-Duty Engine at Different Loads with their EGR% at 2100 rpm when Operated with Glycerine Emulsion Fuel

CHAPTER 5: CONCLUSION and FUTURE WORK

In this study, performance and emissions of various fuels were investigated on two different types of engines: light-duty engine and heavy-duty engine. For the investigation, two fuels which are pure diesel and pure biodiesel were used, and their diesel-biodiesel blends were prepared. Later, these fuels were emulsified using water and glycerine in different percentages (5% and 10%). The glycerine used for the emulsion fuel was the by-product of biodiesel which was purified using orthogonal test method. EGR technology was developed and installed on light duty engine. Several experiments were performed on a light-duty diesel engine to investigate the performance and emission of the fuels used with and without EGR at various speed and load conditions. The heavy-duty engine was used to investigate the emissions of the various fuels at two different idling speed conditions. Below are the conclusions which were investigated while testing.

The investigation results are summarized as follows:

Crude glycerine was obtained as a by-product of biodiesel which was purified to remove the impurities present in it which can affect its stability when used emulsion fuel and can cause ash-related problems.

In case of emulsion fuels, an increase in the droplet size was seen, due to the increase in biodiesel, water and glycerine, which increased viscosity and reduced its stability. On the other hand, with the increase in biodiesel, water and glycerine concentration in diesel, the heating value declined because of the high oxygen content present in the fuel. The lowest heating values were seen in case of emulsion fuels.

The best results for BSFC were found at 2100 rpm, and it decreased with the increase of load. Reduction in the heating value resulted in an increase to BSFC and BSFC was observed to be the lowest at high load. The highest BSFC was noticed for water emulsion fuel blends which were followed by glycerine emulsions and their base fuel. BSFC for B100W10% was 260.311 g/kWh at 1000 rpm, and low load condition and an increase of 4.67% was seen in it as compared to B0 at the same condition. BSFC was also seen to increase with the increase of EGR, even though the increase was not very significant. The lowest BSFC with maximum EGR% was seen at 2100 rpm high load condition which was 231.305 g/kWh for B0.

From the results, it was investigated that BTE increases with the load and the maximum thermal efficiency were achieved at 2100 rpm. An increase in BTE was observed with the increase in the percentages of biodiesel, water, and glycerine. Maximum BTE for glycerine emulsion was achieved at B100G10% which was 39.62% and in case of water emulsions B100W10% showed the maximum BTE noted as 41.63% at high load condition. B50W10% showed 1.32% more BTE than B100G10%. The average BTE of B100G10% was found to be about 4 percentage points higher than the average BTE of B0. BTE was found to decrease with the increase of EGR for all fuels at all speeds and load conditions.

Results showed that NOx decreased with the increase in speed and load. NO_x increased with the increase in biodiesel concentration but declined with the increase in the percentage of water and glycerine. The maximum reduction was observed at high load in each rpm. Average NOx for B100W10% and B100G10% was 20% and 18% lower than that of B100 and about 12% and 10%

lower than B0. Furthermore, NOx was also seen to reduce with the increase in EGR%. The average emission of NOx without EGR were 4.29 g/kWh, 3.44 g/kWh and 3.6 g/kWh for B100, B100W10% and B100G10% which were reduced to 2.99 g/kWh, 2.32 g/kWh and 2.38 g/kWh in case of maximum EGR, about 30% reduction was seen with EGR.

In case of smoke opacity, a similar trend was followed by all the investigated fuels. Smoke decreased with the increase in speed but increased w.r.t. loads. A decrease was seen in smoke levels with the addition of glycerine and water. The lowest smoke emission was shown by B0G10% which was examined to be 0.442% at 3000 rpm and low load condition which showed a reduction of 79% as compared to B0G10% at 1000 rpm and low load condition. B100G10% reduced 53% more smoke than B100. Although higher biodiesel content in the blend emitted higher smoke, B100G10% it still displayed about 20% average smoke reduction compared to B0. Additionally, it was found that with the increase of EGR% smoke opacity increased. The average increase of smoke varied between 25% to 40% at various speeds and loads for without EGR% condition and maximum EGR% condition.

There was a decrease seen in CO and HC emissions with the increase of load and speed. Also, CO and HC emissions were also noted to decline with the increase in biodiesel but increased in the addition of water and glycerine emulsion. B100 emitted 16% lower CO than B0, and there are no change in CO emissions up to 5% glycerin emulsions, but a minute increase was noticed for 5% water emulsion of B100. On an average, water emulsion demonstrated about 10% higher CO emissions than those witnessed for glycerine emulsion. As for HC emissions, it was observed that B100 emitted 40% lower HC than B0, and HC with B100G5% and B100W5% were still 10% and 19% lower than B0 whereas B100W10% showed 12% increase in HC as compared to B0. With the use of EGR, CO and HC emissions increased for all fuels at all speeds and loads. Average increase of CO was calculated in the range of about 30% to 50% for all fuels depending upon their speed and load at maximum EGR condition. The lowest HC observed was for B100W2.5% and B100G2.5% which was 4.376 g/kWh at 3000 rpm and high load condition.

For EGT it was noticed that it increased with increase in speed and load for all fuels. EGT decreased with an increase in glycerine and water concentration in emulsion fuels but increased with the increase in biodiesel concentration. Furthermore, EGT for pure biodiesel was slightly more than pure diesel. With the increase in the EGR decrease in EGT was perceived for all fuels.

Data gathered from the experiments done at two different idling speeds on the heavy-duty engine for various fuels displayed the similar trends. It was seen that NOx emissions for biodiesel fuel were higher than other fuel blends. Emulsion fuels were prepared to decrease the NOx emissions for all fuel blends using water and glycerine. The lowest NOx emissions were seen in B0W10% at both idling speeds than other tested fuels. CO emissions and HC emissions were found to be the lowest for B100. B100 demonstrated a decrease in CO of about 26% and 36% and in HC of about 23% and 57% than B0 at 1000 rpm and 1500 rpm respectively. However, with the use of emulsion fuels, a substantial increase was observed in both, CO and HC emissions. A rise in smoke opacity was noted with the increase in biodiesel, but it decreased with emulsion fuels. A decrease of about 40% for B100G10% and 30% B100W10% was seen in smoke when compared to B100.

FUTURE WORK:

Even though the research undertaken in this study was able to fulfill its objective there is still more research needed to be done in this direction:

1. More research needs to be done on the stability and on the droplet size of the emulsion fuels, especially on glycerine emulsion fuels.
2. Efficient method can be proposed for the purification of glycerine (in sense of time and cost saving). Orthogonal test method gives high percentage of the purity level, but it is time consuming.
3. Research should be done with prime focus on glycerine to test its performance and emission and explore its role as a possible fuel.
4. By using the emulsion fuels and EGR technique, CO and HC levels increase at high percentage. To reduce them, new techniques should be developed or working on the DOC (diesel oxidation catalyst) should be done which can convert CO and HC to CO_2. Its an aftertreatment componen

REFERENCES

[1] E. Foster, M. Contestabile, J. Blazquez, B. Manzano, M. Workman, and N. Shah, "The unstudied barriers to widespread renewable energy deployment: Fossil fuel price responses," *Energy Policy*, vol. 103, pp. 258–264, 2017.

[2] M. Turkensteen, "The accuracy of carbon emission and fuel consumption computations in green vehicle routing," *Eur. J. Oper. Res.*, vol. 262, no. 2, pp. 647–659, 2017.

[3] M. F. Othman, A. Adam, G. Najafi, and R. Mamat, "Green fuel as alternative fuel for diesel engine: A review," *Renewable and Sustainable Energy Reviews*, vol. 80. pp. 694–709, 2017.

[4] P. Geng, E. Cao, Q. Tan, and L. Wei, "Effects of alternative fuels on the combustion characteristics and emission products from diesel engines: A review," *Renewable and Sustainable Energy Reviews*, vol. 71. pp. 523–534, 2017.

[5] J. N. Nair, A. K. Kaviti, and A. K. Daram, "Analysis of performance and emission on compression ignition engine fuelled with blends of neem biodiesel," *Egypt. J. Pet.*, 2016.

[6] Z. Zhang *et al.*, "Effects of fatty acid methyl esters proportion on combustion and emission characteristics of a biodiesel fueled marine diesel engine," *Energy Convers. Manag.*, vol. 159, no. March, pp. 244–253, Mar. 2018.

[7] G. Knothe, "Biodiesel and renewable diesel: A comparison," *Progress in Energy and Combustion Science*, vol. 36, no. 3. pp. 364–373, 2010.

[8] F. Soto *et al.*, "The determination of the activation energy of diesel and biodiesel fuels and the analysis of engine performance and soot emissions," *Fuel Process. Technol.*, vol. 174, no. November 2017, pp. 69–77, 2018.

[9] M. M. Roy, W. Wang, and M. Alawi, "Performance and emissions of a diesel engine fueled by biodiesel-diesel, biodiesel-diesel-additive and kerosene-biodiesel blends," *Energy Convers. Manag.*, vol. 84, pp. 164–173, 2014.

[10] T. Issariyakul and A. K. Dalai, "Biodiesel from vegetable oils," *Renewable and Sustainable Energy Reviews*, vol. 31. pp. 446–471, 2014.

[11] J. Žaglinskis, K. Lukács, and Bereczky, "Comparison of properties of a compression ignition engine operating on diesel-biodiesel blend with methanol additive," *Fuel*, vol. 170, pp. 245–253, 2016.

[12] H. Caliskan, "Environmental and enviroeconomic researches on diesel engines with diesel and biodiesel fuels," *J. Clean. Prod.*, vol. 154, pp. 125–129, 2017.

[13] E. Buyukkaya, "Effects of biodiesel on a di diesel engine performance, emission and combustion characteristics," *Fuel*, vol. 89, no. 10, pp. 3099–3105, 2010.

[14] M. Zheng, M. C. Mulenga, G. T. Reader, M. Wang, D. S. K. Ting, and J. Tjong, "Biodiesel engine performance and emissions in low temperature combustion," *Fuel*, vol. 87, no. 6, pp. 714–722, 2008.

[15] E. E. Oprescu *et al.*, "Performance and emission characteristics of diesel engine powered

with diesel-glycerol derivatives blends," *Fuel Process. Technol.*, vol. 126, pp. 460–468, 2014.

[16] M. Lapuerta, J. Rodríguez-Fernández, and R. García-Contreras, "Effect of a glycerol-derived advanced biofuel -FAGE (fatty acid formal glycerol ester)- on the emissions of a diesel engine tested under the New European Driving Cycle," *Energy*, vol. 93, pp. 568–579, 2015.

[17] C. Beatrice, G. Di Blasio, C. Guido, C. Cannilla, G. Bonura, and F. Frusteri, "Mixture of glycerol ethers as diesel bio-derivable oxy-fuel: Impact on combustion and emissions of an automotive engine combustion system," *Appl. Energy*, vol. 132, pp. 236–247, 2014.

[18] J. Esteban and A. J. Vorholt, "Obtaining glycerol carbonate and glycols using thermomorphic systems based on glycerol and cyclic organic carbonates: Kinetic studies," *J. Ind. Eng. Chem.*, 2018.

[19] L. Leng *et al.*, "Rhamnolipid based glycerol-in-diesel microemulsion fuel: Formation and characterization," *Fuel*, vol. 147, pp. 76–81, 2015.

[20] W. A. Khanday, P. U. Okoye, and B. H. Hameed, "Biodiesel byproduct glycerol upgrading to glycerol carbonate over lithium–oil palm ash zeolite," *Energy Convers. Manag.*, vol. 151, no. September, pp. 472–480, 2017.

[21] S. A. Steinmetz, J. S. Herrington, C. K. Winterrowd, W. L. Roberts, J. O. L. Wendt, and W. P. Linak, "Crude glycerol combustion: Particulate, acrolein, and other volatile organic emissions," *Proc. Combust. Inst.*, vol. 34, no. 2, pp. 2749–2757, 2013.

[22] A. Presciutti, F. Asdrubali, G. Baldinelli, A. Rotili, M. Malavasi, and G. Di Salvia, "Energy and exergy analysis of glycerol combustion in an innovative flameless power plant," *J. Clean. Prod.*, vol. 172, pp. 3817–3824, 2018.

[23] F. Sundus, M. A. Fazal, and H. H. Masjuki, "Tribology with biodiesel: A study on enhancing biodiesel stability and its fuel properties," *Renewable and Sustainable Energy Reviews*, vol. 70. pp. 399–412, 2017.

[24] E. S. Tan, P. Kumaran, T. M. Indra, and K. Yoshikawa, "Effect of Non-Edible Biodiesel Physical and Chemical Properties as Microturbine Fuel," in *Energy Procedia*, 2017, vol. 142, pp. 413–418.

[25] M. S. M. Zaharin, N. R. Abdullah, G. Naja, H. Sharudin, and T. Yusaf, "Effects of physicochemical properties of biodiesel fuel blends with alcohol on diesel engine performance and exhaust emissions : A review," *Renew. Sustain. Energy Rev.*, vol. 79, no. March, pp. 475–493, 2017.

[26] C. Caldeira, F. Freire, E. A. Olivetti, and R. Kirchain, "Fatty acid based prediction models for biodiesel properties incorporating compositional uncertainty," *Fuel*, vol. 196, pp. 13–20, 2017.

[27] S. K. Hoekman, A. Broch, C. Robbins, E. Ceniceros, and M. Natarajan, "Review of biodiesel composition, properties, and specifications," *Renewable and Sustainable Energy Reviews*, vol. 16, no. 1. pp. 143–169, 2012.

[28] A. Patel, N. Arora, J. Mehtani, V. Pruthi, and P. A. Pruthi, “Assessment of fuel properties on the basis of fatty acid profiles of oleaginous yeast for potential biodiesel production,” *Renewable and Sustainable Energy Reviews*, vol. 77. pp. 604–616, 2017.

[29] G. Szabados and Á. Bereczky, “Experimental investigation of physicochemical properties of diesel, biodiesel and TBK-biodiesel fuels and combustion and emission analysis in CI internal combustion engine,” *Renew. Energy*, vol. 121, pp. 568–578, 2018.

[30] H. G. How, H. H. Masjuki, M. A. Kalam, and Y. H. Teoh, “Influence of injection timing and split injection strategies on performance, emissions, and combustion characteristics of diesel engine fueled with biodiesel blended fuels,” *Fuel*, vol. 213, no. October 2017, pp. 106–114, 2018.

[31] K. A. Sorate and P. V. Bhale, “Biodiesel properties and automotive system compatibility issues,” *Renew. Sustain. Energy Rev.*, vol. 41, pp. 777–798, 2015.

[32] P. Zareh, A. A. Zare, and B. Ghobadian, “Comparative assessment of performance and emission characteristics of castor, coconut and waste cooking based biodiesel as fuel in a diesel engine,” *Energy*, vol. 139, 2017.

[33] J. F. Sierra-Cantor and C. A. Guerrero-Fajardo, “Methods for improving the cold flow properties of biodiesel with high saturated fatty acids content: A review,” *Renewable and Sustainable Energy Reviews*, vol. 72. pp. 774–790, 2017.

[34] R. Sakthivel, K. Ramesh, R. Purnachandran, and P. Mohamed Shameer, “A review on the properties, performance and emission aspects of the third generation biodiesels,” *Renew. Sustain. Energy Rev.*, vol. 82, no. 5, pp. 2970–2992, 2018.

[35] K. Venkata Sundar Rao, S. N. Kurbet, and V. V. Kuppast, “A Review on Performance of the IC Engine Using Alternative Fuels,” *Mater. Today Proc.*, vol. 5, no. 1, pp. 1989–1996, 2018.

[36] T. M. Yunus Khan *et al.*, “Effects of engine variables and heat transfer on the performance of biodiesel fueled IC engines,” *Renew. Sustain. Energy Rev.*, vol. 44, pp. 682–691, 2015.

[37] M. A. Akar, E. Kekilli, O. Bas, S. Yildizhan, H. Serin, and M. Ozcanli, “Hydrogen enriched waste oil biodiesel usage in compression ignition engine,” *Int. J. Hydrogen Energy*, pp. 1–7, 2018.

[38] D. N. Thoai, A. Kumar, K. Prasertsit, and C. Tongurai, “Evaluation of Biodiesel Production Process by the Determining of the Total Glycerol Content in Biodiesel,” *Energy Procedia*, vol. 138, pp. 544–551, 2017.

[39] S. Soltani, U. Rashid, R. Yunus, and Y. H. Taufiq-Yap, “Synthesis of Biodiesel through Catalytic Transesterification of Various Feedstocks using Fast Solvothermal Technology: A Critical Review,” *Catalysis Reviews - Science and Engineering*, vol. 57, no. 4. pp. 407–435, 2015.

[40] M. Rehan *et al.*, “Waste to biodiesel: A preliminary assessment for Saudi Arabia,” *Bioresour. Technol.*, vol. 250, no. November 2017, pp. 17–25, 2018.

[41] M. Canakci, A. Erdil, and E. Arcaklioğlu, “Performance and exhaust emissions of a biodiesel engine,” *Appl. Energy*, vol. 83, no. 6, pp. 594–605, 2006.

[42] H. Liu, X. Ma, B. Li, L. Chen, Z. Wang, and J. Wang, “Combustion and emission characteristics of a direct injection diesel engine fueled with biodiesel and PODE/biodiesel fuel blends,” *Fuel*, vol. 209, pp. 62–68, 2017.

[43] M. Cardone *et al.*, “Brassica carinata as an alternative oil crop for the production of biodiesel in Italy: Agronomic evaluation, fuel production by transesterification and characterization,” *Biomass and Bioenergy*, vol. 25, no. 6, pp. 623–636, 2003.

[44] M. N. Nabi, A. Zare, F. M. Hossain, Z. D. Ristovski, and R. J. Brown, “Reductions in diesel emissions including PM and PN emissions with diesel-biodiesel blends,” *J. Clean. Prod.*, vol. 166, pp. 860–868, 2017.

[45] Environment and Climate Change Canada, “Overview of Findings of the National Pollutant Release Inventory (NPRI) Sector Coverage Study for the 2008 Reporting Year,” *Environment and Climate Change Canada*, 2014. [Online]. Available: https://www.ec.gc.ca/inrp-npri/default.asp?lang=En&n=615C413A-1.

[46] “1-s2.0-S1364032115015117-main.pdf.crdownload.” .

[47] I. A. Reşitoɬlu, K. Altinişik, and A. Keskin, “The pollutant emissions from diesel-engine vehicles and exhaust aftertreatment systems,” *Clean Technologies and Environmental Policy*, vol. 17, no. 1. pp. 15–27, 2015.

[48] R. Prasad and V. R. Bella, “A Review on Diesel Soot Emission, its Effect and Control,” *Bull. Chem. React. Eng. Catal.*, vol. 5, no. 2, 2011.

[49] M. Eshani, Y. Gao, S. Gay, and A. Emadi, *Modern electric, hybrid electric and fuel cell vehicles 2nd. Edition*. 2010.

[50] B. Sarkan, O. Stopka, J. Gnap, and J. Caban, “Investigation of Exhaust Emissions of Vehicles with the Spark Ignition Engine within Emission Control,” in *Procedia Engineering*, 2017, vol. 187, pp. 775–782.

[51] M. Vijay Kumar, A. Veeresh Babu, and P. Ravi Kumar, “The impacts on combustion, performance and emissions of biodiesel by using additives in direct injection diesel engine,” *Alexandria Engineering Journal*, 2016.

[52] E. G. Giakoumis, C. D. Rakopoulos, A. M. Dimaratos, and D. C. Rakopoulos, “Exhaust emissions of diesel engines operating under transient conditions with biodiesel fuel blends,” *Prog. Energy Combust. Sci.*, vol. 38, no. 5, pp. 691–715, 2012.

[53] M. A. Ghadikolaei, “Effect of alcohol blend and fumigation on regulated and unregulated emissions of IC engines - A review,” *Renew. Sustain. Energy Rev.*, vol. 57, pp. 1440–1495, 2016.

[54] X. J. Man, C. S. Cheung, Z. Ning, L. Wei, and Z. H. Huang, “Influence of engine load and speed on regulated and unregulated emissions of a diesel engine fueled with diesel fuel blended with waste cooking oil biodiesel,” *Fuel*, vol. 180, pp. 41–49, 2016.

[55] D. A. Carbot-Rojas, R. F. Escobar-Jiménez, J. F. Gómez-Aguilar, and A. C. Téllez-Anguiano, “A survey on modeling, biofuels, control and supervision systems applied in internal combustion engines,” *Renew. Sustain. Energy Rev.*, vol. 73, no. January, pp. 1070–1085, 2017.

[56] A. Roberts, R. Brooks, and P. Shipway, “Internal combustion engine cold-start efficiency: A review of the problem, causes and potential solutions,” *Energy Convers. Manag.*, vol. 82, pp. 327–350, 2014.

[57] J. B. Heywood, *Internal Combustion Engine Fundamentals*, vol. 21. 1988.

[58] J. Hussain, K. Palaniradja, N. Alagumurthi, and R. Manimaran, “Effect of Exhaust Gas Recirculation (EGR) on performance and emission characteristics of a three cylinder direct injection compression ignition engine,” *Alexandria Eng. J.*, vol. 51, no. 4, pp. 241–247, 2012.

[59] B. Jothithirumal and E. Jamesgunasekaran, “Combined impact of biodiesel and exhaust gas recirculation on NOx emissions in di diesel engines,” *Procedia Eng.*, vol. 38, pp. 1457–1466, 2012.

[60] A. Uyumaz, “Combustion, performance and emission characteristics of a DI diesel engine fueled with mustard oil biodiesel fuel blends at different engine loads,” *Fuel*, vol. 212, no. August 2016, pp. 256–267, 2018.

[61] P. Q. Thang, Y. Muto, Y. Maeda, N. Q. Trung, Y. Itano, and N. Takenaka, “Increase in ozone due to the use of biodiesel fuel rather than diesel fuel,” *Environ. Pollut.*, vol. 216, pp. 400–407, 2016.

[62] O. M. Ali, R. Mamat, N. R. Abdullah, and A. A. Abdullah, “Analysis of blended fuel properties and engine performance with palm biodiesel-diesel blended fuel,” *Renew. Energy*, vol. 86, pp. 59–67, 2015.

[63] M. M. Roy, W. Wang, and M. Alawi, “Performance and emissions of a diesel engine fueled by biodiesel-diesel, biodiesel-diesel-additive and kerosene-biodiesel blends,” *Energy Convers. Manag.*, vol. 84, pp. 164–173, 2014.

[64] D. H. Qi, L. M. Geng, H. Chen, Y. Z. Bian, J. Liu, and X. C. Ren, “Combustion and performance evaluation of a diesel engine fueled with biodiesel produced from soybean crude oil,” *Renew. Energy*, vol. 34, no. 12, pp. 2706–2713, 2009.

[65] M. M. Hasan and M. M. Rahman, “Performance and emission characteristics of biodiesel–diesel blend and environmental and economic impacts of biodiesel production: A review,” *Renew. Sustain. Energy Rev.*, vol. 74, no. October 2014, pp. 938–948, 2017.

[66] A. O. Emiroğlu, A. Keskin, and M. Şen, “Experimental investigation of the effects of turkey rendering fat biodiesel on combustion, performance and exhaust emissions of a diesel engine,” *Fuel*, vol. 216, no. December 2017, pp. 266–273, 2018.

[67] M. M. Roy, J. Calder, W. Wang, A. Mangad, and F. C. M. Diniz, “Cold start idle emissions from a modern Tier-4 turbo-charged diesel engine fueled with diesel-biodiesel, diesel-biodiesel-ethanol, and diesel-biodiesel-diethyl ether blends,” *Appl. Energy*, vol. 180, pp. 52–65, 2016.

[68] M. M. Roy, W. Wang, and J. Bujold, “Biodiesel production and comparison of emissions of a DI diesel engine fueled by biodiesel-diesel and canola oil-diesel blends at high idling operations,” *Appl. Energy*, vol. 106, pp. 198–208, 2013.

[69] D. Ogunkoya, S. Li, O. J. Rojas, and T. Fang, “Performance, combustion, and emissions in a diesel engine operated with fuel-in-water emulsions based on lignin,” *Appl. Energy*, vol. 154, no. 2015, pp. 851–861, 2015.

[70] M. R. Seifi, S. R. Hassan-Beygi, B. Ghobadian, U. Desideri, and M. Antonelli, “Experimental investigation of a diesel engine power, torque and noise emission using water-diesel emulsions,” *Fuel*, vol. 166, pp. 392–399, 2016.

[71] N. Debnath, B. K., Saha, U. K., Sahoo, “A comprehensive review on the application of emulsions as an alternative fuel for diesel engines,” *Renew. Sustain. Energy Rev.*, vol. 42, pp. 196–211, 2015.

[72] J. L. Burguera and M. Burguera, “Analytical applications of emulsions and microemulsions,” in *Talanta*, 2012, vol. 96, pp. 11–20.

[73] Z. Guo, S. Wang, and X. Wang, “Stability mechanism investigation of emulsion fuels from biomass pyrolysis oil and diesel,” *Energy*, vol. 66, pp. 250–255, 2014.

[74] O. A. Elsanusi, M. M. Roy, and M. S. Sidhu, “Experimental Investigation on a Diesel Engine Fueled by Diesel-Biodiesel Blends and their Emulsions at Various Engine Operating Conditions,” *Appl. Energy*, vol. 203, pp. 582–593, 2017.

[75] S. Vellaiyan and K. S. Amirthagadeswaran, “The role of water-in-diesel emulsion and its additives on diesel engine performance and emission levels: A retrospective review,” *Alexandria Eng. J.*, vol. 55, no. 3, pp. 2463–2472, 2016.

[76] W. M. Yang *et al.*, “Impact of emulsion fuel with nano-organic additives on the performance of diesel engine,” *Appl. Energy*, vol. 112, pp. 1206–1212, 2013.

[77] S. S. Reham, H. H. Masjuki, M. A. Kalam, I. Shancita, I. M. Rizwanul Fattah, and A. M. Ruhul, “Study on stability, fuel properties, engine combustion, performance and emission characteristics of biofuel emulsion,” *Renewable and Sustainable Energy Reviews*, vol. 52. pp. 1566–1579, 2015.

[78] B. K. Debnath, N. Sahoo, and U. K. Saha, “Adjusting the operating characteristics to improve the performance of an emulsified palm oil methyl ester run diesel engine,” *Energy Convers. Manag.*, vol. 69, pp. 191–198, 2013.

[79] CHEMMUNIQUE, *The HLB System: a time-saving guide to emulsifier selection*, vol. 37, no. 10. 2004.

[80] B. J. Lin, W. H. Chen, W. M. Budzianowski, C. T. Hsieh, and P. H. Lin, “Emulsification analysis of bio-oil and diesel under various combinations of emulsifiers,” *Appl. Energy*, vol. 178, pp. 746–757, 2016.

[81] F. Y. Hagos, O. M. Ali, R. Mamat, and A. A. Abdullah, “Effect of emulsification and blending on the oxygenation and substitution of diesel fuel for compression ignition engine,” *Renewable and Sustainable Energy Reviews*, vol. 75. pp. 1281–1294, 2017.

[82] C. Y. Lin and L. W. Chen, “Comparison of fuel properties and emission characteristics of two- and three-phase emulsions prepared by ultrasonically vibrating and mechanically homogenizing emulsification methods,” *Fuel*, vol. 87, no. 10–11, pp. 2154–2161, 2008.

[83] G. Chen and D. Tao, “An experimental study of stability of oil-water emulsion,” *Fuel Process. Technol.*, vol. 86, no. 5, pp. 499–508, 2005.

[84] A. B. Koc and M. Abdullah, “Performance and NOx emissions of a diesel engine fueled with biodiesel-diesel-water nanoemulsions,” *Fuel Process. Technol.*, vol. 109, pp. 70–77, 2013.

[85] M. S. Kumar, J. Bellettre, and M. Tazerout, “The use of biofuel emulsions as fuel for diesel engines: A review,” *Proceedings of the Institution of Mechanical Engineers, Part A: Journal of Power and Energy*, vol. 223, no. 7. pp. 729–742, 2009.

[86] C. Y. Lin and S. A. Lin, “Effects of emulsification variables on fuel properties of two- and three-phase biodiesel emulsions,” *Fuel*, vol. 86, no. 1–2, pp. 210–217, 2007.

[87] A. M. A. Attia and A. R. Kulchitskiy, “Influence of the structure of water-in-fuel emulsion on diesel engine performance,” *Fuel*, vol. 116, pp. 703–708, 2014.

[88] A. Alahmer, J. Yamin, A. Sakhrieh, and M. A. Hamdan, “Engine performance using emulsified diesel fuel,” *Energy Convers. Manag.*, vol. 51, no. 8, pp. 1708–1713, 2010.

[89] M. S. Kumar and M. Jaikumar, “A comprehensive study on performance, emission and combustion behavior of a compression ignition engine fuelled with WCO (waste cooking oil) emulsion as fuel,” *J. Energy Inst.*, vol. 87, no. 3, pp. 263–271, 2014.

[90] M. Abu-Zaid, “Performance of single cylinder, direct injection Diesel engine using water fuel emulsions,” *Energy Convers. Manag.*, vol. 45, no. 5, pp. 697–705, 2004.

[91] C. R. Coronado, J. A. Carvalho, C. A. Quispe, and C. R. Sotomonte, “Ecological efficiency in glycerol combustion,” *Appl. Therm. Eng.*, vol. 63, no. 1, pp. 97–104, 2014.

[92] M. Ayoub and A. Z. Abdullah, “Critical review on the current scenario and significance of crude glycerol resulting from biodiesel industry towards more sustainable renewable energy industry,” *Renewable and Sustainable Energy Reviews*, vol. 16, no. 5. pp. 2671–2686, 2012.

[93] M. D. Bohon, B. A. Metzger, W. P. Linak, C. J. King, and W. L. Roberts, “Glycerol combustion and emissions,” *Proc. Combust. Inst.*, vol. 33, no. 2, pp. 2717–2724, 2011.

[94] M. M. Roy and A. F. G. Da Silva, “An alternative use of crude glycerin in canadian wood pellet industry,” *Int. J. Mech. Mechatronics Eng.*, vol. 14, no. 2, 2014.

[95] H. Noureddini, W. R. Dailey, and B. A. Hunt, “Production of ethers of glycerol from crude glycerol - The by- product of biodiesel production,” *Pap. Biomater.*, vol. 18, 1998.

[96] S. J. Eaton *et al.*, “Formulation and combustion of glycerol-diesel fuel emulsions,” *Energy and Fuels*, vol. 28, no. 6, pp. 3940–3947, 2014.

[97] G. H. Abd-Alla, “Using exhaust gas recirculation in internal combustion engines: a review,” *Energy Convers. Manag.*, vol. 43, no. 8, pp. 1027–1042, 2002.

[98] M. Y. Kim, D. S. Kim, and C. S. Lee, “Effect of residual gas fraction on the combustion characteristics of butane-air mixtures in the constant-volume chamber,” *Energy and Fuels*, vol. 17, no. 3, pp. 755–761, 2003.

[99] S. S. Hoseini, G. Najafi, and B. Ghobadian, “Experimental and numerical investigation of heat transfer and turbulent characteristics of a novel EGR cooler in diesel engine,” *Appl. Therm. Eng.*, vol. 108, pp. 1344–1356, 2016.

[100] H. J, P. K, A. N, and M. R, “Effect of Exhaust Gas Recirculation (EGR) on Performance and Emission of a Compression Ignition Engine with Staged Combustion (Insertion of Unburned Hydrocarbon),” *Int. J. Energy Eng.*, vol. 2, no. 6, pp. 285–292, 2012.

[101] M. H. M. Yasin, R. Mamat, A. F. Yusop, P. Paruka, T. Yusaf, and G. Najafi, “Effects of Exhaust Gas Recirculation (EGR) on a Diesel Engine fuelled with Palm-biodiesel,” in *Energy Procedia*, 2015, vol. 75, pp. 30–36.

[102] B. Rajesh Kumar and S. Saravanan, “Effect of exhaust gas recirculation (EGR) on performance and emissions of a constant speed di diesel engine fueled with pentanol/diesel blends,” *Fuel*, vol. 160, pp. 217–226, 2015.

[103] M. T. Chaichan, “Performance and emission characteristics of CIE using hydrogen, biodiesel, and massive EGR,” *International Journal of Hydrogen Energy*, 2017.

[104] J. Thangaraja and C. Kannan, “Effect of exhaust gas recirculation on advanced diesel combustion and alternate fuels - A review,” *Applied Energy*, vol. 180. pp. 169–184, 2016.

[105] V. B. Pedrozo, I. May, and H. Zhao, “Exploring the mid-load potential of ethanol-diesel dual-fuel combustion with and without EGR,” *Appl. Energy*, vol. 193, pp. 263–275, 2017.

[106] M. Talibi, P. Hellier, and N. Ladommatos, “The effect of varying EGR and intake air boost on hydrogen-diesel co-combustion in CI engines,” *Int. J. Hydrogen Energy*, vol. 42, no. 9, pp. 6369–6383, 2017.

[107] H. Feng, Z. Zheng, M. Yao, G. Cheng, M. Wang, and X. Wang, “Effects of exhaust gas recirculation on low temperature combustion using wide distillation range diesel,” *Energy*, vol. 51, pp. 291–296, 2013.

[108] J. E *et al.*, “Effect of different technologies on combustion and emissions of the diesel engine fueled with biodiesel: A review,” *Renewable and Sustainable Energy Reviews*, vol. 80. pp. 620–647, 2017.

[109] C. Y. Lin and H. A. Lin, “Effects of NOx-inhibitor agent on fuel properties of three-phase biodiesel emulsions,” *Fuel Process. Technol.*, vol. 89, no. 11, pp. 1237–1242, 2008.

[110] Y. Li, G. Tian, and H. Xu, “Application of Biodiesel in Automotive Diesel Engines,” *Biodiesel - Feed. Prod. Appl.*, 2012.

[111] M. M. Roy, J. Calder, W. Wang, A. Mangad, and F. C. M. Diniz, “Emission analysis of a modern Tier 4 DI diesel engine fueled by biodiesel-diesel blends with a cold flow improver (Wintron Synergy) at multiple idling conditions,” *Appl. Energy*, vol. 179, pp. 45–54, 2016.

[112] G. Knothe and L. F. Razon, “Biodiesel fuels,” *Progress in Energy and Combustion Science*, vol. 58. pp. 36–59, 2017.

[113] L. Leng *et al.*, “Rhamnolipid based glycerol-in-diesel microemulsion fuel: Formation and characterization,” *Fuel*, vol. 96, pp. 11–20, 2014.

[114] Ö. D. Bozkurt, F. M. Tunç, N. Bałlar, S. Çelebi, I. D. Günbaş, and A. Uzun, “Alternative fuel additives from glycerol by etherification with isobutene: Structure-performance relationships in solid catalysts,” *Fuel Processing Technology*, vol. 138. pp. 780–804, 2015.

[115] M. Zhang and H. Wu, “Stability of emulsion fuels prepared from fast pyrolysis bio-oil and glycerol,” *Fuel*, vol. 206, pp. 230–238, 2017.

[116] M. Angeloni, P. Remacha, A. Martínez, and J. Ballester, “Experimental investigation of the combustion of crude glycerol droplets,” *Fuel*, vol. 184, pp. 889–895, 2016.

[117] T. Cai, H. Li, H. Zhao, and K. Liao, “Purification of crude glycerol from waste cooking oil based biodiesel production by orthogonal test method,” *China Pet. Process. Petrochemical Technol.*, vol. 15, no. 1, pp. 48–53, 2013.

[118] C. Y. Lin and C. T. Tsai, “Emulsification characteristics of three-phase emulsion of biodiesel-in nitromethane-in-diesel prepared by microwave irradiation,” *Fuel*, vol. 158, pp. 50–56, 2015.

[119] M. Yahaya Khan, Z. A. Abdul Karim, F. Y. Hagos, A. R. A. Aziz, and I. M. Tan, “Current trends in water-in-diesel emulsion as a fuel,” *The Scientific World Journal*, vol. 2014. 2014.

[120] M. Habibullah, I. M. Rizwanul Fattah, H. H. Masjuki, and M. A. Kalam, “Effects of palm-coconut biodiesel blends on the performance and emission of a single-cylinder diesel engine,” *Energy and Fuels*, vol. 29, no. 2, pp. 734–743, 2015.

[121] H. Firoozmand and D. Rousseau, “Microbial cells as colloidal particles: Pickering oil-in-water emulsions stabilized by bacteria and yeast,” *Food Res. Int.*, vol. 81, pp. 66–73, 2016.

[122] S. Geacai, I. Niţă, O. Iulian, and E. Geacai, “Refractive indices for biodiesel mixtures,” *UPB Sci. Bull. Ser. B Chem. Mater. Sci.*, vol. 74, no. 4, pp. 149–160, 2012.

[123] D. Agarwal, S. K. Singh, and A. K. Agarwal, “Effect of Exhaust Gas Recirculation (EGR) on performance, emissions, deposits and durability of a constant speed compression ignition engine,” *Appl. Energy*, vol. 88, no. 8, pp. 2900–2907, 2011.

[124] S. Less and R. Vilagines, “Light beam reflectance measurement of droplets diameter distribution in crude oil emulsions,” *Fuel*, vol. 109, pp. 542–550, 2013.

[125] M. Silva *et al.*, “Study of the stability and homogeneity of water in oil emulsions of heavy oil,” *Fuel*, vol. 226, no. October 2017, pp. 278–285, 2018.

[126] E. N. Schulz *et al.*, “Evaluation of oil-in-water emulsions with cationic-anionic surfactants mixtures for potential use in the oil industry,” *Colloids Surfaces A Physicochem. Eng.*

Asp., vol. 490, pp. 145–154, 2016.

[127] V. Califano, R. Calabria, and P. Massoli, "Experimental evaluation of the effect of emulsion stability on micro-explosion phenomena for water-in-oil emulsions," *Fuel*, vol. 117, no. PART A, pp. 87–94, 2014.

[128] H. K. Suh and C. S. Lee, "A review on atomization and exhaust emissions of a biodiesel-fueled compression ignition engine," *Renewable and Sustainable Energy Reviews*, vol. 58. pp. 1601–1620, 2016.

[129] H. J. Kim, H. K. Suh, S. H. Park, and C. S. Lee, "An experimental and numerical investigation of atomization characteristics of biodiesel, dimethyl ether, and biodiesel-ethanol blended fuel," *Energy and Fuels*, vol. 22, no. 3, pp. 2091–2098, 2008.

[130] S. H. Yoon, S. H. Park, and C. S. Lee, "Experimental Investigation on the Fuel Properties of Biodiesel and Its Blends at Various Temperatures," *Energy & Fuels*, vol. 22, no. 1, pp. 652–656, 2008.

[131] T. D. O. Macedo, R. G. Pereira, J. M. Pardal, A. S. Soares, V. De, and J. Lameira, "Viscosity of Vegetable Oils and Biodiesel and Energy Generation," vol. 3072, no. 5, pp. 184–189, 2013.

[132] Y. Liang, G. Shu, H. Wei, and W. Zhang, "Effect of oxygen enriched combustion and water-diesel emulsion on the performance and emissions of turbocharged diesel engine," *Energy Convers. Manag.*, vol. 73, pp. 69–77, 2013.

[133] H. E. Mize, A. J. Lucio, C. J. Fhaner, F. S. Pratama, L. A. Robbins, and D. S. Karpovich, "Emulsions of crude glycerin from biodiesel processing with fuel oil for industrial heating," *J. Agric. Food Chem.*, vol. 61, no. 6, pp. 1319–1327, 2013.

[134] R. N. Mehta, U. More, N. Malek, M. Chakraborty, and P. A. Parikh, "Study of stability and thermodynamic properties of water-in-diesel nanoemulsion fuels with nano-Al additive," *Appl. Nanosci.*, vol. 5, no. 8, pp. 891–900, 2015.

[135] H. Sane, N. Purandare, O. Barve, and A. Todakar, "Emission Reduction of Ic Engines By Using Water-in- Diesel Emulsion and Catalytic Converter," pp. 378–383, 2014.

[136] A. O. Emiroğlu and M. Şen, "Combustion, performance and exhaust emission characterizations of a diesel engine operating with a ternary blend (alcohol-biodiesel-diesel fuel)," *Appl. Therm. Eng.*, vol. 133, pp. 371–380, 2018.

[137] A. O. Emiroğlu, A. Keskin, and M. Şen, "Experimental investigation of the effects of turkey rendering fat biodiesel on combustion, performance and exhaust emissions of a diesel engine," *Fuel*, vol. 216, pp. 266–273, 2018.

[138] X. Yuan *et al.*, "Pyrolysis and combustion kinetics of glycerol-in-diesel hybrid fuel using thermogravimetric analysis," *Fuel*, vol. 182, pp. 502–508, 2016.

[139] A Jack, I. Cieślak, and A. Teodorczyk, "Investigation of glycerol doping on ignition delay times and laminar burning velocities of gasoline and diesel fuel," *Combust. ENGINES*, vol. 169(2), no. June, pp. 167–175, 2017.

[140] N. A. Mazlan *et al.*, “Effects of different water percentages in non-surfactant emulsion fuel on performance and exhaust emissions of a light-duty truck,” *J. Clean. Prod.*, vol. 179, pp. 559–566, 2018.

[141] M. N. Nabi, M. S. Akhter, and M. M. Z. Shahadat, “Improvement of engine emissions with conventional diesel fuel and diesel-biodiesel blends,” *Bioresour. Technol.*, vol. 97, no. 3, pp. 372–378, 2006.

[142] M. H. M. Yasin *et al.*, “Study of a Diesel Engine Performance with Exhaust Gas Recirculation (EGR) System Fuelled with Palm Biodiesel,” in *Energy Procedia*, 2017, vol. 110, pp. 26–31.

[143] B. Rajesh Kumar, S. Saravanan, D. Rana, V. Anish, and A. Nagendran, “Effect of a sustainable biofuel - N-octanol - on the combustion, performance and emissions of a di diesel engine under naturally aspirated and exhaust gas recirculation (EGR) modes,” *Energy Convers. Manag.*, vol. 118, pp. 275–286, 2016.

[144] S. V. Khandal, N. R. Banapurmath, and V. N. Gaitonde, “Effect of Hydrogen Fuel Flow Rate, Fuel Injection Timing and Exhaust Gas Recirculation on the Performance of Dual Fuel Engine Powered with Renewable Fuels,” *Renew. Energy*, vol. 126, pp. 79–94, 2018.

APPENDICES

Appendix A: Heavy-Duty Engine Emissions

A1: Emissions at 1000 rpm:

Fuels	NOx (ppm)	CO (ppm)	HC (C1(ppm))	Smoke Opacity (%)
B0	258.44	179.33	43.33	1.164
B50	271.11	152	40	1.389
B100	301.44	131.78	33.33	1.628
B0W5%	213.11	209	60	1.043
B0W10%	194.778	277.67	190	0.802
B50W5%	237.89	188.78	56.67	1.091
B50W10%	212.56	230.22	173.33	0.921
B100W2.5%	273	147.33	40	1.4361
B100W5%	251.67	154.33	46.67	1.158
B100W10%	234.44	177.67	106.67	0.943
B0G5%	224.22	193.22	140	0.873
B0G10%	209.11	251.78	276.67	0.574
B50G5%	246.56	177.44	80	0.943
B50G10%	219.22	203.11	196.67	0.786
B100G2.5%	279.56	135.56	70	1.274
B100G5%	260.44	149	76.67	0.98
B100G10%	238.44	172.22	150	0.89

A2: Emissions at 1500 rpm:

Fuels	NOx (ppm)	CO (ppm)	HC (C1(ppm))	Smoke Opacity (%)
B0	211.5556	237.78	23.33	0.902
B50	227	191.56	13.33	0.992
B100	250.2222	153.78	10	1.273
B0W5%	174.3333	329.44	56.67	0.782
B0W10%	156.2222	389.44	86.67	0.462
B50W5%	196.4444	246.11	46.67	0.872
B50W10%	174.7778	313	86.67	0.805
B100W2.5%	223.6667	175.44	26.67	1.151
B100W5%	207.7778	194.67	36.67	1.014
B100W10%	195.5556	257.22	63.33	0.885
B0G5%	182.2222	272	73.33	0.738
B0G10%	167.3333	364.41	233.33	0.377
B50G5%	201	203.67	60	0.838
B50G10%	185	273.44	170	0.642
B100G2.5%	234.1111	171	50	1.023
B100G5%	220.2222	185.56	53.33	0.86
B100G10%	206.4444	215.67	93.33	0.77

APPENDIX B: Performances and Emissions of the Fuel Blends and Their Emulsion Fuels on Light-Duty Engine without EGR System

B1: Performance: BSFC (g/kWh):

RPM	1000 rpm			2100 rpm			3000 rpm		
Load	Low Load	Medium Load	High Load	Low Load	Medium Load	High Load	Low Load	Medium Load	High Load
Fuels									
B0	248.100	240.511	235.191	239.200	235.400	229.952	243.292	236.464	232.193
B20	249.801	242.201	236.001	240.899	237.125	231.393	244.801	238.837	233.690
B50	252.702	245.890	239.796	244.100	240.542	233.958	247.788	241.307	237.161
B100	257.089	249.901	244.475	250.401	245.183	238.587	252.182	246.877	242.195
B0W5%	249.904	242.502	236.711	241.088	236.994	232.801	245.189	238.880	233.877
B0W10%	251.802	244.198	238.898	242.815	239.088	234.654	246.885	240.838	235.529
B20W5%	251.601	243.805	237.887	242.785	239.005	233.107	246.217	240.920	235.537
B20W10%	254.210	245.711	240.799	244.519	240.928	236.813	249.291	242.959	237.259
B50W5%	254.504	248.121	241.911	246.098	242.416	235.599	250.103	243.104	239.661
B50W10%	256.912	251.200	244.428	248.324	244.399	237.769	252.594	243.934	241.471
B100W5%	258.943	251.659	246.074	251.886	247.033	240.440	253.547	248.686	244.182
B100W10%	260.311	253.567	248.075	253.209	249.003	242.053	255.779	250.448	246.217
B0G5%	249.103	241.212	235.998	240.310	235.716	230.543	244.120	237.443	232.936
B0G10%	251.098	243.099	237.188	242.406	237.285	233.192	245.509	239.195	234.131
B20G5%	250.595	242.889	236.874	241.711	238.222	232.245	245.615	239.847	234.729
B20G10%	252.303	244.587	239.198	243.497	239.830	233.614	248.107	241.971	236.214
B50G5%	253.300	247.500	240.428	245.581	241.443	234.851	248.988	242.435	238.494
B50G10%	255.196	248.986	242.681	247.403	243.679	236.453	251.287	243.574	240.438
B100G5%	258.403	250.710	245.219	251.097	246.007	239.356	252.892	247.810	243.015
B100G10%	259.704	252.598	247.191	252.601	248.046	241.084	254.809	249.576	245.146

B2: BTE (%):

RPM	1000 rpm			2100 rpm			3000 rpm		
Load	Low Load	Medium Load	High Load	Low Load	Medium Load	High Load	Low Load	Medium Load	High Load
Fuels									
B0	32.16	33.17	33.92	33.35	33.89	34.69	32.79	33.74	34.36
B20	32.59	33.61	34.50	33.80	34.33	35.18	33.26	34.09	34.84
B50	33.24	34.16	35.03	34.41	34.92	35.90	33.90	34.81	35.42
B100	34.49	35.48	36.27	35.41	36.17	37.17	35.16	35.92	36.61
B0W5%	34.33	35.38	36.24	35.58	36.20	36.85	34.99	35.91	36.68
B0W10%	36.00	37.13	37.95	37.34	37.92	38.64	36.72	37.64	38.49
B20W5%	34.79	35.91	36.80	36.06	36.63	37.55	35.55	36.34	37.17
B20W10%	36.39	37.65	38.42	37.84	38.40	39.07	37.11	38.08	38.99
B50W5%	35.49	36.40	37.33	36.70	37.26	38.33	36.11	37.15	37.68
B50W10%	37.15	38.00	39.05	38.44	39.05	40.14	37.79	39.13	39.53
B100W5%	36.82	37.89	38.75	37.85	38.60	39.66	37.61	38.34	39.05
B100W10%	38.71	39.74	40.62	39.80	40.47	41.63	39.40	40.24	40.93
B0G5%	33.65	34.75	35.52	34.88	35.56	36.36	34.34	35.30	35.98
B0G10%	34.40	35.53	36.42	35.64	36.40	37.04	35.19	36.11	36.90
B20G5%	34.12	35.20	36.09	35.37	35.89	36.81	34.81	35.65	36.42
B20G10%	34.90	36.01	36.82	36.17	36.72	37.70	35.50	36.40	37.28
B50G5%	34.80	35.61	36.66	35.89	36.51	37.53	35.40	36.36	36.96
B50G10%	35.55	36.44	37.38	36.67	37.23	38.37	36.10	37.24	37.73
B100G5%	35.96	37.07	37.90	37.01	37.78	38.83	36.75	37.50	38.24
B100G10%	36.78	37.81	38.64	37.81	38.51	39.62	37.48	38.27	38.96

B3: Emissions: NOx (g/kWh):

RPM	1000 rpm			2100 rpm			3000 rpm		
Load	Low Load	Medium Load	High Load	Low Load	Medium Load	High Load	Low Load	Medium Load	High Load
Fuels									
B0	10.222	5.288	4.081	7.142	3.355	2.535	5.913	2.956	2.269
B20	10.797	5.532	4.196	7.216	3.482	2.598	6.165	3.154	2.362
B50	11.368	5.653	4.276	7.505	3.600	2.669	6.510	3.344	2.484
B100	11.911	5.973	4.436	7.854	3.713	2.762	6.878	3.434	2.557
B0W5%	9.426	4.717	3.783	6.277	3.089	2.349	5.416	2.750	2.065
B0W10%	8.473	4.441	3.558	5.606	2.769	2.080	4.802	2.425	1.845
B20W5%	10.021	4.838	3.862	6.475	3.133	2.372	5.703	2.838	2.121
B20W10%	8.702	4.550	3.667	5.696	2.858	2.119	5.050	2.568	1.917
B50W5%	10.120	4.994	3.987	6.585	3.245	2.425	5.916	2.933	2.183
B50W10%	9.040	4.617	3.747	5.954	2.949	2.191	5.243	2.656	1.990
B100W5%	10.725	5.238	4.081	6.805	3.364	2.508	6.190	3.095	2.277
B100W10%	9.485	4.741	3.813	6.081	3.053	2.287	5.512	2.775	2.035
B0G5%	9.836	4.981	3.877	6.439	3.133	2.434	5.568	2.861	2.187
B0G10%	8.828	4.573	3.732	5.840	2.895	2.147	5.205	2.546	1.923
B20G5%	10.284	5.070	3.978	6.654	3.244	2.458	5.875	2.940	2.255
B20G10%	9.064	4.682	3.767	6.005	2.984	2.229	5.317	2.623	1.999
B50G5%	10.561	5.223	4.065	6.927	3.319	2.511	6.203	2.980	2.269
B50G10%	9.273	4.760	3.819	6.098	3.089	2.273	5.512	2.720	2.071
B100G5%	10.903	5.380	4.154	7.166	3.447	2.581	6.517	3.166	2.375
B100G10%	9.638	4.939	3.893	6.246	3.141	2.330	5.799	2.870	2.138

B4: CO (g/kWh):

RPM	1000 rpm			2100 rpm			3000 rpm		
Load	Low Load	Medium Load	High Load	Low Load	Medium Load	High Load	Low Load	Medium Load	High Load
Fuels									
B0	13.147	5.115	3.108	7.954	3.030	1.808	7.277	2.672	1.564
B20	12.430	4.952	2.987	7.486	2.906	1.710	6.674	2.510	1.460
B50	10.900	4.280	2.666	7.052	2.714	1.648	6.283	2.363	1.403
B100	10.326	4.198	2.559	6.651	2.495	1.533	5.644	2.158	1.242
B0W5%	21.895	9.028	5.573	9.859	3.921	2.384	8.236	3.171	1.924
B0W10%	28.779	11.372	6.953	11.998	4.551	2.703	11.573	4.448	2.664
B20W5%	18.310	7.214	4.501	9.391	3.756	2.313	7.774	2.995	1.830
B20W10%	23.186	9.599	6.001	11.330	4.359	2.623	10.330	3.905	2.436
B50W5%	15.872	6.623	4.032	8.957	3.564	2.171	7.561	2.936	1.754
B50W10%	20.748	8.294	5.198	10.528	4.140	2.561	9.691	3.743	2.332
B100W5%	14.676	5.767	3.671	8.422	3.276	1.976	6.887	2.745	1.526
B100W10%	18.071	7.377	4.581	9.926	3.852	2.349	9.052	3.391	2.086
B0G5%	19.075	7.520	4.354	9.157	3.633	2.154	7.845	3.009	1.820
B0G10%	27.919	10.434	6.564	11.196	4.304	2.632	10.259	3.905	2.398
B20G5%	17.640	6.868	4.072	8.790	3.441	2.109	7.419	2.877	1.678
B20G10%	21.608	8.600	5.332	10.929	4.167	2.535	9.620	3.714	2.332
B50G5%	15.202	6.134	3.845	8.389	3.304	2.065	7.135	2.833	1.668
B50G10%	19.792	8.131	5.010	10.260	4.003	2.464	9.372	3.538	2.199
B100G5%	14.294	5.665	3.563	7.854	3.112	1.905	6.603	2.554	1.450
B100G10%	16.828	7.031	4.381	9.759	3.742	2.251	8.804	3.273	2.000

B5: HC (C1) (g/kWh):

RPM	1000 rpm			2100 rpm			3000 rpm		
Load	Low Load	Medium Load	High Load	Low Load	Medium Load	High Load	Low Load	Medium Load	High Load
Fuels									
B0	30.436	12.494	7.897	18.914	7.435	4.598	16.741	6.577	4.024
B20	29.309	12.014	7.581	17.338	7.111	4.389	15.904	6.230	4.024
B50	24.800	10.572	6.634	14.973	5.818	3.762	13.393	4.846	3.129
B100	18.036	7.689	5.054	11.033	4.525	2.508	10.045	3.461	1.788
B0W5%	36.072	15.377	9.476	23.642	9.051	5.852	21.764	8.307	5.365
B0W10%	45.090	19.222	12.004	29.947	11.637	7.523	26.786	10.384	6.706
B20W5%	31.563	13.455	8.845	20.490	8.404	5.016	20.089	7.615	4.918
B20W10%	40.581	17.299	10.740	26.795	10.990	6.269	25.112	10.384	6.259
B50W5%	27.054	11.533	7.581	17.338	7.111	4.180	16.741	6.230	4.024
B50W10%	38.327	15.377	10.108	23.642	9.697	6.269	23.438	9.692	5.812
B100W5%	24.800	9.611	6.318	14.185	5.818	3.344	13.393	5.538	3.129
B100W10%	31.563	13.455	8.213	20.490	7.758	5.016	18.415	7.615	4.471
B0G5%	38.327	16.338	10.740	25.218	10.344	6.269	23.438	9.692	5.812
B0G10%	47.345	20.183	13.267	31.523	12.283	7.523	28.460	11.076	7.153
B20G5%	36.072	14.416	9.477	22.066	9.051	5.434	21.764	8.307	4.918
B20G10%	45.091	19.222	12.635	29.947	11.637	7.105	28.460	11.076	6.706
B50G5%	29.309	12.494	8.213	18.914	7.758	5.016	18.415	6.923	4.471
B50G10%	42.836	17.299	10.740	26.795	10.344	6.687	25.112	9.692	6.259
B100G5%	27.054	11.533	7.581	17.338	6.465	3.762	15.067	5.538	3.129
B100G10%	36.072	14.416	8.845	22.066	9.051	5.434	21.764	8.307	4.918

B6: Smoke Opacity (%):

RPM	1000 rpm			2100 rpm			3000 rpm		
Load	Low Load	Medium Load	High Load	Low Load	Medium Load	High Load	Low Load	Medium Load	High Load
Fuels									
B0	4.467	5.688	7.729	3.621	4.322	5.131	2.063	2.742	3.643
B20	6.282	7.532	8.775	4.004	4.805	5.907	2.529	3.065	3.959
B50	11.265	12.960	13.771	5.645	6.610	7.779	3.344	4.375	5.303
B100	20.867	21.186	24.094	7.017	7.995	8.389	4.981	5.464	5.811
B0W5%	4.359	5.269	6.256	2.592	3.095	3.738	1.586	2.051	2.845
B0W10%	3.328	3.743	4.391	1.299	1.725	2.582	0.593	0.860	1.173
B20W5%	5.811	6.256	7.028	3.254	3.910	4.358	2.261	2.962	3.925
B20W10%	3.648	4.910	5.203	2.242	2.807	3.484	1.057	1.465	1.695
B50W5%	7.917	8.902	9.004	4.414	4.910	5.616	2.841	3.395	4.183
B50W10%	4.545	5.890	7.296	3.019	3.732	3.973	1.094	1.627	2.280
B100W5%	16.494	17.979	20.033	4.945	5.243	5.829	3.387	3.728	4.248
B100W10%	12.410	13.779	14.656	3.676	3.798	4.347	1.986	2.604	3.050
B0G5%	4.210	4.690	5.902	2.281	2.771	3.632	1.500	1.701	2.097
B0G10%	2.113	2.963	4.134	0.760	1.253	1.754	0.442	0.607	0.646
B20G5%	5.056	5.937	6.704	3.185	3.736	4.313	2.080	3.014	3.729
B20G10%	3.117	4.311	4.972	1.752	2.201	2.607	0.909	1.085	1.333
B50G5%	7.695	7.949	8.299	3.196	3.918	4.565	2.800	3.191	3.902
B50G10%	3.470	5.468	6.497	2.553	2.918	2.938	1.197	1.570	2.189
B100G5%	14.871	17.780	18.892	3.817	4.190	4.808	2.827	3.240	3.928
B100G10%	8.313	10.358	11.726	3.069	3.576	3.953	1.621	1.976	2.264

B7: EGT (°C):

RPM	1000 rpm			2100 rpm			3000 rpm		
Load	Low Load	Medium Load	High Load	Low Load	Medium Load	High Load	Low Load	Medium Load	High Load
Fuels									
B0	160.3	185.4	230.2	220.1	245	280.6	255.4	295.2	340.1
B20	161.2	187	231.8	220.9	246.1	281.3	257.1	296.7	342.2
B50	163.7	189.2	234.1	222.2	247.4	282.8	258.7	298	342.9
B100	169.5	194.4	239.1	226	252.3	288.1	263.6	301.8	347.9
B0W5%	144.5	162.7	211.6	197.2	216.6	257.9	231.7	270.2	319.9
B0W10%	129	150.2	203.1	188.5	210	244.4	221.6	259.3	308
B20W5%	147.2	164.3	212.9	199.9	218.6	260.1	233.9	272.4	320.9
B20W10%	131.6	152.3	204.5	191.7	211.7	248.2	223.6	261.4	311.4
B50W5%	148.9	167.1	215.4	202.2	223.7	264.5	237.8	275.8	323.2
B50W10%	135.6	155.4	206.7	195.8	215.3	253.9	226.6	264.3	315.5
B100W5%	153.2	172.4	220.1	207.4	231.7	270.9	243.8	282.6	330.5
B100W10%	141.4	162.6	211.7	199.3	221.1	259.8	234.6	271.9	322.5
B0G5%	149.2	165.1	214.6	200	221.1	261.5	234.4	274.8	322.7
B0G10%	135.5	154.4	206.3	193.6	213.1	248.2	224.5	262.3	313.6
B20G5%	151.1	168.7	216.9	202.8	223.5	264.4	236.9	277.4	325.2
B20G10%	137.3	157.8	208.5	196.8	215	251.1	227.2	264.3	315.9
B50G5%	152.6	173.9	220.7	207.4	228.6	267.1	240	281.2	328.1
B50G10%	140.5	161.7	212.9	200.1	217.5	254.8	230.1	267.9	318.5
B100G5%	157.3	179.8	225.1	210.4	236.4	273.5	247.1	286.3	334.5
B100G10%	145.6	166.1	216.5	203.8	222.7	264.5	236.3	274.7	325.3

APPENDIX C: Performances and Emissions of the Fuel Blends and Their Emulsion Fuels on Light-Duty Engine with EGR System

C1: Performance: BSFC (g/kWh) at 1000 rpm:

RPM	1000 rpm								
Load	Low Load			Medium Load			High Load		
EGR %	0%	2.51%	7.62%	0%	4.13%	8.72%	0%	5.77%	9.93%
Fuels									
B0	248.100	248.302	248.704	240.511	240.769	241.190	235.191	235.475	235.983
B50	252.702	253.014	253.552	245.890	246.146	246.657	239.796	240.219	240.914
B100	257.089	257.571	258.230	249.901	250.428	250.964	244.475	244.945	245.601
B0W5%	249.904	250.165	250.713	242.502	242.853	243.547	236.711	237.106	237.801
B0W10%	251.802	252.111	252.636	244.198	244.477	245.039	238.898	239.213	239.803
B50W5%	254.504	254.862	255.433	248.121	248.506	249.185	241.911	242.420	243.128
B50W10%	256.912	257.271	257.798	251.200	251.509	252.093	244.428	244.774	245.502
B100W2.5%		258.514	259.128		251.431	251.992		245.778	246.491
B100W5%	258.943	259.286	259.918	251.659	252.142	252.787	246.074	246.594	247.217
B100W10%	260.311	260.771	261.363	253.567	254.006	254.568	248.075	248.406	249.050
B0G5%	249.103	249.355	249.908	241.212	241.519	242.550	235.998	236.365	236.919
B0G10%	251.098	251.358	251.975	243.099	243.425	244.087	237.188	237.588	238.217
B50G5%	253.300	253.675	254.306	247.500	247.967	248.656	240.428	240.902	241.535
B50G10%	255.196	255.538	256.239	248.986	250.355	251.126	242.681	243.050	243.773
B100G2.5%		258.057	258.718		250.829	251.544		245.342	246.075
B100G5%	258.403	258.709	259.230	250.710	251.249	251.959	245.219	245.834	246.617
B100G10%	259.704	260.040	260.508	252.598	252.992	253.547	247.191	247.590	248.165

C2: BSFC (g/kWh) at 2100 rpm:

RPM	2100 rpm								
Load	Low Load			Medium Load			High Load		
EGR %	0%	7.20%	11.99%	0%	8.52%	13.86%	0%	9.75%	15.58%
Fuels									
B0	239.200	239.546	240.107	235.400	235.810	236.507	229.952	230.433	231.305
B50	244.100	244.681	245.472	240.542	241.104	241.872	233.958	234.571	235.486
B100	250.401	251.225	251.948	245.183	245.927	246.666	238.587	239.490	240.256
B0W5%	241.088	241.511	242.330	236.994	237.397	238.036	232.801	233.280	234.014
B0W10%	242.815	243.358	243.738	239.088	239.597	240.409	234.654	235.419	236.263
B50W5%	246.098	246.462	247.202	242.416	242.741	243.556	235.599	235.951	236.711
B50W10%	248.324	248.848	249.451	244.399	245.117	245.987	237.769	238.433	239.313
B100W2.5%		251.935	252.700		247.014	247.825		240.400	241.245
B100W5%	251.886	252.519	253.293	247.033	247.808	248.632	240.440	241.223	241.956
B100W10%	253.209	253.873	254.529	249.003	249.518	250.152	242.053	242.665	243.410
B0G5%	240.310	240.772	241.491	235.716	236.258	237.029	230.543	231.020	231.854
B0G10%	242.406	242.856	243.440	237.285	237.791	238.399	233.192	233.807	234.398
B50G5%	245.581	246.088	246.906	241.443	242.040	243.013	234.851	235.415	236.424
B50G10%	247.403	247.799	248.680	243.679	244.103	245.012	236.453	236.920	237.923
B100G2.5%		251.498	252.193		246.357	247.150		240.012	240.764
B100G5%	251.097	251.826	252.756	246.007	246.593	247.542	239.356	240.118	240.988
B100G10%	252.601	253.121	253.744	248.046	248.522	249.149	241.084	241.522	242.300

C3: BSFC (g/kWh) at 3000 rpm:

RPM	3000 rpm								
Load	Low Load			Medium Load			High Load		
EGR %	0%	8.08%	12.77%	0%	10.09%	15.43%	0%	12.36%	17.94%
Fuels									
B0	243.292	243.928	244.843	236.464	237.356	238.400	232.193	232.238	233.352
B50	247.788	248.842	249.651	241.307	241.430	242.365	237.161	237.295	237.294
B100	252.182	253.341	254.138	246.877	248.101	248.848	242.195	243.333	244.282
B0W5%	245.189	245.803	247.100	238.880	239.523	240.644	233.877	234.613	235.905
B0W10%	246.885	247.676	248.700	240.838	241.600	242.672	235.529	236.352	237.384
B50W5%	250.103	250.431	251.111	243.104	243.499	244.218	239.661	239.994	240.372
B50W10%	252.594	253.437	254.518	243.934	244.905	245.946	241.471	242.753	243.936
B100W2.5%		253.880	254.741		248.690	249.670		244.089	244.932
B100W5%	253.547	254.355	255.104	248.686	249.630	250.499	244.182	245.147	245.926
B100W10%	255.779	256.393	257.156	250.448	251.183	251.969	246.217	246.963	247.748
B0G5%	244.120	244.748	245.821	237.443	238.085	239.112	232.936	233.605	234.702
B0G10%	245.509	246.288	247.305	239.195	239.751	240.981	234.131	234.837	235.940
B50G5%	248.988	249.671	250.640	242.435	243.126	244.223	238.494	239.236	240.269
B50G10%	251.287	252.164	253.166	243.574	244.659	245.748	240.438	241.524	242.673
B100G2.5%		253.430	254.239		248.100	249.084		243.566	244.643
B100G5%	252.892	253.581	254.387	247.810	248.648	249.526	243.015	244.158	245.167
B100G10%	254.809	255.373	256.268	249.576	250.227	251.287	245.146	245.638	246.813

C4: BTE (%) at 1000 rpm:

RPM	1000 rpm								
Load	Low Load			Medium Load			High Load		
EGR %	0%	2.51%	7.62%	0%	4.13%	8.72%	0%	5.77%	9.93%
Fuels									
B0	32.16	32.13	32.08	33.17	33.14	33.08	33.92	33.88	33.81
B50	33.24	33.20	33.13	34.16	34.12	34.05	35.03	34.97	34.86
B100	34.49	34.43	34.34	35.48	35.41	35.33	36.27	36.20	36.11
B0W5%	34.33	34.29	34.22	35.38	35.32	35.22	36.24	36.18	36.07
B0W10%	36.00	35.96	35.89	37.13	37.08	37.00	37.95	37.90	37.81
B50W5%	35.49	35.44	35.36	36.40	36.34	36.24	37.33	37.26	37.15
B50W10%	37.15	37.10	37.02	38.00	37.95	37.86	39.05	38.99	38.88
B100W2.5%		35.92	35.83		36.93	36.85		37.78	37.67
B100W5%	36.82	36.77	36.69	37.89	37.82	37.72	38.75	38.67	38.57
B100W10%	38.71	38.64	38.56	39.74	39.67	39.58	40.62	40.57	40.46
B0G5%	33.65	33.62	33.54	34.75	34.71	34.56	35.52	35.46	35.38
B0G10%	34.40	34.37	34.28	35.53	35.49	35.39	36.42	36.36	36.26
B50G5%	34.80	34.75	34.66	35.61	35.55	35.45	36.66	36.59	36.49
B50G10%	35.55	35.50	35.40	36.44	36.24	36.12	37.38	37.33	37.21
B100G2.5%		35.53	35.44		36.56	36.45		37.37	37.26
B100G5%	35.96	35.92	35.85	37.07	36.99	36.88	37.90	37.80	37.68
B100G10%	36.78	36.73	36.66	37.81	37.75	37.67	38.64	38.58	38.49

C5: BTE (%) at 2100 rpm:

RPM	2100 rpm								
Load	Low Load			Medium Load			High Load		
EGR %	0%	7.20%	11.99%	0%	8.52%	13.86%	0%	9.75%	15.58%
Fuels									
B0	33.35	33.30	33.23	33.89	33.83	33.73	34.69	34.62	34.49
B50	34.41	34.33	34.22	34.92	34.84	34.73	35.90	35.81	35.67
B100	35.41	35.30	35.20	36.17	36.06	35.95	37.17	37.03	36.91
B0W5%	35.58	35.52	35.40	36.20	36.14	36.04	36.85	36.77	36.66
B0W10%	37.34	37.25	37.20	37.92	37.84	37.71	38.64	38.51	38.37
B50W5%	36.70	36.64	36.54	37.26	37.21	37.08	38.33	38.28	38.15
B50W10%	38.44	38.36	38.26	39.05	38.94	38.80	40.14	40.03	39.88
B100W2.5%		36.86	36.75		37.59	37.47		38.63	38.49
B100W5%	37.85	37.76	37.64	38.60	38.48	38.35	39.66	39.53	39.41
B100W10%	39.80	39.69	39.59	40.47	40.39	40.28	41.63	41.53	41.40
B0G5%	34.88	34.81	34.71	35.56	35.48	35.36	36.36	36.28	36.15
B0G10%	35.64	35.57	35.48	36.40	36.33	36.23	37.04	36.95	36.85
B50G5%	35.89	35.82	35.70	36.51	36.42	36.27	37.53	37.44	37.28
B50G10%	36.67	36.61	36.48	37.23	37.16	37.03	38.37	38.29	38.13
B100G2.5%		36.46	36.36		37.22	37.10		38.20	38.08
B100G5%	37.01	36.90	36.77	37.78	37.69	37.54	38.83	38.70	38.56
B100G10%	37.81	37.73	37.64	38.51	38.43	38.34	39.62	39.55	39.42

C6: BTE (%) at 3000 rpm:

RPM	3000 rpm								
Load	Low Load			Medium Load			High Load		
EGR %	0%	8.08%	12.77%	0%	10.09%	15.43%	0%	12.36%	17.94%
Fuels									
B0	32.79	32.71	32.58	33.74	33.61	33.46	34.36	34.35	34.19
B50	33.90	33.75	33.64	34.81	34.79	34.66	35.42	35.40	35.40
B100	35.16	35.00	34.89	35.92	35.74	35.63	36.61	36.44	36.30
B0W5%	34.99	34.90	34.72	35.91	35.82	35.65	36.68	36.56	36.36
B0W10%	36.72	36.60	36.45	37.64	37.52	37.36	38.49	38.36	38.19
B50W5%	36.11	36.06	35.97	37.15	37.09	36.98	37.68	37.63	37.57
B50W10%	37.79	37.66	37.50	39.13	38.97	38.81	39.53	39.32	39.13
B100W2.5%		36.57	36.45		37.34	37.19		38.04	37.91
B100W5%	37.61	37.49	37.38	38.34	38.20	38.06	39.05	38.90	38.77
B100W10%	39.40	39.30	39.19	40.24	40.12	39.99	40.93	40.80	40.67
B0G5%	34.34	34.25	34.10	35.30	35.21	35.06	35.98	35.88	35.71
B0G10%	35.19	35.07	34.93	36.11	36.03	35.85	36.90	36.78	36.61
B50G5%	35.40	35.30	35.17	36.36	36.25	36.09	36.96	36.84	36.68
B50G10%	36.10	35.98	35.83	37.24	37.08	36.92	37.73	37.56	37.38
B100G2.5%		36.18	36.07		36.96	36.81		37.65	37.48
B100G5%	36.75	36.65	36.53	37.50	37.37	37.24	38.24	38.06	37.91
B100G10%	37.48	37.40	37.27	38.27	38.17	38.01	38.96	38.88	38.70

C7: Emissions: NOx (g/kWh) at 1000 rpm:

RPM	1000 rpm								
Load	Low Load			Medium Load			High Load		
EGR %	0%	2.51%	7.62%	0%	4.13%	8.72%	0%	5.77%	9.93%
Fuels									
B0	10.222	9.045	8.124	5.288	4.630	4.124	4.081	3.504	3.153
B50	11.368	9.966	8.817	5.653	5.054	4.489	4.276	3.788	3.330
B100	11.911	10.438	9.249	5.973	5.222	4.649	4.436	3.918	3.435
B0W5%	9.426	8.327	7.434	4.717	4.169	3.714	3.783	3.299	2.919
B0W10%	8.473	7.458	6.741	4.441	3.830	3.390	3.558	2.990	2.747
B50W5%	10.120	9.169	7.888	4.994	4.486	3.875	3.987	3.485	3.042
B50W10%	9.040	7.885	7.031	4.617	4.022	3.511	3.747	3.177	2.813
B100W2.5%		9.917	8.770		4.938	4.408		3.746	3.323
B100W5%	10.725	9.494	8.269	5.238	4.623	4.036	4.081	3.539	3.199
B100W10%	9.485	8.285	7.390	4.741	4.170	3.655	3.813	3.240	2.905
B0G5%	9.836	8.550	7.601	4.981	4.305	3.814	3.877	3.416	2.957
B0G10%	8.828	7.881	6.933	4.573	4.031	3.441	3.732	3.140	2.819
B50G5%	10.561	9.392	8.247	5.223	4.527	4.047	4.065	3.560	3.102
B50G10%	9.273	8.209	7.270	4.760	4.222	3.611	3.819	3.279	2.898
B100G2.5%		10.091	8.889		5.012	4.478		3.788	3.350
B100G5%	10.903	9.717	8.555	5.380	4.739	4.167	4.154	3.719	3.245
B100G10%	9.638	8.508	7.532	4.939	4.337	3.704	3.893	3.403	2.990

C8: NOx (g/kWh) at 2100 rpm:

RPM	2100 rpm								
Load	Low Load			Medium Load			High Load		
EGR %	0%	7.20%	11.99%	0%	8.52%	13.86%	0%	9.75%	15.58%
Fuels									
B0	7.142	5.778	4.957	3.355	2.762	2.398	2.535	2.046	1.722
B50	7.505	6.336	5.404	3.600	2.989	2.577	2.669	2.199	1.843
B100	7.854	6.672	5.805	3.713	3.132	2.700	2.762	2.298	1.952
B0W5%	6.277	5.276	4.483	3.089	2.492	2.113	2.349	1.913	1.586
B0W10%	5.606	4.590	4.052	2.769	2.242	1.916	2.080	1.706	1.461
B50W5%	6.585	5.584	4.707	3.245	2.657	2.298	2.425	2.022	1.658
B50W10%	5.954	5.015	4.231	2.949	2.374	2.000	2.191	1.807	1.522
B100W2.5%		6.188	5.314		2.909	2.572		2.186	1.820
B100W5%	6.805	5.803	4.712	3.364	2.760	2.394	2.508	2.100	1.739
B100W10%	6.081	5.199	4.535	3.053	2.489	2.078	2.287	1.893	1.591
B0G5%	6.439	5.460	4.543	3.133	2.587	2.145	2.434	1.995	1.630
B0G10%	5.840	4.891	4.243	2.895	2.330	1.973	2.147	1.788	1.497
B50G5%	6.927	5.767	4.852	3.319	2.766	2.375	2.511	2.082	1.736
B50G10%	6.098	5.199	4.405	3.089	2.502	2.089	2.273	1.889	1.562
B100G2.5%		6.221	5.440		2.969	2.592		2.203	1.860
B100G5%	7.166	6.088	5.029	3.447	2.889	2.465	2.581	2.191	1.816
B100G10%	6.246	5.301	4.663	3.141	2.577	2.199	2.330	1.966	1.664

C9: NOx (g/kWh) at 3000 rpm:

RPM	3000 rpm								
Load	Low Load			Medium Load			High Load		
EGR %	0%	8.08%	12.77%	0%	10.09%	15.43%	0%	12.36%	17.94%
Fuels									
B0	5.913	4.990	4.265	2.956	2.545	2.103	2.269	1.891	1.621
B50	6.510	5.431	4.685	3.344	2.739	2.271	2.484	2.017	1.689
B100	6.878	5.694	4.836	3.434	2.853	2.398	2.557	2.075	1.735
B0W5%	5.416	4.418	3.542	2.750	2.255	1.787	2.065	1.678	1.378
B0W10%	4.802	3.809	2.992	2.425	1.978	1.614	1.845	1.526	1.261
B50W5%	5.916	4.700	3.945	2.933	2.405	1.970	2.183	1.803	1.521
B50W10%	5.243	4.107	3.261	2.656	2.142	1.695	1.990	1.597	1.333
B100W2.5%		5.242	4.517		2.718	2.212		1.960	1.627
B100W5%	6.190	4.963	4.117	3.095	2.527	2.024	2.277	1.853	1.543
B100W10%	5.512	4.421	3.732	2.775	2.228	1.791	2.035	1.683	1.430
B0G5%	5.568	4.698	3.659	2.861	2.390	1.841	2.187	1.762	1.491
B0G10%	5.205	4.105	3.175	2.546	2.042	1.675	1.923	1.566	1.324
B50G5%	6.203	4.945	4.115	2.980	2.492	2.051	2.269	1.857	1.529
B50G10%	5.512	4.421	3.496	2.720	2.164	1.777	2.071	1.634	1.371
B100G2.5%		5.346	4.634		2.873	2.265		2.000	1.648
B100G5%	6.517	5.261	4.234	3.166	2.627	2.118	2.375	1.947	1.597
B100G10%	5.799	4.612	3.832	2.870	2.312	1.857	2.138	1.749	1.451

C10: CO (g/kWh) at 1000 rpm:

RPM	1000 rpm								
Load	Low Load			Medium Load			High Load		
EGR %	0%	2.51%	7.62%	0%	4.13%	8.72%	0%	5.77%	9.93%
Fuels									
B0	13.147	24.119	25.608	5.115	9.536	10.214	3.108	5.625	5.871
B50	10.900	13.527	17.894	4.280	5.402	7.306	2.666	3.339	4.528
B100	10.326	12.610	16.572	4.198	5.090	6.728	2.559	3.162	4.213
B0W5%	21.895	26.595	32.087	9.028	10.609	12.767	5.573	6.336	7.663
B0W10%	28.779	38.792	45.926	11.372	15.660	18.918	6.953	9.370	10.774
B50W5%	15.872	22.973	26.489	6.623	9.439	10.885	4.032	5.815	6.755
B50W10%	20.748	33.932	41.695	8.294	13.787	16.924	5.198	8.774	10.266
B100W2.5%		15.315	20.539		6.240	8.257		3.898	5.181
B100W5%	14.676	21.184	22.963	5.767	8.659	9.301	3.671	5.523	5.690
B100W10%	18.071	29.943	33.321	7.377	12.442	13.755	4.581	7.923	8.741
B0G5%	19.075	24.761	30.191	7.520	10.102	12.320	4.354	6.158	7.554
B0G10%	27.919	36.408	39.315	10.434	14.704	16.215	6.564	9.129	10.326
B50G5%	15.202	20.634	25.211	6.134	8.386	10.233	3.845	5.003	6.271
B50G10%	19.792	31.593	37.552	8.131	13.183	15.004	5.010	8.367	9.128
B100G2.5%		14.444	20.186		5.928	8.033		3.784	5.024
B100G5%	14.294	19.717	22.214	5.665	7.645	8.965	3.563	4.888	5.617
B100G10%	16.828	29.484	32.439	7.031	12.130	13.513	4.381	7.656	8.668

C11: CO (g/kWh) at 2100 rpm:

RPM	2100 rpm								
Load	Low Load			Medium Load			High Load		
EGR %	0%	7.20%	11.99%	0%	8.52%	13.86%	0%	9.75%	15.58%
Fuels									
B0	7.954	9.782	10.161	3.030	3.589	3.736	1.808	2.080	2.130
B50	7.052	8.667	9.574	2.714	3.289	3.536	1.648	1.904	2.056
B100	6.651	8.172	9.280	2.495	3.151	3.324	1.533	1.737	1.975
B0W5%	9.859	11.980	13.626	3.921	4.740	5.122	2.384	2.900	3.088
B0W10%	11.998	14.023	17.591	4.551	5.352	6.825	2.703	3.139	4.149
B50W5%	8.957	11.113	12.598	3.564	4.289	4.828	2.171	2.629	2.984
B50W10%	10.528	13.806	15.741	4.140	5.265	5.967	2.561	3.036	3.652
B100W2.5%		9.410	10.484		3.702	4.006		2.271	2.375
B100W5%	8.422	10.587	11.688	3.276	4.114	4.476	1.976	2.590	2.776
B100W10%	9.926	13.404	15.300	3.852	5.077	5.639	2.349	2.900	3.355
B0G5%	9.157	11.670	12.775	3.633	4.414	4.664	2.154	2.717	2.858
B0G10%	11.196	13.032	16.768	4.304	5.065	6.473	2.632	3.036	3.875
B50G5%	8.389	10.649	11.482	3.304	4.239	4.429	2.065	2.613	2.680
B50G10%	10.260	12.506	15.094	4.003	4.915	5.556	2.464	2.948	3.355
B100G2.5%		9.256	10.220		3.614	3.912		2.231	2.316
B100G5%	7.854	10.370	11.101	3.112	4.052	4.323	1.905	2.478	2.643
B100G10%	9.759	12.320	14.478	3.742	4.877	5.192	2.251	2.852	3.021

C12: CO (g/kWh) at 3000 rpm:

RPM	3000 rpm								
Load	Low Load			Medium Load			High Load		
EGR %	0%	8.08%	12.77%	0%	10.09%	15.43%	0%	12.36%	17.94%
Fuels									
B0	7.277	8.294	10.082	2.672	3.055	3.786	1.564	1.778	2.126
B50	6.283	6.519	9.309	2.363	2.397	3.476	1.403	1.406	2.003
B100	5.644	6.196	8.969	2.158	2.331	3.377	1.242	1.348	1.902
B0W5%	8.236	8.810	12.773	3.171	3.358	4.874	1.924	1.993	2.907
B0W10%	11.573	12.134	15.649	4.448	4.728	5.950	2.664	2.821	3.611
B50W5%	7.561	8.423	12.123	2.936	3.134	4.503	1.754	1.787	2.683
B50W10%	9.691	11.909	15.123	3.743	4.662	5.666	2.332	2.730	3.425
B100W2.5%		7.035	9.835		2.753	3.724		1.613	2.180
B100W5%	6.887	8.326	10.794	2.745	2.924	4.045	1.526	1.712	2.343
B100W10%	9.052	11.650	14.257	3.391	4.478	5.505	2.086	2.663	3.193
B0G5%	7.845	8.326	11.969	3.009	3.108	4.355	1.820	1.861	2.513
B0G10%	10.259	11.844	15.247	3.905	4.583	5.827	2.398	2.746	3.510
B50G5%	7.135	8.100	10.670	2.833	2.937	3.996	1.668	1.745	2.412
B50G10%	9.372	11.618	14.752	3.538	4.491	5.456	2.199	2.655	3.232
B100G2.5%		6.809	9.587		2.674	3.600		1.588	2.126
B100G5%	6.603	7.810	10.268	2.554	2.805	3.823	1.450	1.696	2.273
B100G10%	8.804	11.199	13.237	3.273	4.359	5.010	2.000	2.614	3.015

C13: HC (C1) (g/kWh) at 1000 rpm:

RPM	1000 rpm								
Load	Low Load			Medium Load			High Load		
EGR %	0%	2.51%	7.62%	0%	4.13%	8.72%	0%	5.77%	9.93%
Fuels									
B0	30.436	35.681	40.532	12.494	14.715	16.701	7.897	8.982	10.848
B50	24.800	32.437	37.414	10.572	12.876	14.943	6.634	7.784	9.706
B100	18.036	28.112	33.257	7.689	11.036	13.185	5.054	6.587	8.564
B0W5%	36.072	38.924	45.729	15.377	16.554	18.459	9.476	10.179	11.989
B0W10%	45.090	49.737	54.043	19.222	21.153	22.854	12.004	13.173	14.273
B50W5%	27.054	36.762	41.571	11.533	14.715	17.580	7.581	9.581	11.418
B50W10%	38.327	45.412	51.964	15.377	19.313	21.096	10.108	11.976	13.131
B100W2.5%		28.112	33.257		11.036	14.064		7.185	9.135
B100W5%	24.800	32.437	39.493	9.611	12.876	15.822	6.318	8.383	10.277
B100W10%	31.563	38.924	45.729	13.455	15.635	18.459	8.213	10.179	11.989
B0G5%	38.327	43.249	49.886	16.338	18.394	20.217	10.740	11.377	13.131
B0G10%	47.345	54.062	58.200	20.183	22.992	24.612	13.267	14.371	15.986
B50G5%	29.309	36.762	43.650	12.494	15.635	18.459	8.213	9.581	11.418
B50G10%	42.836	47.574	54.043	17.299	19.313	21.975	10.740	12.575	13.702
B100G2.5%		30.275	35.336		11.956	14.943		7.784	9.135
B100G5%	27.054	32.437	39.493	11.533	13.795	15.822	7.581	8.982	10.277
B100G10%	36.072	41.087	45.729	14.416	16.554	19.338	8.845	10.778	12.560

C14: HC (C1) (g/kWh) at 2100 rpm:

RPM	2100 rpm								
Load	Low Load			Medium Load			High Load		
EGR %	0%	7.20%	11.99%	0%	8.52%	13.86%	0%	9.75%	15.58%
Fuels									
B0	18.914	21.898	24.929	7.435	8.552	9.418	4.598	5.073	5.776
B50	14.973	18.978	22.159	5.818	7.077	8.310	3.762	4.509	4.901
B100	11.033	16.058	19.389	4.525	5.898	7.756	2.508	3.758	4.901
B0W5%	23.642	24.817	27.699	9.051	9.436	10.526	5.852	5.636	6.651
B0W10%	29.947	30.657	34.623	11.637	12.385	13.850	7.523	7.891	8.402
B50W5%	17.338	21.898	26.314	7.111	8.257	10.526	4.180	4.885	6.301
B50W10%	23.642	27.737	31.853	9.697	10.616	12.188	6.269	6.764	7.351
B100W2.5%		16.058	20.774		6.487	7.756		3.758	4.901
B100W5%	14.185	18.978	23.544	5.818	7.667	9.418	3.344	4.885	5.601
B100W10%	20.490	23.358	27.699	7.758	9.436	11.080	5.016	6.012	6.651
B0G5%	25.218	27.737	30.469	10.344	10.616	12.188	6.269	6.764	7.352
B0G10%	31.523	33.576	37.393	12.283	13.564	14.404	7.523	8.267	8.752
B50G5%	18.914	23.358	27.699	7.758	9.436	10.526	5.016	5.636	6.651
B50G10%	26.795	30.657	33.238	10.344	11.795	12.742	6.687	7.140	7.702
B100G2.5%		17.518	22.159		6.487	8.310		4.133	4.901
B100G5%	17.338	20.438	24.929	6.465	8.257	9.418	3.762	4.885	5.951
B100G10%	22.066	24.817	29.084	9.051	10.026	11.634	5.434	6.388	7.001

C15: HC (C1) (g/kWh) at 3000 rpm:

RPM	3000 rpm								
Load	Low Load			Medium Load			High Load		
EGR %	0%	8.08%	12.77%	0%	10.09%	15.43%	0%	12.36%	17.94%
Fuels									
B0	16.741	19.786	23.336	6.577	7.764	9.335	4.024	4.681	5.652
B50	13.393	16.742	20.419	4.846	6.211	8.168	3.129	3.901	4.740
B100	10.045	13.698	18.961	3.461	5.590	7.001	1.788	3.121	4.011
B0W5%	21.764	22.829	26.253	8.307	8.695	9.918	5.365	5.461	6.199
B0W10%	26.786	28.917	33.546	10.384	11.801	13.419	6.706	7.022	8.022
B50W5%	16.741	19.786	24.795	6.230	7.453	9.335	4.024	4.681	5.470
B50W10%	23.438	25.873	30.629	9.692	10.559	11.668	5.812	6.241	7.293
B100W2.5%		15.220	18.961		5.590	7.001		3.121	4.376
B100W5%	13.393	18.264	21.878	5.538	7.453	8.751	3.129	4.291	5.105
B100W10%	18.415	22.829	26.253	7.615	9.316	9.918	4.471	5.461	6.199
B0G5%	23.438	25.873	29.170	9.692	10.559	11.668	5.812	6.241	6.928
B0G10%	28.460	31.961	35.005	11.076	12.422	13.419	7.153	7.412	8.387
B50G5%	18.415	21.308	26.253	6.923	8.074	10.502	4.471	5.071	6.199
B50G10%	25.112	28.917	30.629	9.692	11.180	12.252	6.259	7.022	7.657
B100G2.5%		15.220	20.419		6.211	7.584		3.511	4.376
B100G5%	15.067	19.786	23.336	5.538	7.453	9.335	3.129	4.681	5.470
B100G10%	21.764	24.351	27.712	8.307	9.938	11.085	4.918	5.851	6.564

C16: Smoke Opacity (%) at 1000 rpm:

RPM	1000 rpm								
Load	Low Load			Medium Load			High Load		
EGR %	0%	2.51%	7.62%	0%	4.13%	8.72%	0%	5.77%	9.93%
Fuels									
B0	4.4671	7.1817	7.4551	5.6881	7.6235	7.8105	7.7285	7.8827	8.5792
B50	11.2646	12.1212	16.5303	12.9596	14.0879	18.72	13.7714	16.0806	24.9891
B100	20.8669	22.492	23.3382	21.1862	22.9828	25.1306	24.0942	25.4894	28.7117
B0W5%	4.3592	4.4832	6.4892	5.2685	6.2916	6.8243	6.2562	7.1134	7.6217
B0W10%	3.3279	3.5112	3.7341	3.7429	3.9488	4.2734	4.3913	4.4844	5.5012
B50W5%	7.917	9.4388	14.4515	8.9024	11.923	15.8031	9.0041	13.0655	16.6077
B50W10%	4.5451	5.882	9.4388	5.8895	8.8711	11.923	7.2962	12.912	14.0655
B100W2.5 %		21.6438	23.3189		22.6083	24.0433		23.7297	24.8729
B100W5%	16.4941	20.169	22.6911	17.9791	20.8175	23.3563	20.0331	23.7283	24.6603
B100W10%	12.4099	12.803	15.3904	13.779	14.9841	16.5364	14.6564	16.7792	18.9452
B0G5%	4.2101	5.0919	5.5495	4.6896	5.83	6.0865	5.9022	6.3922	7.2084
B0G10%	2.1128	2.1588	3.31	2.9632	3.2805	3.68	4.1342	4.8143	5.3132
B50G5%	7.6948	8.5993	13.774	7.9493	9.8097	15.0084	8.2989	12.8513	15.6454
B50G10%	3.47	4.6632	8.1403	5.4677	6.7916	11.1106	6.4974	10.1134	13.5038
B100G2.5%		20.5632	21.6934		20.8458	22.1174		23.0581	24.1187
B100G5%	14.8705	18.7204	20.7204	17.7796	20.6531	21.8175	18.892	22.4729	23.9083
B100G10%	8.313	9.898	10.1796	10.3575	11.2486	13.2882	11.7256	13.2639	15.627

C17: Smoke Opacity (%) at 2100 rpm:

RPM	2100 rpm								
Load	Low Load			Medium Load			High Load		
EGR %	0%	7.20%	11.99%	0%	8.52%	13.86%	0%	9.75%	15.58%
Fuels									
B0	3.6209	3.7087	5.0091	4.3224	5.0424	5.6452	5.1309	5.756	6.0445
B50	5.6448	6.217	7.0097	6.6099	7.5919	8.8907	7.7788	7.8368	10.9776
B100	7.0169	7.7691	10.1892	7.9947	8.7586	10.5502	8.3892	11.0487	12.6553
B0W5%	2.5915	3.0326	3.9154	3.0952	3.4277	4.1652	3.7375	4.0936	5.1808
B0W10%	1.2993	1.7484	2.0183	1.7252	2.08	2.7273	2.5819	2.7296	4.3052
B50W5%	4.414	4.5883	5.409	4.9101	5.006	7.4015	5.6155	5.6806	8.6314
B50W10%	3.019	3.2167	3.5075	3.7322	3.8044	3.8116	3.9733	4.3346	4.5152
B100W2.5%		6.072	6.6831		6.6387	8.2127		6.8755	11.0619
B100W5%	4.9452	4.9788	6.5156	5.2432	5.4801	7.9048	5.8291	6.0706	9.4874
B100W10%	3.6758	3.7231	4.6494	3.7981	4.5458	4.8814	4.347	4.8675	4.962
B0G5%	2.2808	2.3804	2.7207	2.7709	3.0194	3.1279	3.6315	3.6772	4.562
B0G10%	0.7602	1.1723	1.2448	1.2527	1.8236	1.8621	1.7535	2.5523	2.6564
B50G5%	3.1961	3.5002	4.85	3.9175	4.0613	5.5664	4.5653	5.3203	6.5049
B50G10%	2.5526	2.6596	3.0422	2.9184	3.3794	3.7344	2.9381	4.4236	4.4712
B100G2.5%		4.7275	6.1886		5.8699	6.5063		6.5892	6.8376
B100G5%	3.8166	4.4802	5.4036	4.1897	5.0649	6.3101	4.8081	5.5813	6.7072
B100G10%	3.0692	3.9501	4.4849	3.5756	4.0009	4.6181	3.9531	4.5612	5.0313

C18: Smoke Opacity (%) at 3000 rpm:

RPM	3000 rpm								
Load	Low Load			Medium Load			High Load		
EGR %	0%	8.08%	12.77%	0%	10.09%	15.43%	0%	12.36%	17.94%
Fuels									
B0	2.0628	2.1569	2.9798	2.7416	2.9531	3.5129	3.6429	3.7913	4.1093
B50	3.3435	4.1529	5.1074	4.3754	5.0664	5.8095	5.3031	5.5882	6.4648
B100	4.9806	5.4475	7.0192	5.4644	7.7552	8.7667	5.8106	9.6048	10.7535
B0W5%	1.5864	2.031	2.741	2.0514	2.4216	2.9383	2.8447	3.0599	3.157
B0W10%	0.5928	0.7457	0.8166	0.8604	0.9805	1.2986	1.1728	1.7777	1.8707
B50W5%	2.8405	3.8749	5.0012	3.3945	3.9519	5.1426	4.1832	4.5408	5.8101
B50W10%	1.0944	2.2798	2.6204	1.6265	2.7713	3.1557	2.2802	3.4577	3.6664
B100W2.5%		3.6562	4.3294		4.4565	5.0093		5.1945	6.7191
B100W5%	3.3874	3.484	6.4804	3.7283	4.131	6.6957	4.2478	4.9069	9.1328
B100W10%	1.9862	2.4615	2.9992	2.6041	2.9538	3.4642	3.0502	4.0059	4.1131
B0G5%	1.4995	1.5307	1.5587	1.7008	2.1646	2.3094	2.0974	3.0555	3.6404
B0G10%	0.4417	0.4965	0.5467	0.6067	0.6576	0.6753	0.6457	0.9564	1.251
B50G5%	2.8003	2.8705	2.9909	3.1909	3.4434	3.9242	3.9019	4.1449	4.9562
B50G10%	1.1969	1.6993	2.005	1.5696	2.1037	2.5859	2.1894	2.4426	2.9936
B100G2.5%		3.1661	4.1584		3.8526	4.5552		4.614	5.5751
B100G5%	2.8272	2.9594	3.3961	3.2404	3.6969	4.1814	3.9284	4.8237	5.3018
B100G10%	1.6205	1.7029	2.2592	1.9762	2.1968	2.678	2.2636	2.5668	3.2582

C19: EGT (°C) at 1000 rpm:

RPM	1000 rpm								
Load	Low Load			Medium Load			High Load		
EGR %	0%	2.51%	7.62%	0%	4.13%	8.72%	0%	5.77%	9.93%
Fuels									
B0	160.3	157.4	154.1	185.4	182.3	177.6	230.2	226.1	220
B50	163.7	160.9	158.3	189.2	186	182.5	234.1	230.4	226.3
B100	169.5	166.8	163.8	194.4	190.9	187.6	239.1	235.3	231.3
B0W5%	144.5	141.7	139.4	162.7	160.3	157.8	211.6	207.6	204.1
B0W10%	129	125.8	122.9	150.2	146.3	142.8	203.1	198.8	194.2
B50W5%	148.9	146.1	143.2	167.1	164.1	160.7	215.4	211.3	207.5
B50W10%	135.6	132.7	129.8	155.4	152.3	149.1	206.7	200.4	196
B100W2.5%		158.52	156.1		180.6	177.3		225.7	222.1
B100W5%	153.2	149.8	147.5	172.4	169.6	166.7	220.1	216.8	212.9
B100W10%	141.4	139.4	137	162.6	160	156.9	211.7	207.9	203.7
B0G5%	149.2	144.4	141.9	165.1	162.5	159.5	214.6	210.5	205.9
B0G10%	135.5	130.6	126.8	154.4	148.3	145	206.3	201.3	195.5
B50G5%	152.6	149.7	144.7	173.9	168.9	164.3	220.7	214.5	208.7
B50G10%	140.5	136.1	132.7	161.7	157.2	152.9	212.9	205.9	199.5
B100G2.5%		161.2	157.8		182.5	179.2		228.8	225.2
B100G5%	157.3	153.5	149.2	179.8	174.8	170.2	225.1	219.3	214
B100G10%	145.6	143	140.5	166.1	163.3	160.7	216.5	212.2	207.5

C20: EGT (°C) at 2100 rpm:

RPM	2100 rpm								
Load	Low Load			Medium Load			High Load		
EGR %	0%	7.20%	11.99%	0%	8.52%	13.86%	0%	9.75%	15.58%
Fuels									
B0	220.1	215.5	210.8	245	239.4	234.6	280.6	274.4	268.4
B50	222.2	217.5	212.7	247.4	242.2	237.9	282.8	276.6	270.2
B100	226	221.7	217.7	252.3	247.8	242.3	288.1	282.1	275.9
B0W5%	197.2	193.8	190.1	216.6	212.3	207.8	257.9	253	247.9
B0W10%	188.5	184.5	179.9	210	204.8	200.1	244.4	238.4	232.7
B50W5%	202.2	197.5	193.4	223.7	219.2	214.4	264.5	258.4	253
B50W10%	195.8	191.5	187.7	215.3	210.6	206.1	253.9	249.1	242.4
B100W2.5%		211.1	207.1		238.1	233.3		274.2	268.7
B100W5%	207.4	204.1	200.2	231.7	227.8	224.4	270.9	265.5	260.7
B100W10%	199.3	195.5	192	221.1	217.3	213	259.8	254.9	250.5
B0G5%	200	196.6	192	221.1	217.3	210.2	261.5	255.3	249.7
B0G10%	193.6	187.1	182.9	213.1	207.9	203.9	248.2	242.7	236.1
B50G5%	207.4	201.8	195.5	228.6	222	215.3	267.1	260.7	253.9
B50G10%	200.1	194.5	189.8	217.5	211.4	208	254.8	250	243.5
B100G2.5%		214.6	210.9		242.4	237.8		276.7	272
B100G5%	210.4	205.4	201.3	236.4	230.5	226.11	273.5	268.3	262.4
B100G10%	203.8	199.7	194.9	222.7	217.8	214.3	264.5	259.8	253.3

C21: EGT (°C) at 3000 rpm:

RPM	3000 rpm								
Load	Low Load			Medium Load			High Load		
EGR %	0%	8.08%	12.77%	0%	10.09%	15.43%	0%	12.36%	17.94%
Fuels									
B0	255.4	248.8	242.1	295.2	286.6	278.9	340.1	330.9	321.3
B50	258.7	252.2	245.6	298	290.2	282.4	342.9	333.6	325.3
B100	263.6	255.7	248.3	301.8	293.3	285.1	347.9	338.9	329.7
B0W5%	231.7	227.5	223	270.2	264.5	259.5	319.9	313.8	307.2
B0W10%	221.6	215.2	210.3	259.3	253.1	247.3	308	299.7	291.6
B50W5%	237.8	233	227.6	275.8	270	264.6	323.2	316.4	309.4
B50W10%	226.6	222	216.5	264.3	259.3	253.6	315.5	307.9	301.5
B100W2.5%		248.2	242		287.2	280		333.4	325.4
B100W5%	243.8	239.7	234.7	282.6	277.2	272.5	330.5	323.9	318.4
B100W10%	234.6	229.7	225.5	271.9	266.5	261.7	322.5	317	310.7
B0G5%	234.4	229.5	224.9	274.8	268.5	261.1	322.7	315.3	309
B0G10%	224.5	218.8	211.5	262.3	255.1	249.3	313.6	303.1	294.6
B50G5%	240	234.7	230	281.2	273.9	265.9	328.1	320.2	311.2
B50G10%	230.1	223.7	217.2	267.9	260.7	256.7	318.5	310.5	302.5
B100G2.5%		252.8	245.7		291.7	285.1		337.7	329.3
B100G5%	247.1	240.9	235.4	286.3	280.9	273.6	334.5	325.1	319.2
B100G10%	236.3	232.5	227.9	274.7	268.6	262.2	325.3	319.4	313.1

APPENDIX D: Pictures of Instruments Used

Gas Analyzer

Smoke Opacity Meter

CO Analyzer

Thermometer

APPENDIX E: Power, Torque and BSFC Curve of the Light-Duty Engine

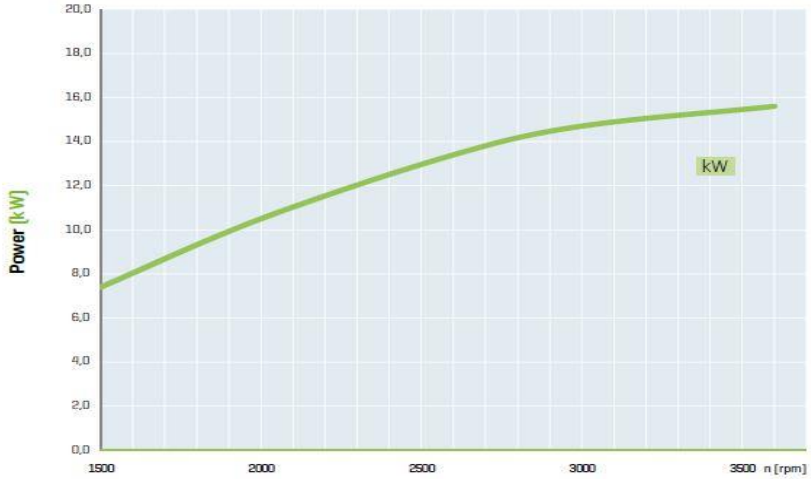

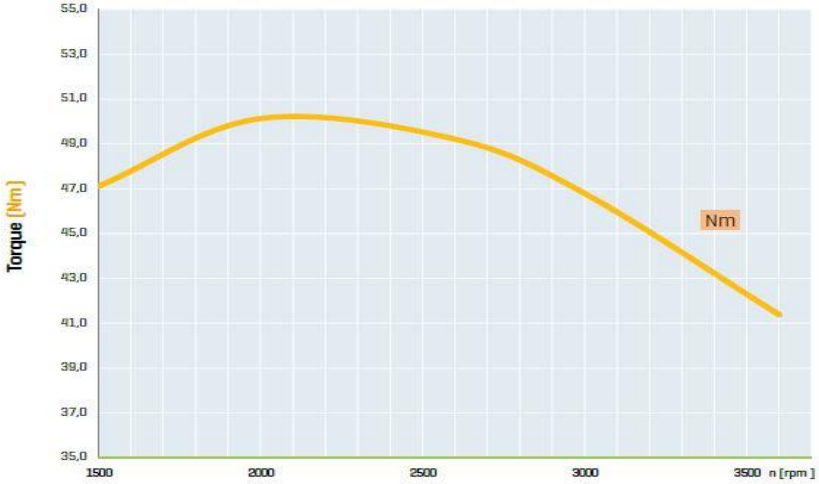

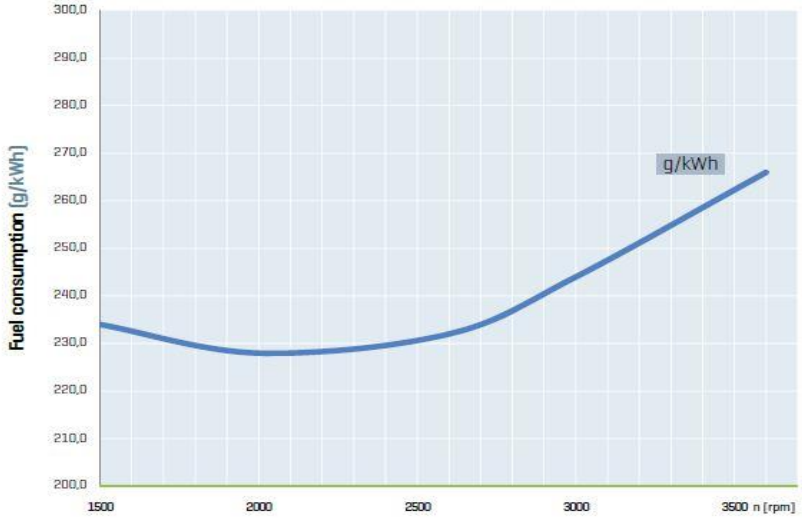

APPENDIX F: Calculations & Conversions
Emissions:

1. CO: ppm*1.25 = CO mg/m^3

   (CO (mg/m^3) * mass flow rate of (air+fuel (m^3/hr)))/ (1000*BP (kW)) = CO g/kWh

2. NO: ppm*1.34 = NO mg/m^3

   NO2: ppm*2.056 = NO2 mg/m^3

   NOx = NO+NO2 mg/m^3

   (NOx (mg/m^3) * mass flow rate of (air+fuel (m^3/hr)))/ (1000*BP (kW)) = NOx g/kWh

3. HC: ppm*1.965 = HC mg/m^3

   (HC (mg/m^3) * mass flow rate of (air+fuel (m^3/hr)))/ (1000*BP (kW)) = HC g/kWh

Mass Flow Rate of Fuel & Air:

1. Mass flow rate of fuel:

Density of fuel in (g/cm^3) given or found.

Fuel Consumption in (ml/min) was noted.

F.C in (g/min) = (ml/min)*density (g/cm^3).

1ml = 1cm^3

F.C in (g/hr) = (g/min)*60 was found.

F.C in (cm^3/hr) = (g/hr)/density (g/cm^3).

F.C in (m^3/hr) = (cm^3/hr)/(10^6).

2. Mass flow rate of air:

Given:

Area of the pipe (a) = 0.0016619 (m^2)

Acc. due to gravity (g) = 9.8 (m/s^2)

Density of air @25°C (ρa) = 1.184 (kg/m^3)

Density of liquid used in manometer (ρl) = 1000 (kg/m^3)

$\rho = \rho l / \rho a$

1. Deflection in the manometer reading due to intake air was calculated and noted to be Δh in m.
2. For calculating the velocity of the intake air, the formula used was: $V = \sqrt{2 * g * \rho * \Delta h}$ in m/s.
3. Then, volumetric flow rate, Q= area*velocity in m^3/s.
4. Mdot of intake air (kg/s) = Q* ρ.
5. Mdot of intake air (m^3/hr) = (Mdot of air (kg/s)/ density (ρ))*3600
6. The total Mdot was calculated (Mdot of intake air+ Mdot of fuel) in (m^3/hr)

- BSFC (g/kWh) = F.C (g/hr)/ B.P (kW)
- BTE (%) = (3600*100)/(BSFC (g/kWh)*H.V (Kj/g))
- B.P (kW) = (2*3.14*N*T)/60000

1 kW = 1.34 hp